Development of Advanced Methods of Structural and Trajectory Analysis for Transport Aircraft

Final Report

Dr. Mark D. Ardema
Principal Investigator

October 1, 1995 - February 28, 1998

Santa Clara University
Santa Clara, CA 95053

NASA Ames Research Center Grant NCC2-5167

Introduction

This report summarizes work accomplished under NASA Grant NCC2-5167, "Development of Advanced Methods of Structural and Trajectory Analysis for Transport Aircraft," October 1, 1995 - February 28, 1998. The effort was in two areas: (1) development of advanced methods of structural weight estimation, and (2) development of advanced methods of flight path optimization.

During the Spring of 1996 both graduate student research assistants working on the project, H.C. Chou and Mark Chambers, resigned to take positions in industry. This required assigning three new Santa Clara people to the project: Dr. Lee Hornberger, Associate Professor of Mechanical Engineering; Robert Windhorst, graduate student research assistant; and Frank Dickerson, undergraduate student. These new people inevitably required time to learn the ACSYNT code and the nature of the ongoing research. The result is that the grant was extended at no additional cost from September 30, 1997, to February 28, 1998.

Dr. H. Miura, M. Moore, and J. Phillips were the NASA collaborators on the Grant. All publications resulting from the grant were co-authored by Santa Clara and NASA Ames personnel.

Structural Weight Estimation

A report that was prepared under a previous grant was published in May 1996 ("Analytical Fuselage and Wing Weight Estimation of Transport Aircraft," by M. Ardema, M. Chambers, A. Patron, A. Hahn, H. Miura, and M. Moore, NASA TM 110392). A paper that summarizes this report was accepted for presentation at the World Aviation Congress held in October 1996; a copy of this paper appears in Appendix A.

Throughout the first year, integration of the structural weight computer code, PDCYL, into ACSYNT continued. Input variables used by PDCYL but already in ASCYNT have been removed from PDCYL. Infrequently used input variables have been defaulted. Data transfer has been modified so that optimization runs with ACSYNT can be done with PDCYL as an integral part of the code.

The major effort of the first year of the grant was to develop an improved method of estimating the weight of wing and fuselage structures made from composite materials. This involved an extensive literature search, the coding of a composite materials subroutine, and demonstrating the code. This work is discussed in detail in Appendix B.

Previously in ACSYNT, the weight of composite material structures was estimated assuming quasi-isotropic materials, maximum stress failure theory, and smeared structural elements. The new capability accounts for realistic lay-ups of unidirectional fiber/matrix

composites and uses a bi-axial strain failure theory. The new composite routine has been implemented for the fuselage and wing weight calculations.

A user's manual for the new composite subroutine may be found in Appendix B. As a check case for the new subroutine, the weight of a composite fuselage of the ASA 2150 has been estimated.

The final effort in the structures area was support of the project to design and analyze a 150 passenger advanced transport airplane, the ASA 2150. PDCYL has been used as an integral part of ACSYNT to estimate the fuselage and wing weights of this aircraft. Appendix C gives the details of the weight calculations for both Aluminum and Graphite/Epoxy fuselage versions of the ASA 2150.

Appendix C shows that at a gross take-off weight of 152,181 pounds, the ASA 2150 is estimated to have a wing weight of 10,315 pounds and a fuselage weight of 15,652 pounds when made of Aluminum. Figure 1 shows the ASA 2150 fuselage bending moment distribution. The critical loading condition for most of the fuselage is either the landing condition (L) or the runway bump condition (B), with a small portion governed by the maneuver condition (M). The shell unit weight distribution is shown on Figure 2. Approximately the first half of the fuselage is sized by minimum gage, with most of the rest yield strength critical.

When the fuselage is made of composite material, the weight is estimated to be 15,375 pounds, a weight savings of about 2% relative to aluminum. The composite material is a uni-directional tape made from Hercules AS4 carbon fiber in Fiberite 12K/938 resin. The reason for this relatively low weight savings is that for relatively small and lightly loaded aircraft such as the ASA 2150, the fact that the composite material thickness must be in integer thicknesses of the basic stack thickness means that the structure is in many places considerably overdesigned. The basic stack used was a quasi-isotropic lay-up of eight unidirectional plys. Also, the nonoptimun factor used for the composite was 17% higher than that for the Aluminum design. As for the Aluminum design, the composite fuselage was sized by minimum gage and yield strength.

Trajectory Optimization

The last year of the grant focused on development of trajectory optimization routines for supersonic transport aircraft. The results of this research were published as NASA/TM-1998-112223, included as Appendix D. Since this report gives a comprehensive description of this work, it will not be further discussed here.

Figure 1. **Bending Moment Distribution (ASA 2150)**

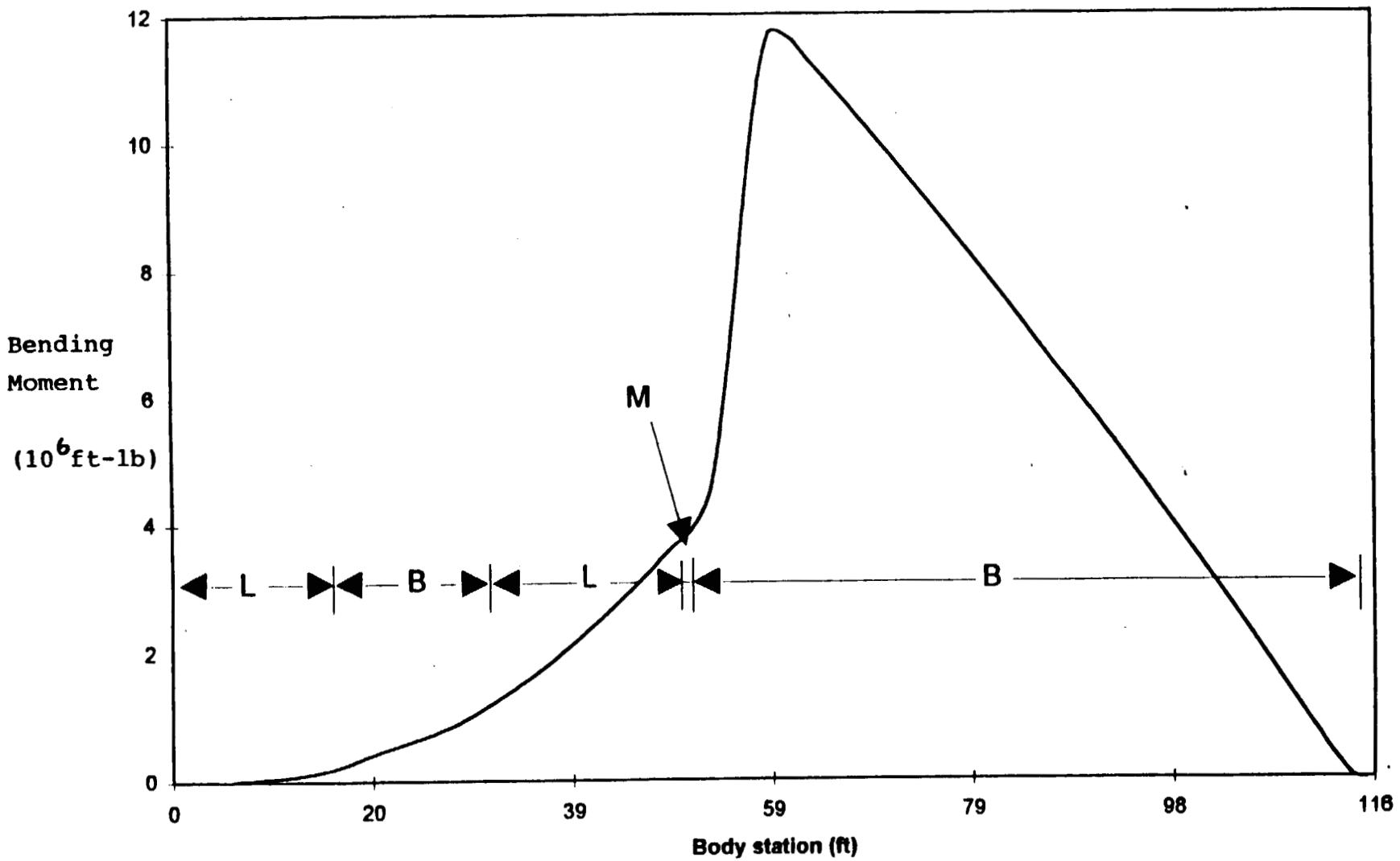

Figure 2. **Shell Unit Weight Distribution (ASA 2150)**

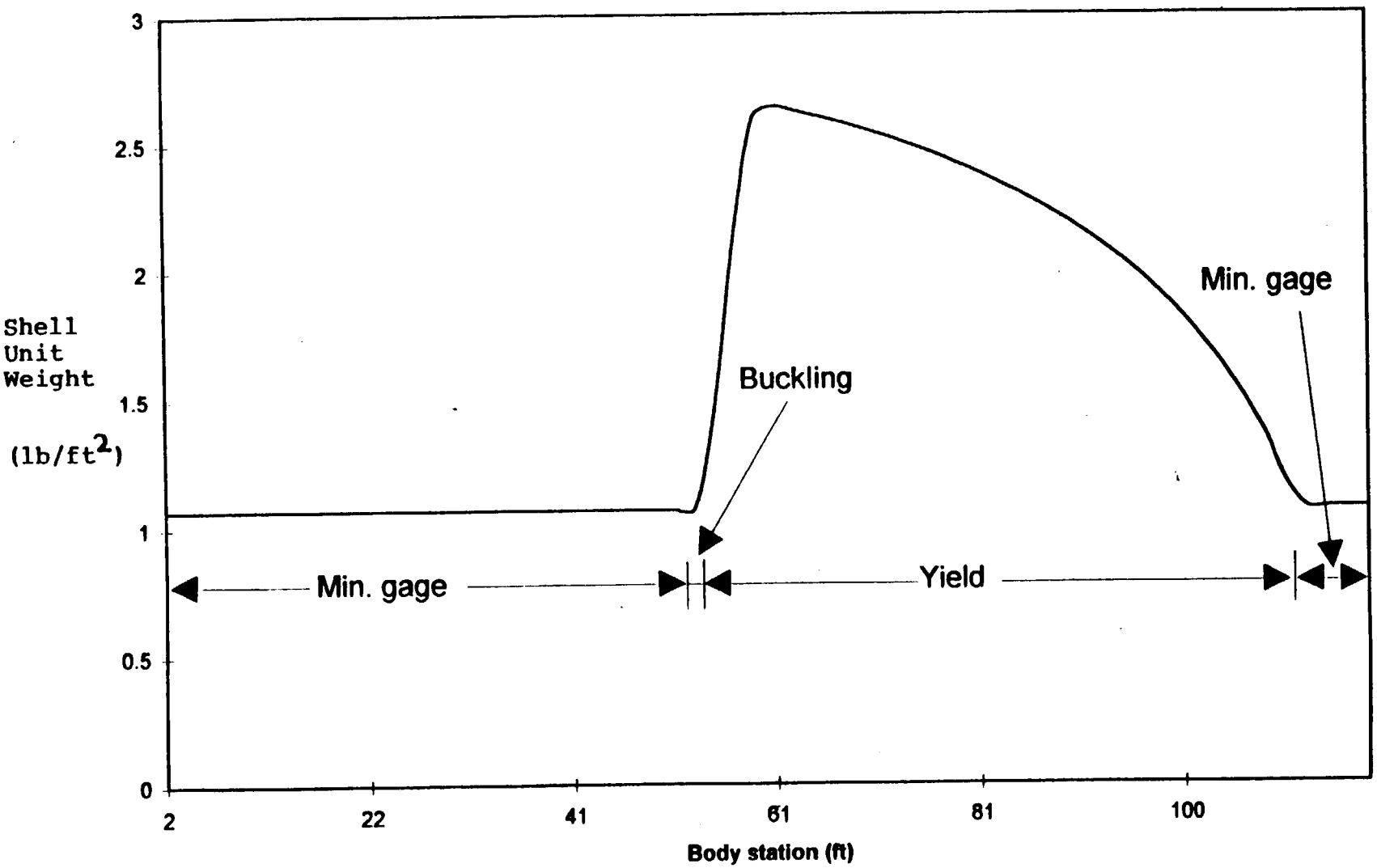

Appendix A

"Fuselage and Wing Weight of Transport Aircraft"

by

M. Ardema, M. Chambers, A. Patron, A. Hahn, H. Miura, and M. Moore

to be presented at

World Aviation Congress
October 22 - 24, 1996
Los Angeles, California

October 1996

965583

Fuselage and Wing Weight of Transport Aircraft

Mark D. Ardema, Mark C. Chambers, and Anthony P. Patron
Santa Clara Univ.

Andrew S. Hahn, Hirokazu Miura, and Mark D. Moore
NASA Ames Research Center

1996 World Aviation Congress
October 21-24, 1996
Los Angeles, CA

SAE The Engineering Society For Advancing Mobility Land Sea Air and Space INTERNATIONAL

SAE International
400 Commonwealth Drive
Warrendale, PA 15096-0001 U.S.A.

AIAA

American Institute of Aeronautics and Astronautics
370 L'Enfant Promenade, S.W.
Washington, D.C. 20024

Published by the American Institute of Aeronautics and Astronautics (AIAA) at 1801 Alexander Bell Drive, Suite 500, Reston, VA 22091 U.S.A., and the Society of Automotive Engineers (SAE) at 400 Commonwealth Drive, Warrendale, PA 15096 U.S.A.

Produced in the U.S.A. Non-U.S. purchasers are responsible for payment of any taxes required by their governments.

ISSN #0148-7191

All AIAA papers are abstracted and indexed in International Aerospace Abstracts and Aerospace Database.

All SAE papers, standards and selected books are abstracted and indexed in the Global Mobility Database.

Copies of this paper may be purchased from:

AIAA's document delivery service
Aeroplus Dispatch
1722 Gilbreth Road
Burlingame, California 94010-1305
Phone: (800) 662-2376 or (415) 259-6011
Fax: (415) 259-6047

or from:

SAExpress Global Document Service
c/o SAE Customer Sales and Satisfaction
400 Commonwealth Drive
Warrendale, PA 15096
Phone: (412) 776-4970
Fax: (412) 776-0790

SAE routinely stocks printed papers for a period of three years following date of publication. Quantity reprint rates are available.

Positions and opinions advanced in this paper are those of the author(s) and not necessarily those of SAE or AIAA. The author is solely responsible for the content of the paper. A process is available by which discussions will be printed with the paper if it is published in SAE Transactions.

Fuselage and Wing Weight of Transport Aircraft

Mark D. Ardema, Mark C. Chambers, and Anthony P. Patron
Santa Clara Univ.

Andrew S. Hahn, Hirokazu Miura, and Mark D. Moore
NASA Ames Research Center

ABSTRACT

A method of estimating the load-bearing fuselage weight and wing weight of transport aircraft based on fundamental structural principles has been developed. This method of weight estimation represents a compromise between the rapid assessment of component weight using empirical methods based on actual weights of existing aircraft, and detailed, but time-consuming, analysis using the finite element method. The method was applied to eight existing subsonic transports for validation and correlation. Integration of the resulting computer program, PDCYL, has been made into the weights-calculating module of the AirCraft SYNThesis (ACSYNT) computer program. ACSYNT has traditionally used only empirical weight estimation methods; PDCYL adds to ACSYNT a rapid, accurate means of assessing the fuselage and wing weights of unconventional aircraft. PDCYL also allows flexibility in the choice of structural concept, as well as a direct means of determining the impact of advanced materials on structural weight.

INTRODUCTION

A methodology based on fundamental structural principles has been developed to estimate the load-carrying weight of the fuselage and basic box weight of the wing for aircraft, and has been incorporated into the AirCraft SYNThesis program (ACSYNT). This weight routine is also available to run independently of ACSYNT, and is a modification of a collection of previously developed structural programs.[1-4] The main subroutine called by ACSYNT is PDCYL. This study has concentrated on modern transport aircraft because of the detailed weight information available, allowing the weights output from PDCYL to be compared to actual structural weights. The detailed weight statements also allow *nonoptimum* factors to be computed which, when multiplied by the load-bearing structural weights calculated by PDCYL, will give good representative total structure weight estimates. These nonoptimum factors will be computed through a regression analysis of a group of eight transport aircraft.

PDCYL is able to model both skin-stringer-frame and composite sandwich shell fuselage and wing box constructions. Numerous modifications were made to PDCYL and its associated collection of subroutines. These modifications include the addition of detailed fuselage shell geometry calculations; optional integration of a cylindrical fuselage midsection between the nose and tail sections; addition of landing and bump maneuvers to the load cases sizing the fuselage; ability to introduce an elliptical spanwise lift load distribution on the wing; variation of wing thickness ratio from tip to root; ability to place landing gear on the wing to relieve spanwise bending loads; distribution of propulsion system components between wing and fuselage; and the determination of maximum wingtip deflection.

BRIEF DESCRIPTION OF ACSYNT

The Aircraft Synthesis Computer program, ACSYNT, is an integrated design tool used in the modeling of advanced aircraft for conceptual design studies.[5] ACSYNT development began at NASA Ames Research Center in the 1970s and continues to this day. The ACSYNT program is quite flexible and can model a wide range of aircraft configurations and sizes, from remotely piloted high altitude craft to the largest transport.

The ACSYNT program uses the following modules, not necessarily in this order: Geometry, Trajectory, Aerodynamics, Propulsion, Stability, Weights, Cost, Advanced Aerodynamic Methods, and Takeoff. An ACSYNT run would normally progress as follows: the Geometry module is called to define the aircraft shape and configuration; the Trajectory module then runs the vehicle through a specified mission; finally the Weight and Cost modules are executed. To determine the performance of the vehicle at each mission point, the Trajectory module will call the Aerodynamics and Propulsion modules.

* Work of the first two authors was supported by NASA Ames Research Center Grant NCC2-5068.

After the mission is completed, the calculated weight of the aircraft may be compared with the initial estimate and an iteration scheme run to converge upon the required aircraft weight. This process is necessarily iterative as the aircraft weight ACSYNT calculates is dependent upon the initial weight estimate.

ACSYNT is able to perform a *sensitivity analysis* on any design variable, such as aspect ratio, thickness-to-chord ratio, fuselage length or maximum fuselage diameter. Sensitivity is defined as (change in objective function/value of objective function) divided by (change in design variable/design variable). As an example, if gross weight is the objective function and decreases when the wing thickness-to-chord ratio increases, then the sensitivity of thickness-to-chord ratio is negative. It is important to note that while this increase in thickness-to-chord ratio lowers the gross weight of the aircraft, it may also have a detrimental effect on aircraft performance.

ACSYNT is also able to size multiple design variables by optimizing the objective function. The objective function represents the interactions between design disciplines such as structures, aerodynamics and propulsion. The automated sizing of design variables during the optimization process is accomplished using the gradient method. Two types of constraints may be imposed during the optimization process. These are performance-based constraints such as runway length or maximum roll angle, and side constraints on design variables such as limitations on wing span or fuselage length. ACSYNT never violates constraints during the optimization process so that each iteration produces a valid aircraft.

METHODS OF WEIGHT ESTIMATION

Two methods are commonly available to estimate the load-bearing fuselage weight and wing box structure weight of aircraft. These methods, in increasing order of complexity and accuracy, are empirical regression and detailed finite element structural analysis. Each method has particular advantages and limitations which will be briefly discussed in the following sections. There is an additional method based on classical plate theory (CPT) which may be used to estimate the weight of the wing box structure.

EMPIRICAL

The empirical approach is the simplest weight estimation tool. It requires knowledge of fuselage and wing weights from a number of similar existing aircraft in addition to various key configuration parameters of these aircraft in order to produce a linear regression. This regression is a function of the configuration parameters of the existing aircraft and is then scaled to give an estimate of fuselage and wing weights for an aircraft under investigation. Obviously, the accuracy of this method is dependent upon the quality and quantity of data available for existing aircraft. Also, the accuracy of the estimation will depend on how closely the existing aircraft match the configuration and weight of the aircraft under investigation. All of the empirical regression functions currently in the ACSYNT program give total fuselage weight and total wing weight.

FINITE ELEMENT

Finite element analysis is the matrix method of solution of a discretized model of a structure. This structure, such as an aircraft fuselage or wing, is modeled as a system of elements connected to adjacent elements at nodal points. An element is a discrete (or finite) structure that has a certain geometric makeup and set of physical characteristics. A nodal force acts at each nodal point, which is capable of displacement. A set of mathematical equations may be written for each element relating its nodal displacements to the corresponding nodal forces. For skeletal structures, such as those composed of rods or beams, the determination of element sizing and corresponding nodal positioning is relatively straightforward. Placement of nodal points on these simple structures would naturally fall on positions of concentrated external force application or joints, where discontinuities in local displacement occur.

Continuum structures, such as an aircraft fuselage or wing, which would use some combination of solid, flat plate, or shell elements, are not as easily discretizable. An approximate mesh of elements must be made to model these structures. In effect, an idealized model of the structure is made, where the element selection and sizing is tailored to local loading and stress conditions.

The assembly of elements representing the entire structure is a large set of simultaneous equations that, when combined with the loading condition and physical constraints, can be solved to find the unknown nodal forces and displacements. The nodal forces and displacements are then substituted back into the each element to produce stress and strain distributions for the entire structural model.

CLASSICAL PLATE THEORY

CPT has been applied to wing structure design and weight estimation for the past 20 years. Using CPT a mathematical model of the wing based on an equivalent plate representation is combined with global Ritz analysis techniques to study the structural response of the wing. An equivalent plate model does not require detailed structural design data as required for finite element analysis model generation and has been shown to be a reliable model for low aspect ratio fighter wings. Generally, CPT will overestimate the stiffness of more flexible, higher aspect ratio wings, such as those employed on modern transport aircraft. Recently, transverse shear deformation has been included in equivalent plate models to account for this added flexibility. This new technique has been shown to give closer representations of tip deflection and natural frequencies of higher aspect ratio wings, although it still overestimates the wing stiffness. No fuselage weight estimation technique which corresponds to the equivalent plate model for wing structures is available.

NEED FOR BETTER, INTERMEDIATE METHOD

Preliminary weight estimates of aircraft are traditionally made using empirical methods based on the weights of existing aircraft, as has been described. These methods, however, are undesirable for studies of unconventional aircraft concepts for two reasons. First, since the weight estimating

ormulas are based on existing aircraft, their application to nconventional configurations (i.e., canard aircraft or area uled bodies) is suspect. Second, they provide no straightorward method to assess the impact of advanced technologies nd materials (i.e., bonded construction and advanced omposite laminates).

On the other hand, finite-element based methods of tructural analysis, commonly used in aircraft detailed design, re not appropriate for conceptual design, as the idealized tructural model must be built off-line. The solution of even a oderately complex model is also computationally intensive nd will become a bottleneck in the vehicle synthesis. Two pproaches which may simplify finite-element structural nalysis also have drawbacks. The first approach is to create etailed analyses at a few critical locations on the fuselage and ving, then extrapolate the results to the entire aircraft, but this an be misleading because of the great variety of structural, oad, and geometric characteristics in a typical design. The econd method is to create an extremely coarse model of the ircraft, but this scheme may miss key loading and stress oncentrations in addition to suffering from the problems ssociated with a number of detailed analyses.

The fuselage and wing structural weight estimation nethod employed in PDCYL is based on another approach, eam theory structural analysis. This results in a weight stimate that is directly driven by material properties, load onditions, and vehicle size and shape, and is not confined to n existing data base. Since the analysis is done station-bytation along the vehicle longitudinal axis, and along the wing tructural chord, the distribution of loads and vehicle geometry s accounted for, giving an integrated weight that accounts for ocal conditions. An analysis based solely on fundamental rinciples will give an accurate estimate of structural weight nly. Weights for fuselage and wing secondary structure, ncluding control surfaces and leading and trailing edges, and ome items from the primary structure, such as doublers, utouts, and fasteners, must be estimated from correlation to xisting aircraft.

The equivalent plate representation, which is unable to nodel the fuselage structure, is not used in PDCYL.

METHODS

OVERVIEW

Since it is necessary in systems analysis studies to be able o rapidly evaluate a large number of specific designs, the nethods employed in PDCYL are based on idealized vehicle nodels and simplified structural analysis. The analyses of the fuselage and wing structures are performed in different outines within PDCYL, and, as such, will be discussed eparately. The PDCYL weight analysis program is initiated at he point where ACSYNT performs its fuselage weight calculation. PDCYL first performs a basic geometrical sizing of the aircraft in which the overall dimensions of the aircraft are determined and the propulsion system, landing gear, wing, and lifting surfaces are placed.

Fuselage

The detailed fuselage analysis starts with a calculation of vehicle loads on a station-by-station basis. Three types of loads are considered—longitudinal acceleration (applicable to high-thrust propulsion systems), tank or internal cabin pressure, and longitudinal bending moment. All of these loads occur simultaneously, representing a critical loading condition. For longitudinal acceleration, longitudinal stress resultants caused by acceleration are computed as a function of longitudinal fuselage station; these stress resultants are compressive ahead of the propulsion system and tensile behind the propulsion system. For internal pressure loads, the longitudinal distribution of longitudinal and circumferential (hoop) stress resultants is computed for a given shell gage pressure (generally 12 psig). There is an option to either use the pressure loads to reduce the compressive loads from other sources or not to do this; in either case, the pressure loads are added to the other tensile loads.

The following is a summary of the methods used; the details may be found in Ref. 6.

Longitudinal bending moment distributions from three load cases are examined for the fuselage. Loads on the fuselage are computed for a quasi-static pull-up maneuver, a landing maneuver, and travel over runway bumps. These three load cases occur at user-specified fractions of gross takeoff weight. Aerodynamic loads are computed as a constant fraction of fuselage planform area and are considered negligible for subsonic transports. For pitch control there is an option to use either elevators mounted on the horizontal tail (the conventional configuration) or elevons mounted on the trailing edges of the wing. The envelope of maximum bending moments is computed for all three load cases and is then used to determine the net stress resultants at each fuselage station.

After the net stress resultants are determined at each fuselage station, a search is conducted at each station to determine the amount of structural material required to preclude failure in the most critical condition at the most critical point on the shell circumference. This critical point is assumed to be the outermost fiber at each station. Failure modes considered are tensile yield, compressive yield, local buckling, and gross buckling of the entire structure. A minimum gage restriction is also imposed as a final criterion. It is assumed that the material near the neutral fiber of the fuselage (with respect to longitudinal bending loads) is sufficient to resist the shear and torsion loads transmitted through the fuselage. For the shear loads this is a good approximation as the fibers farthest from the neutral axis will carry no shear. Also, for beams with large fineness ratios (fuselage length/maximum diameter) bending becomes the predominant failure mode.

The maximum stress failure theory is used for predicting yield failures. Buckling calculations assume stiffened shells behave as wide columns and sandwich shells behave as cylinders. The frames required for the stiffened shells are sized by the Shanley criterion. This criterion is based on the premise that, to a first-order approximation, the frames act as elastic supports for the wide column.[7]

There are a variety of structural geometries available for the fuselage. There is a simply stiffened shell concept using

longitudinal frames. There are three concepts with Z-stiffened shells and longitudinal frames; one with structural material proportioned to give minimum weight in buckling, one with buckling efficiency compromised to give lighter weight in minimum gage, and one a buckling-pressure compromise. Similarly, there are three truss-core sandwich designs, two for minimal weight in buckling with and without frames, and one a buckling-minimum gage compromise.

It is assumed that the structural materials exhibit elasto-plastic behavior. Further, to account for the effects of creep, fatigue, stress-corrosion, thermal cycling and thermal stresses, options are available to scale the material properties of strength and Young's modulus of elasticity. In the numerical results of this study, all materials were considered elastic and the full room-temperature material properties were used.

Composite materials can be modeled with PDCYL by assuming them to consist of orthotropic lamina formed into quasi-isotropic (two-dimensionally, or planar, isotropic) laminates. Each of the lamina is assumed to be composed of filaments placed unidirectionally in a matrix material. Such a laminate has been found to give very nearly minimum weight for typical aircraft structures.

Wing

The wing structure is a multi-web box beam designed by spanwise bending and shear. The wing-fuselage carrythrough structure, defined by the wing-fuselage intersection, carries the spanwise bending, shear, and torsion loads introduced by the outboard portion of the wing.

The load case used for the wing weight analysis is the quasi-static pull-up maneuver. The applied loads to the wing include the distributed lift and inertia forces, and the point loads of landing gear and propulsion, if placed on the wing. Fuel may also be stored in the wing, which will relieve bending loads during the pull-up maneuver.

The wing weight analysis proceeds in a similar fashion to that of the fuselage. The weight of the structural box is determined by calculating the minimum amount of material required to satisfy static buckling and strength requirements at a series of spanwise stations. The covers of the multi-web box are sized by buckling due to local instability and the webs by flexure-induced crushing. Required shear material is computed independently of buckling material. Aeroelastic effects are not accounted for directly, although an approximation of the magnitude of the tip deflection during the pull-up maneuver is made. For the carrythrough structure, buckling, shear, and torsion material are computed independently and summed.

As for the fuselage, there are a variety of structural geometries available. There are a total of six structural concepts, three with unstiffened covers and three with truss-stiffened covers. Both cover configurations use webs that are either Z-stiffened, unflanged, or trusses.

GEOMETRY

Fuselage

The fuselage is assumed to be composed of a nose section, an optional cylindrical midsection, and a tail section. The gross density and fineness ratio are defined as

$$\rho_B = \frac{W_B}{V_B} \tag{1}$$

$$R_{fin} = \frac{l_B}{D} \tag{2}$$

where W_B is the fuselage weight (W_B = gross takeoff weight excluding the summed weight of the wing, tails, wing-mounted landing gear, wing-mounted propulsion, and fuel if stored in the wing), V_B is the total fuselage volume, l_B is the fuselage length, and D is the maximum fuselage diameter. The fuselage outline is defined by two power-law bodies of revolution placed back-to-back, with an optional cylindrical midsection between them (Fig. 1). (For the present study, all eight transports used for validation of the analysis used the optional cylindrical midsection.)

The horizontal tail is placed according to its quarter chord location as a fraction of the fuselage length.

Propulsion may be either mounted on the fuselage or placed on the wing. In the case of fuselage mounted propulsion, the starting and ending positions of the propulsion unit are again calculated from their respective fractions of fuselage length

Similarly, the nose landing gear is placed on the fuselage as a fraction of vehicle length; the main gear, on the other hand, may be placed either on the fuselage as a single unit, also as a fraction of fuselage length, or on the wing in multiple units.

Wing

The lifting planforms are assumed to be tapered, swept wings with straight leading and trailing edges. The planform shape is trapezoidal as the root chord and tip chord are parallel. The wing is placed on the fuselage according to the location of the leading edge of its root chord, determined as a fraction of the fuselage length (Fig. 2). It is assumed that specified portions of the streamwise (aerodynamic) chord are required for controls and high lift devices, leaving the remainder for the structural wing box. The intersection of this structural box with the fuselage contours determines the location of the rectangular carrythrough structure. The width of the carrythrough structure is defined by the corresponding fuselage diameter.

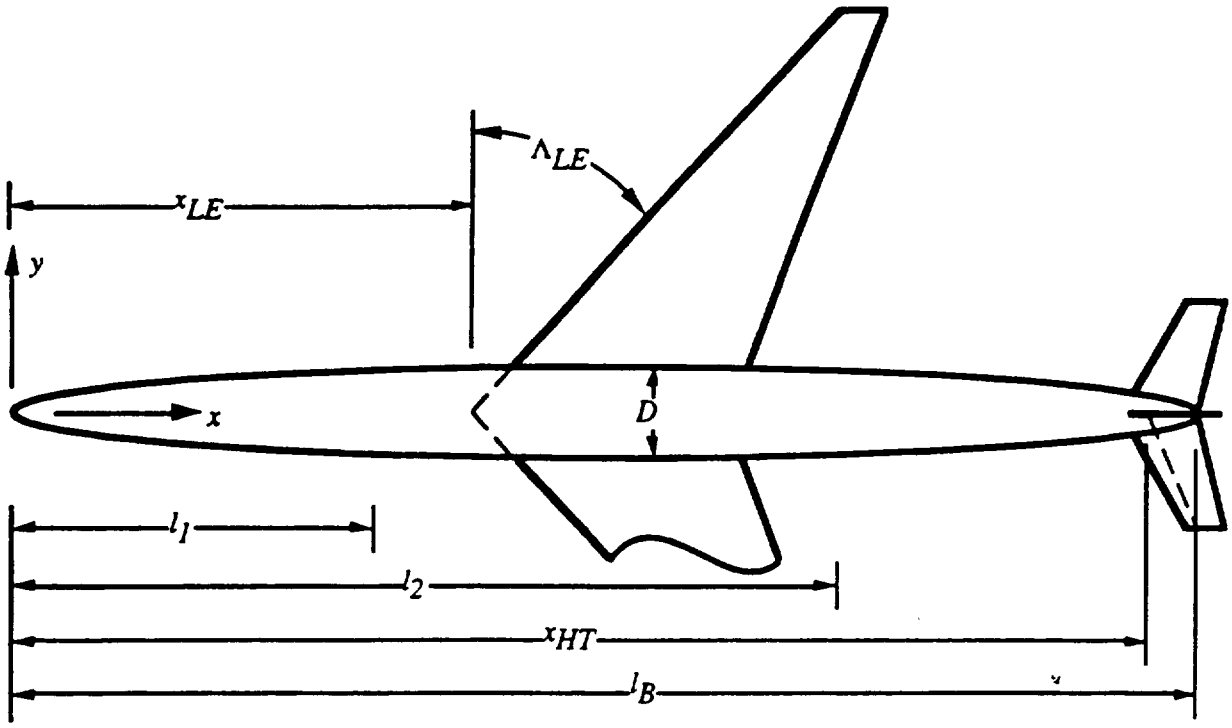

Fig. 1 The body configuration.

For the transports in the present study, all the fuel is carried within the wing structure. An option is also available to carry the fuel entirely within the fuselage, negating any bending relief in the wing.

LOADS

Fuselage

Fuselage loading is determined on a station-by-station basis along the length of the vehicle. Three types of fuselage loads are considered—longitudinal acceleration, tank pressure, and bending moment. In the present study, all three load types are assumed to occur simultaneously to determine maximum compressive and tensile loads at the outer shell fibers at each station.

Bending loads applied to the vehicle fuselage are obtained by simulating vehicle pitch-plane motion during a quasi-static pull-up maneuver; a landing; and movement over a runway bump. Simplified vehicle loading models are used where it is assumed that: (1) fuselage lift forces (nominally zero for subsonic transports) are distributed uniformly over the fuselage plan area; (2) wing loading, determined independently, is transferred by a couple of vertical force and torque through the wing carrythrough structure; (3) fuselage weight is distributed uniformly over fuselage volume; (4) control surface forces and landing gear reactions are point loads; and (5) the propulsion system weight, if mounted on the fuselage, is uniformly distributed. A factor of safety (nominally 1.5) is applied to each load case. The aircraft weight for each case is selected as a fraction of gross takeoff weight. All fuselage lift forces are assumed to be linear functions of angle of attack. Longitudinal bending moments are computed for each of the three loading cases and the envelope of the maximum values taken as the design loading condition. The bending moment computation is given in detail in Ref. 4 and will only be summarized here.

Considering first the pull-up maneuver loading, the motion is assumed to be a quasi-static pitch-plane pull-up of given normal load factor n (nominally 2.5 for transport aircraft). The vehicle is trimmed with the appropriate control surface (a horizontal tail for all eight transport used for validation in the present study), after which the angle of attack is calculated.

Landing loads are developed as the aircraft descends at a given vertical speed after which it impacts the ground; thereafter the main and nose landing gears are assumed to exert a constant, or optionally a $(1 - \cos(\omega t))$, force during its stroke until the aircraft comes to rest. The vehicle weight is set equal to the nominal landing weight. Wing lift as a fraction of landing weight is specified, which reduces the effective load the landing gear carries. Likewise, the portion of total vehicle load the main gear carries is specified. No pitch-plane motion is considered during the landing.

Runway bump loads are handled by inputting the bump load factor into the landing gear. Bump load factor is applied according to Ref. 8. This simulates the vehicle running over a bump during taxi. In a similar fashion to the landing, the wing lift as a fraction of gross takeoff weight is specified, as is the portion of effective load input through the main gear. No pitch-plane motion is considered during the bump.

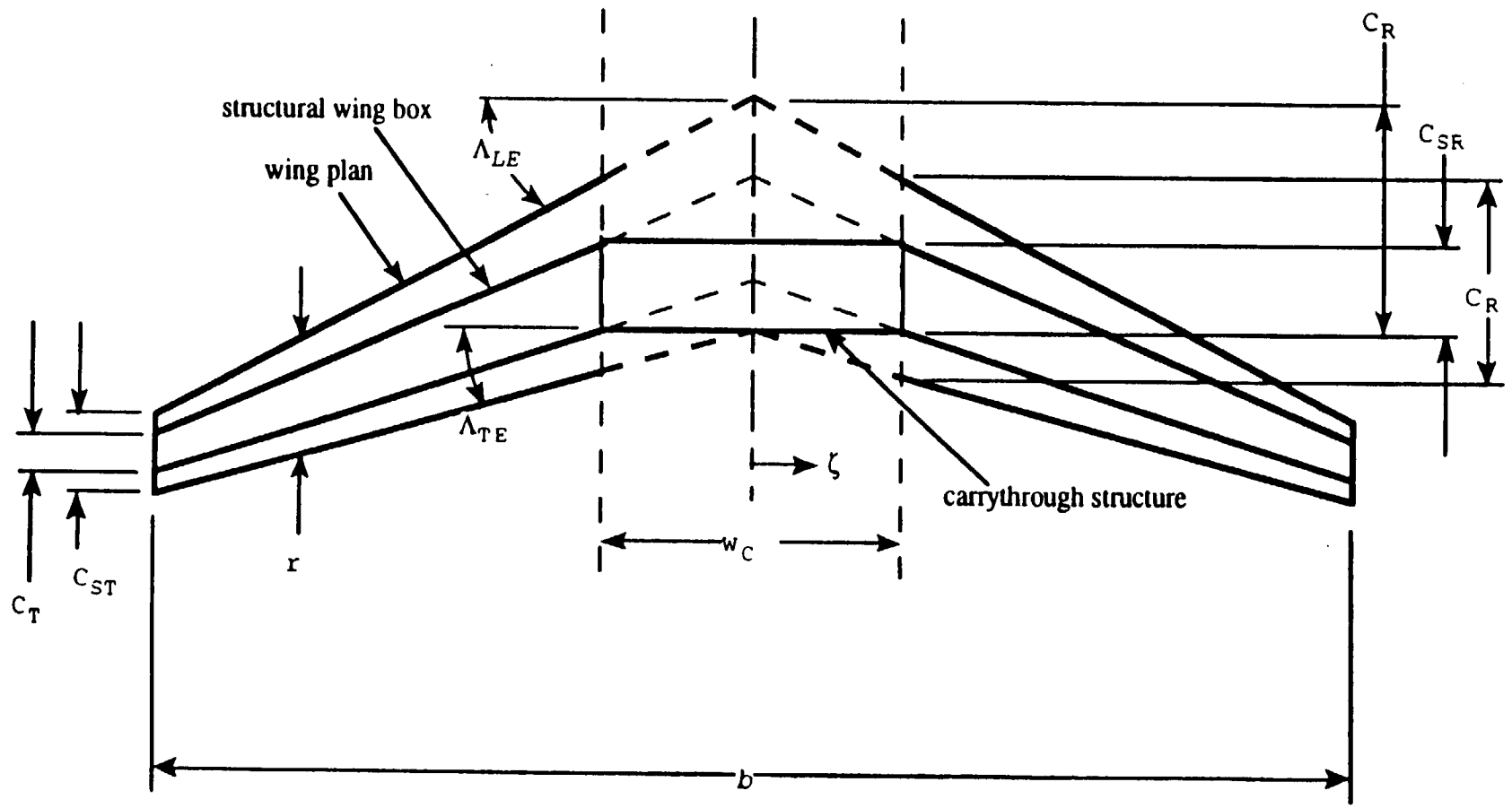

Figure 2 Wing structural planform geometry.

Wing

For the wing, only a quasi-static pull-up maneuver condition at load factor n is considered for determining loads. At each spanwise station along the quarter chord, from the wingtip to the wing-fuselage intersection, the lift load, center of pressure, inertia load, center of gravity, shear force, and bending moment are computed. For the inertia load, it is assumed that the fuel weight is distributed uniformly with respect to the wing volume.

There is an option for either a trapezoidal or a Schrenk[9] lift load distribution along the wingspan; the trapezoidal distribution represents a uniform lift over the wing area (which has a trapezoidal planform) while the Schrenk distribution is an average of the trapezoidal distribution with an elliptical distribution, where the lift is zero at the wingtip and maximum at the wing-fuselage intersection. Prandtl has shown that a true elliptical lift load distribution will have a minimum induced drag, but a combination of the elliptical and trapezoidal distributions will give a better representation of actual aircraft loading.[9]

STRUCTURAL ANALYSIS

Fuselage

Weight estimating relationships are now developed for the load-carrying fuselage structure. In addition, the volume taken up by the fuselage structure is also determined.

Considering first the circular shell, the stress resultants in the axial direction caused by longitudinal bending, axial acceleration, and pressure at a fuselage station x are

$$N_{x_B} = \frac{Mr}{I'_y} \tag{3}$$

$$N_{x_A} = \frac{N_x W_S}{P} \tag{4}$$

$$N_{x_P} = \frac{AP_g}{P} \tag{5}$$

respectively, where $r = D/2$ is the fuselage radius, $A = \pi r^2$ is the fuselage cross-sectional area, and $P = 2\pi r$ is the fuselage perimeter. In EQ (3), $I'_y = \pi r^3$ is the moment of inertia of the shell divided by the shell thickness. In EQ (4), for the case of fuselage-mounted propulsion, W_s is the portion of vehicle weight ahead of station x if x is ahead of the inlet entrance, or the portion of vehicle weight behind x if x is behind the nozzle exit. In EQ (5), P_g is the limit gage pressure differential for the passenger compartment during cruise. The total tension stress resultant is then

$$N_x^+ = N_{x_B} + N_{x_P} \tag{6}$$

if x is ahead of the nozzle exit, and

$$N_x^+ = N_{x_B} + N_{x_P} + N_{x_A} \tag{7}$$

if x is behind it. Similarly, the total compressive stress resultant is

$$N_x^- = N_{x_B} + N_{x_A} - \begin{Bmatrix} 0, & \text{if not pressure stabilized} \\ N_{x_P}, & \text{if stabilized} \end{Bmatrix} \tag{8}$$

if x is ahead of the inlet entrance, and

$$N_x^- = N_{x_B} - \begin{Bmatrix} 0, & \text{if not pressure stabilized} \\ N_{x_P}, & \text{if stabilized} \end{Bmatrix} \tag{9}$$

if x is behind it. These relations are based on the premise that acceleration loads never decrease stress resultants, but pressure loads may relieve stress, if pressure stabilization is chosen as an option. The stress resultant in the hoop direction is

$$N_y = rP_g K_P \tag{10}$$

where K_p accounts for the fact that not all of the shell material (for example, the core material in sandwich designs) is available for resisting hoop stress.

The equivalent isotropic thicknesses of the shell are given by

$$\bar{t}_{S_C} = \frac{N_x^-}{F_{cy}} \tag{11}$$

$$\bar{t}_{S_T} = \frac{1}{F_{tu}} \max\left(N_x^+, N_y\right) \tag{12}$$

$$\bar{t}_{S_G} = K_{mg} t_{mg} \tag{13}$$

for designs limited by compressive yield strength (F_{cy}), ultimate tensile strength (F_{tu}), and minimum gage, respectively. In EQ (13), t_{mg} is a specified minimum material thickness and K_{mg} is a parameter relating $\bar{t}_{S_G}$ to t_{mg} which depends on the shell geometry.

A fourth thickness that must be considered is that for buckling critical designs, $\bar{t}_{S_B}$, which will now be developed. The nominal vehicles of this study have integrally stiffened shells stabilized by ring frames. In the buckling analysis of these structures, the shell is analyzed as a wide column and the frames are sized by the Shanley criteria.[7] Expressions are derived for the equivalent isotropic thickness of the shell required to preclude buckling, $\bar{t}_{S_B}$, and for the *smeared* equivalent isotropic thickness of the ring frames required to preclude general instability, $\bar{t}_F$. The analysis will be restricted to the case of cylindrical shells. The major assumptions are that the structural shell behaves as an Euler beam and that all structural materials behave elastically.

For the stiffened shell with frames concept, the common procedure of assuming the shell to be a wide column is adopted. If the frame spacing is defined as d and Young's

modulus of the shell material is defined as E, the buckling equation is then

$$\frac{N_x^-}{dE} = \varepsilon\left(\frac{\bar{t}_{S_B}}{d}\right)^2 \tag{14}$$

or, solving for $\bar{t}_{S_B}$

$$\bar{t}_{S_B} = \sqrt{\frac{N_x^- d}{E\varepsilon}} \tag{15}$$

Fuselage structural geometry concepts are presented in Table 1; values of the shell efficiency ε for the various structural concepts are given in Table 2. The structural shell geometries available are simply stiffened, Z-stiffened, and truss-core sandwich. We next size the frames to prevent general instability failure. The Shanley criterion is based on the premise that the frames act as elastic supports for the wide column; this criterion gives the smeared equivalent thickness of the frames as

$$\bar{t}_{F_B} = 2r^2\sqrt{\frac{\pi C_F N_x^-}{K_{F1} d^3 E_F}} \tag{16}$$

where C_F is Shanley's constant, K_{F1} is a frame geometry parameter, and E_F is Young's modulus for the frame material. (See Ref. 3 for a discussion of the applicability of this criterion and for a detailed derivation of the equations presented here.) If the structure is buckling critical, the total thickness is

$$\bar{t} = \bar{t}_{S_B} + \bar{t}_{F_B} \tag{17}$$

Minimizing $\bar{t}$ with respect to d results in

$$\bar{t} = \frac{4}{27^{1/4}}\left(\frac{\pi C_F}{K_{F1}\varepsilon^3 E_F E^3}\right)^{\frac{1}{8}}\left(\frac{2r^2\rho_F\left(N_x^-\right)^2}{\rho}\right)^{\frac{1}{4}} \tag{18}$$

$$\bar{t}_{S_B} = \frac{3}{4}\bar{t} \tag{19}$$

$$\bar{t}_{F_B} = \frac{1}{4}\bar{t} \tag{20}$$

$$d = \left(6r^2\frac{\rho_F}{\rho}\sqrt{\frac{\pi C_F \varepsilon E}{K_{F1} E_F}}\right)^{\frac{1}{2}} \tag{21}$$

where ρ_F is the density of the frame material and ρ is the density of the shell material, so that the shell is three times as heavy as the frames.

Frameless sandwich shell concepts may also be used. For these concepts, it is assumed that the elliptical shell buckles at the load determined by the maximum compressive stress resultant N_x^- on the cylinder. The buckling equation for these frameless sandwich shell concepts is

$$\frac{N_x^-}{rE} = \varepsilon\left(\frac{\bar{t}_{S_B}}{r}\right)^m \tag{22}$$

where m is the buckling equation exponent. Or, solving for $\bar{t}_{S_B}$

$$\bar{t}_{S_B} = r\left(\frac{N_x^-}{rE\varepsilon}\right)^{\frac{1}{m}} \tag{23}$$

This equation is based on small deflection theory, which seems reasonable for sandwich cylindrical shells, although it is known to be inaccurate for monocoque cylinders. Values of m and ε may be found, for example in Refs. 10 and 11 for many shell geometries. Table 2 gives values for sandwich structural concepts available in PDCYL, numbers 8 and 9, both of which are truss-core sandwich. The quantities N_x^-, r, and consequently $\bar{t}_{S_B}$, will vary with fuselage station dimension x.

At each fuselage station x, the shell must satisfy all failure criteria and meet all geometric constraints. Thus, the shell thickness is selected according to compression, tension, minimum gage, and buckling criteria, or

$$\bar{t}_S = \max\left(\bar{t}_{S_C}, \bar{t}_{S_T}, \bar{t}_{S_G}, \bar{t}_{S_B}\right) \tag{24}$$

If $\bar{t}_S = \bar{t}_{S_B}$, the structure is buckling critical and the equivalent isotropic thickness of the frames, $\bar{t}_F$, is computed from EQ (20). If $\bar{t}_S > \bar{t}_{S_B}$, the structure is not buckling critical at the optimum frame sizing and the frames are resized to make $\bar{t}_S = \bar{t}_{S_B}$. Specifically, a new frame spacing is computed from EQ (15) as

$$d = \frac{E\varepsilon\bar{t}_S^2}{N_x^-} \tag{25}$$

and this value is used in EQ (16) to determine $\bar{t}_F$.

The total thickness of the fuselage structure is then given by the summation of the smeared weights of the shell and the frames

$$\bar{t}_B = \bar{t}_S + \bar{t}_F \tag{26}$$

The shell gage thickness may be computed from $\bar{t}_g = \bar{t}_S / K_{mg}$. The *ideal* fuselage structural weight is obtained by summation over the vehicle length

$$W_I = 2\pi\sum\left(\rho\bar{t}_{S_i} + \rho_F\bar{t}_{F_i}\right)r_i\Delta x_i \tag{27}$$

where the quantities subscripted i depend on x.

Since the preceding analysis gives only the ideal weight, W_I, the *nonoptimum* weight, W_{NO} (including fasteners, cutouts, surface attachments, uniform gage penalties,

Table 1 Fuselage structural geometry concepts

KCON sets concept number	
2	Simply stiffened shell, frames, sized for minimum weight in buckling
3	Z-stiffened shell, frames, best buckling
4	Z-stiffened shell, frames, buckling-minimum gage compromise
5	Z-stiffened shell, frames, buckling-pressure compromise
6	Truss-core sandwich, frames, best buckling
8	Truss-core sandwich, no frames, best buckling
9	Truss-core sandwich, no frames, buckling-minimum gage-pressure compromise

Table 2 Fuselage structural geometry parameters

Structural concept (KCON)	m	ε	K_{mg}	K_p	K_{th}
2	2	0.656	2.463	2.463	0.0
3	2	0.911	2.475	2.475	0.0
4	2	0.760	2.039	1.835	0.0
5	2	0.760	2.628	1.576	0.0
6	2	0.605	4.310	3.965	0.459
8	1.667	0.4423	4.820	3.132	0.405
9	1.667	0.3615	3.413	3.413	0.320

manufacturing constraints, etc.) has yet to be determined. The method used will be explained in a later section.

Wing

Using the geometry and loads applied to the wing developed above, the structural dimensions and weight of the structural box may now be calculated. The wing structure is assumed to be a rectangular multi-web box beam with the webs running in the direction of the structural semispan. Reference 10 indicates that the critical instability mode for multi-web box beams is simultaneous buckling of the covers due to local instability and of the webs due to flexure induced crushing. This reference gives the solidity (ratio of volume of structural material to total wing box volume) of the least weight multi-web box beams as

$$\Sigma = \varepsilon\left(\frac{M}{Z_S t^2 E}\right)^e \tag{28}$$

where ε and e depend on the cover and web geometries (Table 3), M is the applied moment, t is the thickness, E is the elastic modulus, and Z_S is obtained from Ref. 10. The solidity is therefore

$$\Sigma = \frac{W'_{BEND}(y)}{\rho Z_S t} \tag{29}$$

where W'_{BEND} is the weight of bending material per unit span and ρ is the material density. W'_{BEND} is computed from EQS (28) and (29). The weight per unit span of the shear material is

$$W'_{SHEAR}(y) = \frac{\rho F_S}{\sigma_S} \tag{30}$$

where F_S is the applied shear load and σ_S is the allowable shear stress. The optimum web spacing is computed from[2]

$$d_W = t\left[\frac{(1-2e_C)}{(1-e_C)\sqrt{2\varepsilon_W}}\left(\frac{M}{Z_S t^2 E}\right)^{\frac{2e_C-3}{2e_C}} \varepsilon_C^{\frac{3}{2e_C}}\right]^{\frac{2e_C}{4e_C-3}} \tag{31}$$

where subscripts W and C refer to webs and covers, respectively. The equivalent isotropic thicknesses of the covers and webs are

Table 3 Wing structural coefficients and exponents

Covers	Webs	ε	e	ε	e_C	ε_W	K_{g_C}	K_{g_W}
Unstiffened	Truss	2.25	0.556	3.62	3	0.605	1.000	0.407
Unstiffened	Unflanged	2.21	0.556	3.62	3	0.656	1.000	0.505
Unstiffened	Z-stiffened	2.05	0.556	3.62	3	0.911	1.000	0.405
Truss	Truss	2.44	0.600	1.108	2	0.605	0.546	0.407
Truss	Unflanged	2.40	0.600	1.108	2	0.656	0.546	0.505
Truss	Z-stiffened	2.25	0.600	1.108	2	0.911	0.546	0.405

$$\bar{t}_C = d_W\left(\frac{M}{Z_S t E \varepsilon_C d_W}\right)^{\frac{1}{e_C}} \tag{32}$$

$$\bar{t}_W = t\sqrt{\left(\frac{M}{Z_S t^2 E}\right)^{\left(2-\frac{1}{e_C}\right)}\left(\frac{\varepsilon_C d_W}{t}\right)^{\frac{1}{e_C}}\left(\frac{2}{\varepsilon_W}\right)} \tag{33}$$

spectively, and the gage thicknesses are

$$t_{gC} = K_{gC}\bar{t}_C \tag{34}$$

$$t_{gW} = K_{gW}\bar{t}_W \tag{35}$$

Values of ε, e, ε_C, E_C, ε_W, K_{g_W}, and K_{g_C} are found in able 3 for various structural concepts.[10] If the wing structural emispan is divided into N equal length segments, the total *deal* weight of the wing box structure is

$$W_{BOX} = \frac{2b_S}{N}\sum_{i=1}^{N}\left(W'_{BEND_i} + W'_{SHEAR_i}\right) \tag{36}$$

The wing carrythrough structure consists of torsion material in addition to bending and shear material. The torsion material is required to resist the twist induced due to the sweep of the wing. The bending material is computed in a similar manner as that of the box except that only the longitudinal component of the bending moment contributes. Letting $t_0 = t(y = 0)$ and $M_0 = M(y = 0)$,

$$\Sigma_C = \varepsilon\left(\frac{M_0\cos(\Lambda_S)}{t_0^2 C_{SR} E}\right)^e \tag{37}$$

The weight of the bending material is then

$$W_{BEND_C} = \rho\Sigma_C C_{SR} t_0 w_C \tag{38}$$

where w_C is the width of the carrythrough structure. (When the wing-fuselage intersection occurs entirely within the cylindrical midsection, as is the case with all eight transport used for validation in the present study, $w_C = D$.) The quantities d_W, t_W, and t_C are computed in the same manner as for the box. The weight of the shear material is

$$W_{SHEAR_C} = \rho\frac{F_{S_0}}{\sigma_S} w_C \tag{39}$$

where $F_{S_0} = F_S(0)$.

The torque on the carrythrough structure is

$$T = M_0\sin(\Lambda_S) \tag{40}$$

and the weight of the torsion material is then

$$W_{TORSION_C} = \frac{\rho T(t_0 + C_{SR})w_C}{t_0 C_{SR}\sigma_S} \tag{41}$$

Finally, the *ideal* weight of the carrythrough structure is computed from a summation of the bending shear and torsion material, or

$$W_C = W_{BEND_C} + W_{SHEAR_C} + W_{TORSION_C} \tag{42}$$

As in the case of the fuselage structural weight, *non-optimum* weight must be added to the ideal weight to obtain the true wing structural weight. The method used will be discussed below.

REGRESSION ANALYSIS

Overview

Using fuselage and wing weight statements of eight subsonic transports, a relation between the calculated load-bearing structure weights obtained through PDCYL and the actual load-bearing structure weights, primary structure weights, and total weights is determined using statistical analysis techniques. A basic application which is first described is linear regression, wherein the estimated weights of the aircraft are related to the weights calculated by PDCYL with a straight line, $y = mx + b$, where y is the value of the estimated weight, m is the slope of the line, x is the value obtained through PDCYL, and b is the y-intercept. This line is termed a *regression* line, and is found by using the *method of least squares*, in which the sum of the squares of the residual

errors between actual data points and the corresponding points on the regression line is minimized. Effectively, a straight line is drawn through a set of ordered pairs of data (in this case eight weights obtained through PDCYL and the corresponding actual weights) so that the aggregate deviation of the actual weights above or below this line is minimized. The estimated weight is therefore dependent upon the independent PDCYL weight.

Of key importance is the degree of accuracy to which the prediction techniques are able to estimate actual aircraft weight. A measure of this accuracy, the correlation coefficient, denoted R, represents the reduction in residual error due to the regression technique. R is defined as

$$R = \sqrt{\frac{E_l - E_r}{E_r}} \tag{43}$$

where E_l and E_r refer to the residual errors associated with the regression before and after analysis is performed, respectively. A value of $R = 1$ denotes a perfect fit of the data with the regression line. Conversely, a value of $R = 0$ denotes no improvement in the data fit due to regression analysis.

There are two basic forms of equations which are implemented in this study. The first is of the form

$$y_{est} = mx_{calc} \tag{44}$$

The second general form is

$$y_{est} = mx^{a}_{calc} \tag{45}$$

Fuselage

The analysis above is used to develop a relationship between weight calculated by PDCYL and actual wing and fuselage weights. The data were obtained from detailed weight breakdowns of eight transport aircraft[12–16] and are shown in Table 4 for the fuselage. Because the theory used in the PDCYL analysis only predicts the load-carrying structure of the aircraft components, a correlation between the predicted weight and the actual load-carrying structural weight and primary weight, as well as the total weight of the fuselage, was made.

Structural weight consists of all load-carrying members including bulkheads and frames, minor frames, covering, covering stiffeners, and longerons. For the linear curve-fit, the resulting regression equation is

$$W_{actual} = 1.3503 W_{calc} \qquad R = 0.9946 \tag{46}$$

This shows that the *nonoptimum* factor for fuselage structure is 1.3503; in other words, the calculated weight must be increased by about 35 percent to get the actual structural weight. For the alternative power-intercept curve fitting analysis, the resulting load-carrying regression equation is

$$W_{actual} = 1.1304 W_{calc}^{1.0179} \qquad R = 0.9946 \tag{47}$$

To use either of these equations to estimate total fuselage weight, nonstructural weight items must be estimated independently and added to the structural weight.

Primary weight consists of all load-carrying members as well as any secondary structural items such as joints fasteners, keel beam, fail-safe straps, flooring, flooring structural supplies, and pressure web. It also includes the lavatory structure, galley support, partitions, shear ties, tie rods, structural firewall, torque boxes, and attachment fittings. The linear curve fit for this weight yields the following primary regression equation

$$W_{actual} = 1.8872 W_{calc} \qquad R = 0.9917 \tag{48}$$

The primary power-intercept regression equation is

$$W_{actual} = 1.6399 W_{calc}^{1.0141} \qquad R = 0.9917 \tag{49}$$

Table 4 Fuselage weight breakdowns for eight transport aircraft

	Weight, lb			
Aircraft	PDCYL	Load-carrying structure	Primary structure	Total structure
B-720	6545	9013	13336	19383
B-727	5888	8790	12424	17586
B-737	3428	5089	7435	11831
B-747	28039	39936	55207	72659
DC-8	9527	13312	18584	24886
MD-11	20915	25970	34999	54936
MD-83	7443	9410	11880	16432
L-1011	21608	28352	41804	52329

The total fuselage weight accounts for all members of the dy, including the structural weight and primary weight. It es not include passenger accommodations, such as seats, ratories, kitchens, stowage, and lighting; the electrical stem; flight and navigation systems; alighting gear; fuel and opulsion systems; hydraulic and pneumatic systems; the mmunication system; cargo accommodations; flight deck commodations; air conditioning equipment; the auxiliary wer system; and emergency systems. Linear regression sults in the following total fuselage weight equation

$$W_{actual} = 2.5686 W_{calc} \qquad R = 0.9944 \qquad (50)$$

This shows that the nonoptimum factor for the total selage weight is 2.5686; in other words, the fuselage ructure weight estimated by PDCYL must be increased by out 157 percent to get the actual total fuselage weight. This noptimum factor is used to compare fuselage structure eight estimates from PDCYL with total fuselage weight stimates from the Sanders and the Air Force equations used y ACSYNT.

The total fuselage weight power-intercept regression quation is

$$W_{actual} = 3.9089 W_{calc}^{0.9578} \qquad R = 0.9949 \qquad (51)$$

Plots of actual fuselage component weight versus DCYL-calculated weight, as well as the corresponding linear egressions, are shown in Figs. 3–5.

Wing

The same analysis was performed on the wing weight for the sample aircraft and is shown in Table 5. The wing box, or load-carrying structure, consists of spar caps, interspar coverings, spanwise stiffeners, spar webs, spar stiffeners, and interspar ribs. The wing box linear regression equation is

$$W_{actual} = 0.9843 W_{calc} \qquad R = 0.9898 \qquad (52)$$

so that the nonoptimum factor is 0.9843. Power-intercept regression results in

$$W_{actual} = 1.3342 W_{calc}^{0.9701} \qquad R = 0.9902 \qquad (53)$$

Wing primary structural weight includes all wing box items in addition to auxiliary spar caps and spar webs, joints and fasteners, landing gear support beam, leading and trailing edges, tips, structural firewall, bulkheads, jacket fittings, terminal fittings, and attachments. Linear regression results in

$$W_{actual} = 1.3442 W_{calc} \qquad R = 0.9958 \qquad (54)$$

Power-intercept regression yields

$$W_{actual} = 2.1926 W_{calc}^{0.9534} \qquad R = 0.9969 \qquad (55)$$

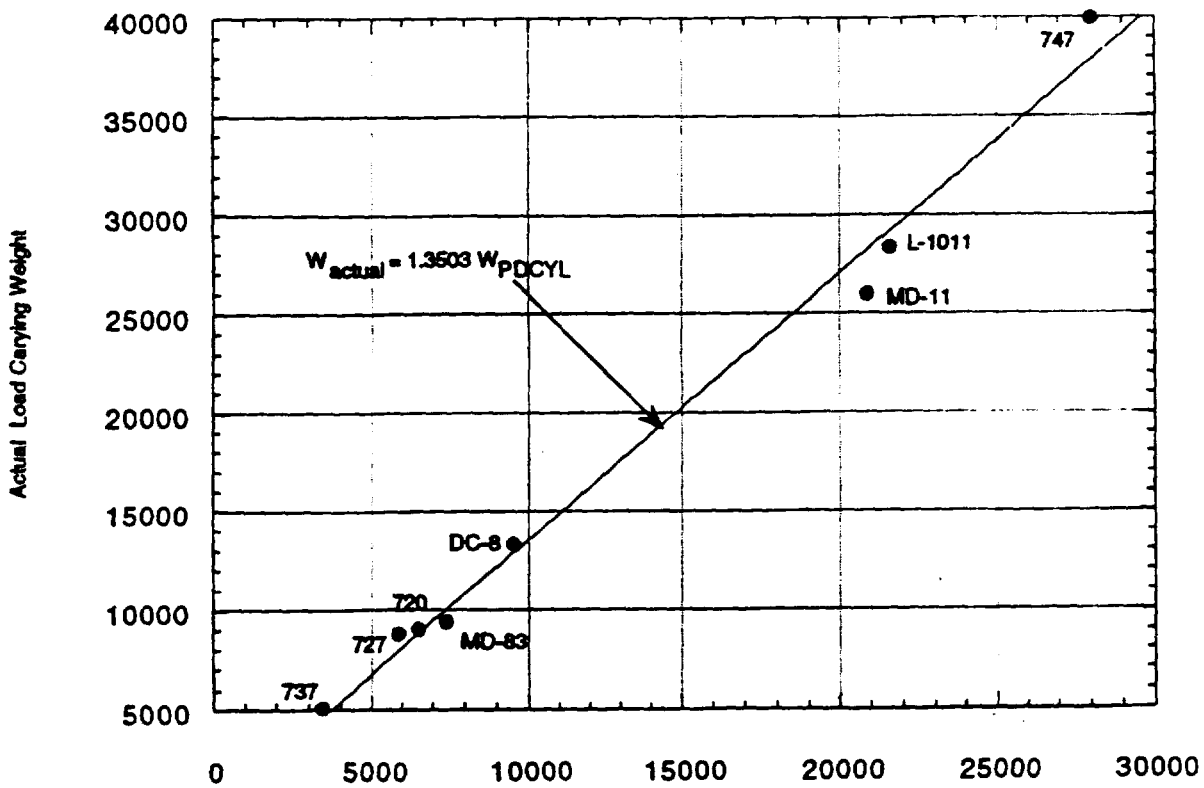

Fig. 3 Fuselage load-carrying structure and linear regression.

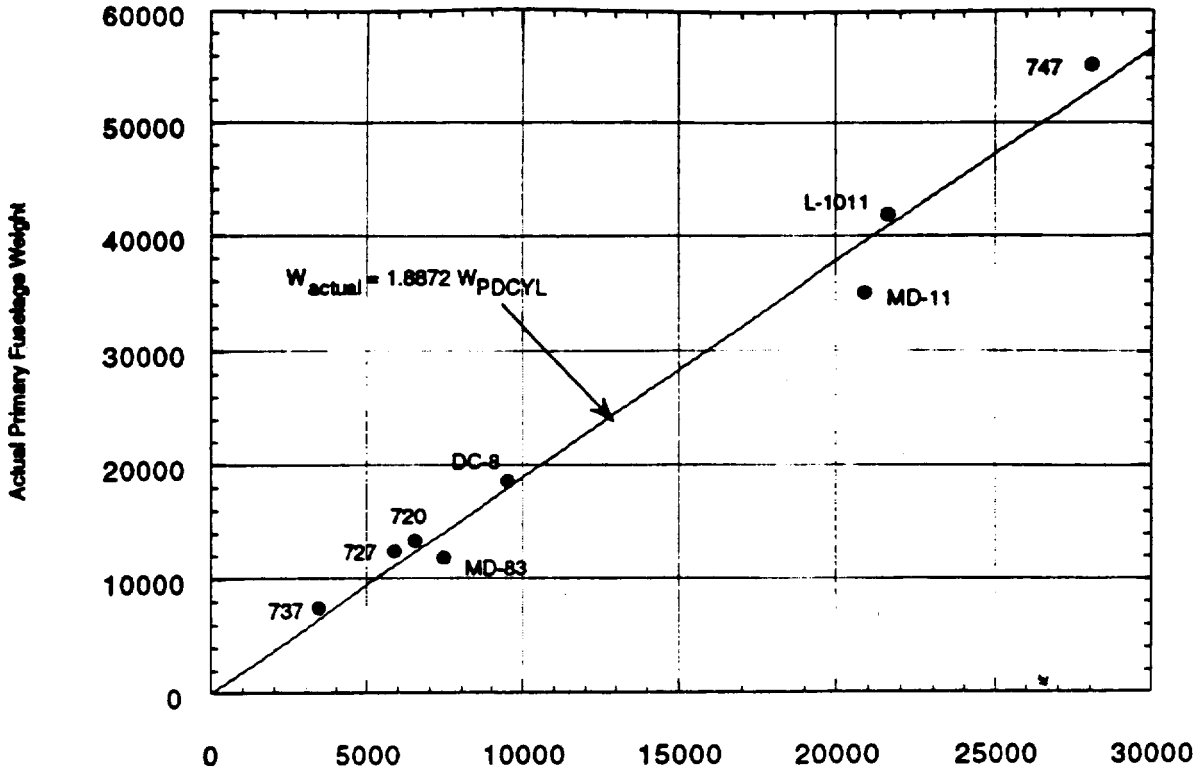

Fig. 4 Fuselage primary structure and linear regression.

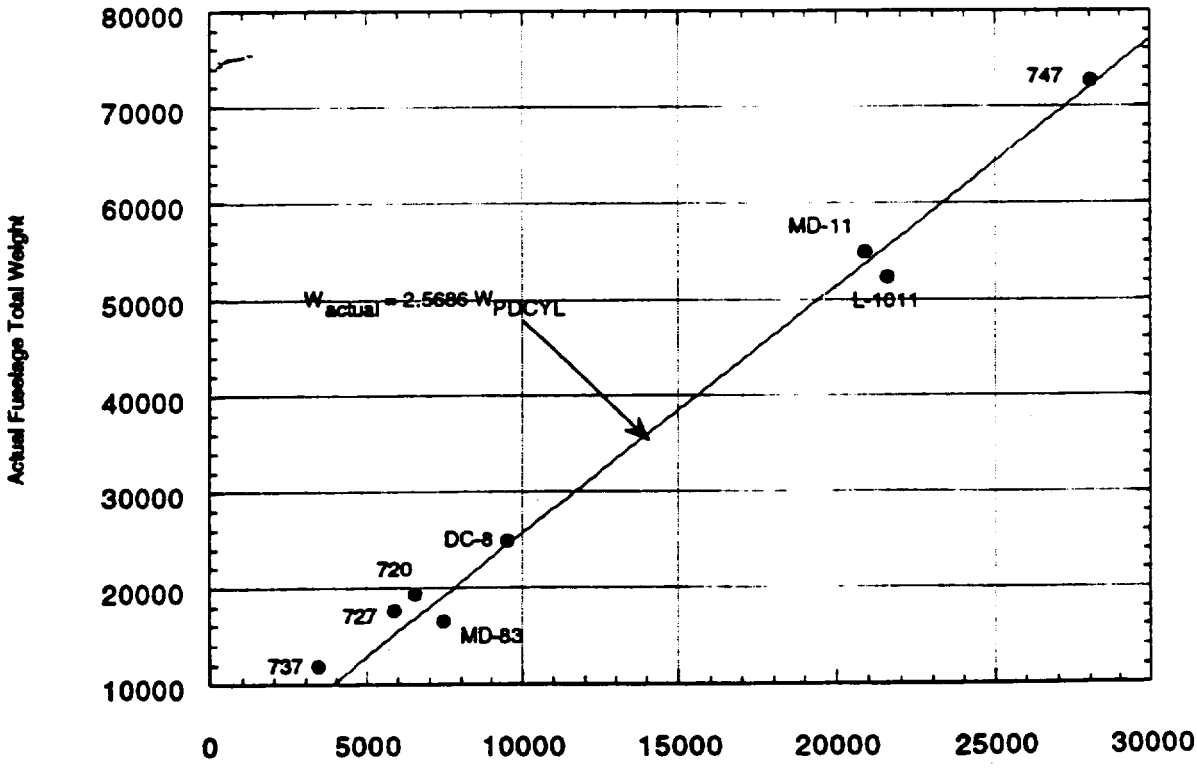

Fig. 5 Fuselage total structure and linear regression.

Table 5. Wing weight breakdowns for eight transport aircraft

	Weight, lb			
Aircraft	PDCYL	Load-carrying structure	Primary structure	Total structure
B-720	13962	11747	18914	23528
B-727	8688	8791	12388	17860
B-737	5717	5414	7671	10687
B-747	52950	50395	68761	88202
DC-8	22080	19130	27924	35330
MD-11	33617	35157	47614	62985
MD-83	6953	8720	11553	15839
L-1011	25034	28355	36101	46233

The total wing weight includes wing box and primary
ght items in addition to high-lift devices, control surfaces,
access items. It does not include the propulsion system,
system, and thrust reversers; the electrical system;
nting gear; hydraulic and pneumatic systems; anti-icing
ces; and emergency systems. The resulting total weight
ar regression equation is

$$W_{actual} = 1.7372 W_{calc} \qquad R = 0.9925 \qquad (56)$$

This shows that the nonoptimum factor for the total wing
ght is 1.7372; in other words, the wing box weight esti-
ted by PDCYL must be increased by about 74 percent to
the actual total wing weight. This nonoptimum factor is
d to compare wing box weight estimates from PDCYL with
al wing weight estimates from the Sanders and the Air
rce equations used by ACSYNT.

The power-intercept equation for total wing weight is

$$W_{actual} = 3.7464 W_{calc}^{0.9268} \qquad R = 0.9946 \qquad (57)$$

Plots of actual wing component weight versus PDCYL-
lculated weight, as well as the corresponding linear
gressions, are shown in Figs. 6–8.

Discussion

Both fuselage and wing weight linear and power regressions give excellent correlation with the respective weights of existing aircraft, as evidenced by the high values of the correlation coefficient, R. It should be noted that even though the power-based regressions give correlations equal to or better than the linear regressions their factors may vary distinctly from the linear cases. This is due to their powers not equaling unity.

Because estimates of non-load-bearing primary structure are generally not available at the conceptual design stage, and because nonprimary structure is probably not well estimated by a nonoptimum factor, EQS (48) and (54) are recommended for estimating the primary structural weights of the respective transport fuselage and wing structures (Figs. 4 and 7).

A comparison may be made between weight estimates from weight estimating relationships currently used by ACSYNT, PDCYL output, and actual aircraft component weights. Figure 9(a) shows a comparison between fuselage weight estimated from the Sanders equation, the Air Force equation, and PDCYL output with the actual fuselage weight of the 747-21P. Figure 9(b) shows a similar comparison for the wing weight.

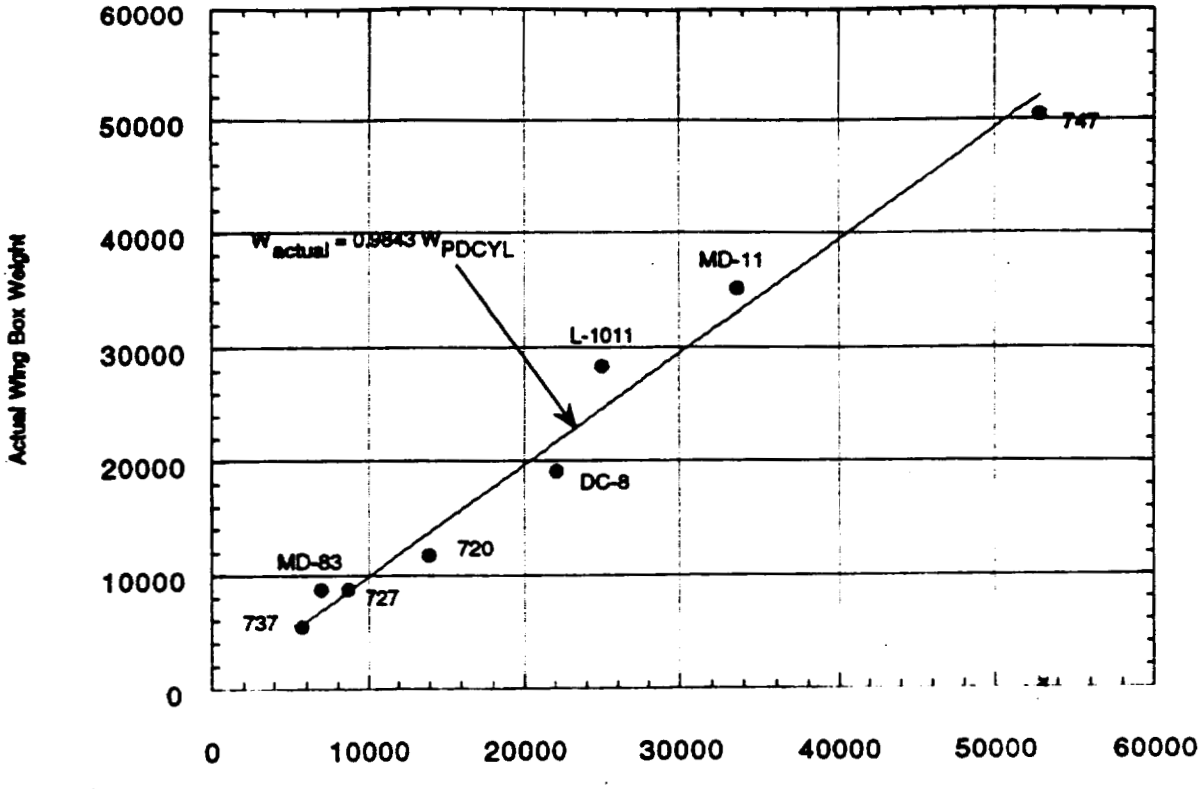

Fig. 6 Wing load-carrying structure and linear regression.

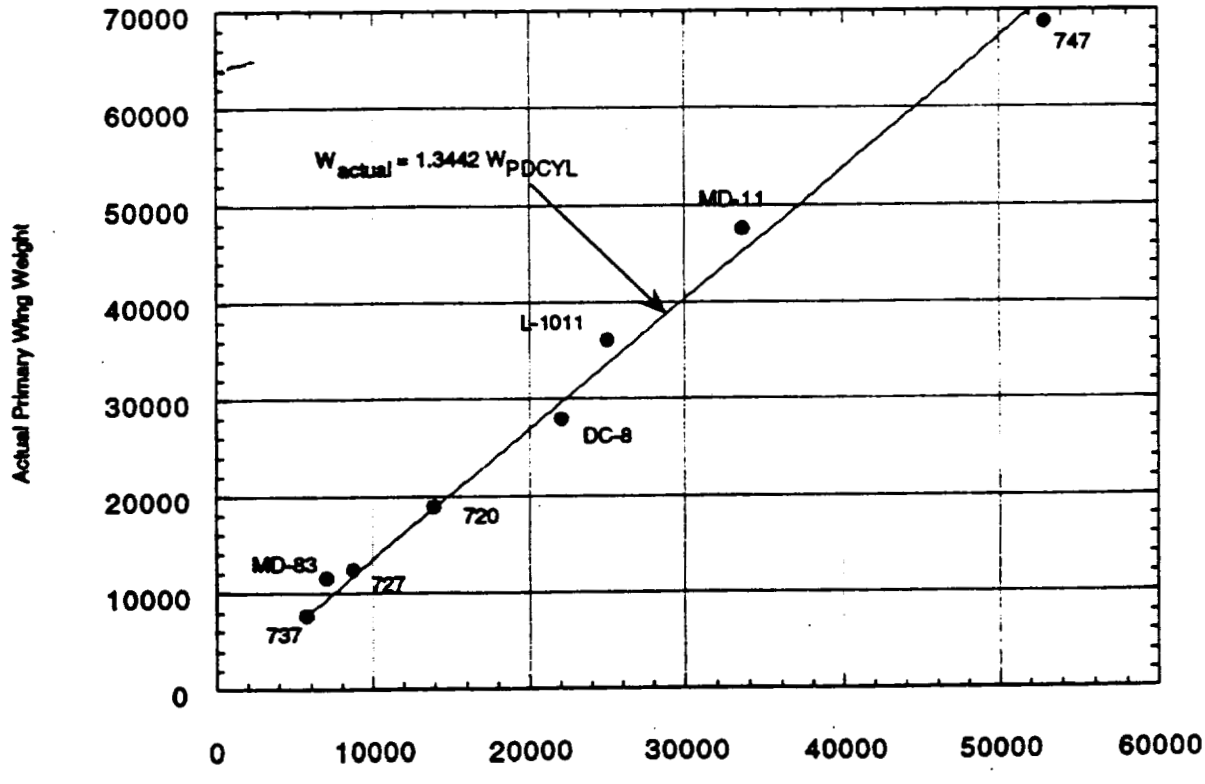

Fig. 7 Wing primary structure and linear regression.

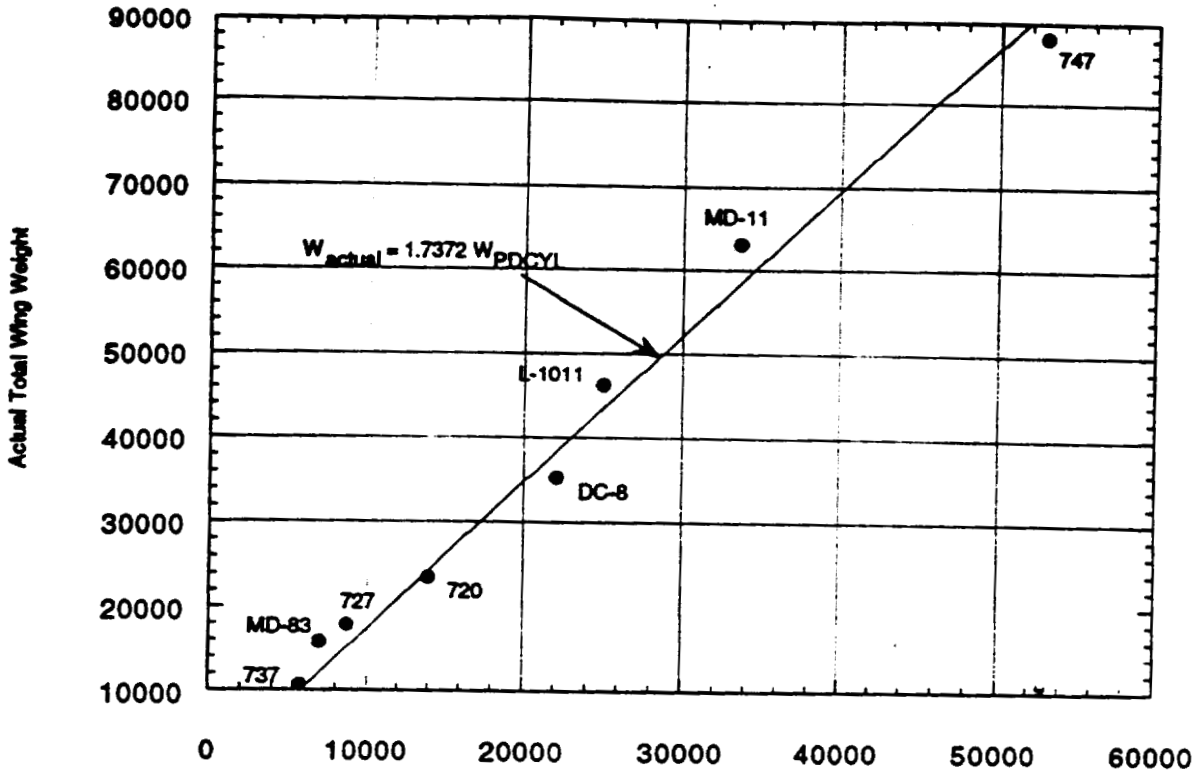

Fig. 8 Wing total structure and linear regression.

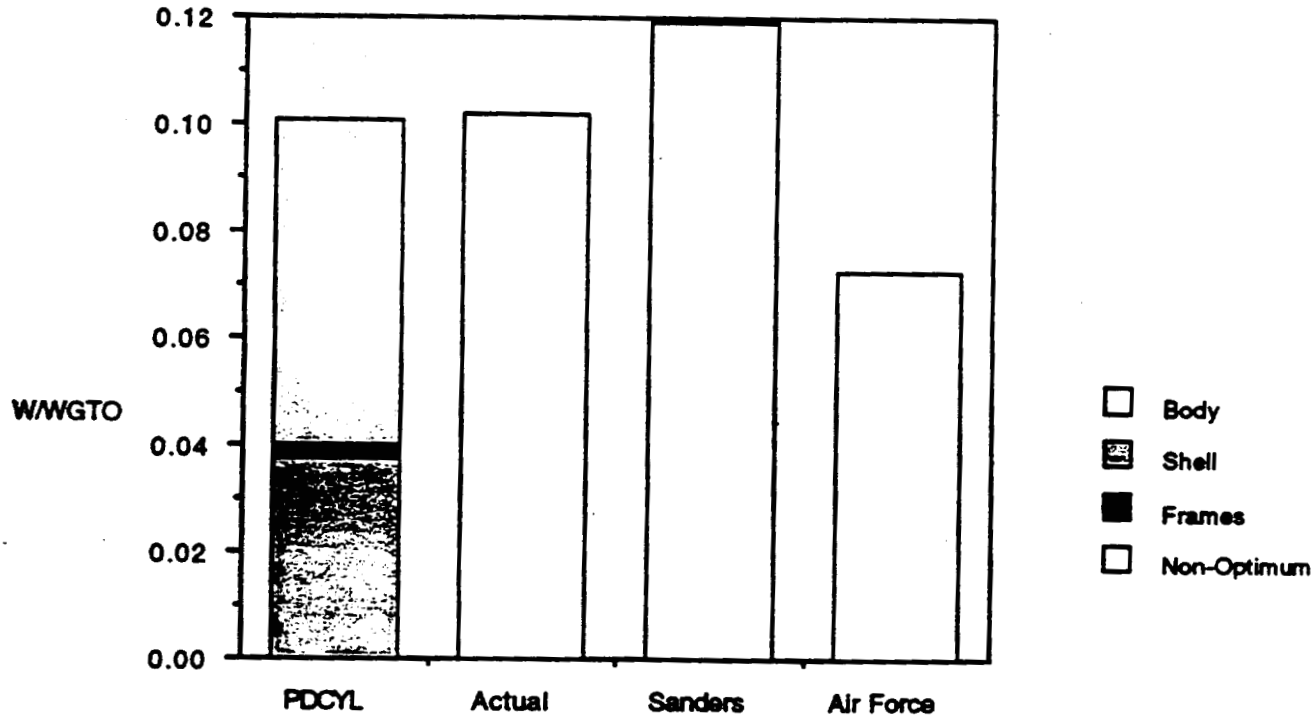

Fig. 9(a) Fuselage weight estimation comparison for 747-21P.

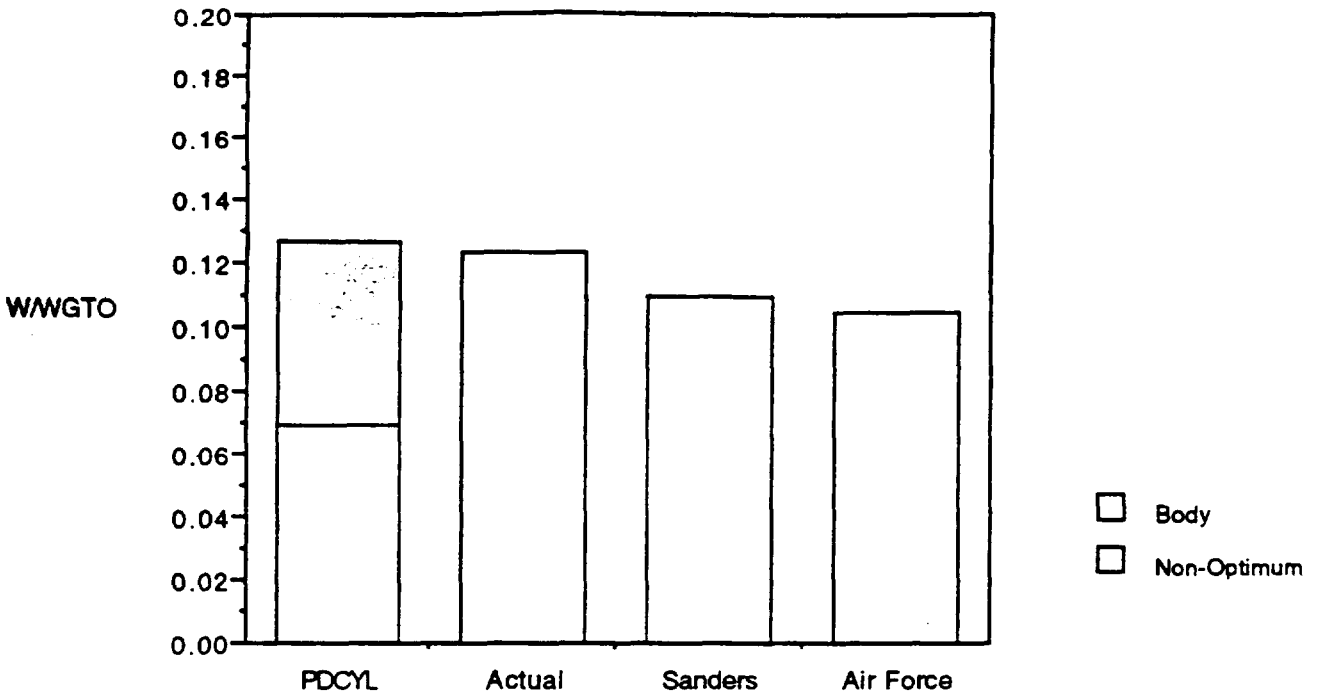

Fig. 9(b) Wing weight estimation comparison for 747-21P.

REFERENCES

[1]Ardema, M. D.: Body Weight of Hypersonic Aircraft: Part 1. NASA TM-101028, Oct. 1988.

[2]Ardema, M. D.; and Williams, L. J.: Transonic Transport Study – Structures and Aerodynamics, NASA TM X-62,157, May 1972.

[3]Ardema, M. D.: Structural Weight Analysis of Hypersonic Aircraft. NASA TN D-6692, Mar. 1972.

[4]Ardema, M. D.: Analysis of Bending Loads of Hypersonic Aircraft. NASA TM X-2092, 1970.

[5]Moore, M.; and Samuels, J.: ACSYNT Aircraft Synthesis Program – User's Manual. Systems Analysis Branch, NASA Ames Research Center, Sept. 1990.

[6]Ardema, Mark D.; Chambers, Mark C.; Patron, Anthony P.; Hahn, Andrew S.; Miura, Hirokazu; and Moore, Mark D.: Analytical Fuselage and Wing Weight Estimation of Transport Aircraft. NASA TM-110392, May 1996.

[7]Shanley, F. R.: Weight-Strength Analysis of Aircraft Structures. Second Edition, Dover, N.Y., 1960.

[8]Megson, T. H. G.: Aircraft Structures for Engineering Students. Second Edition, Halsted Press, 1990.

[9]McCormick, B. W.: Aerodynamics, Aeronautics, and Flight Mechanics. John Wiley & Sons, 1979.

[10]Crawford, R. F.; and Burns, A. B.: Strength, Efficiency, and Design Data for Beryllium Structures. ASD-TR-61-692, Feb. 1962.

[11]Crawford, R. F.; and Burns, A. B.: Minimum Weight Potentials for Stiffened Plates and Shells. AIAA J., vol. 1, no. 4, Apr. 1963, pp. 879–886.

[12]Niu, M. C.-Y.: Airframe Structural Design: Practical Design Information and Data on Aircraft Structures. Conmilit Press, 1991.

[13]York, P.; and Labell, R. W.: Aircraft Wing Weight Build-Up Methodology with Modification for Materials and Construction Techniques. NASA CR-166173, Sept. 1980.

[14]Thomas, R. B.; and Parsons, S. P.: Weight Data Base. The Boeing Company, Commercial Airplane Division, Weight Research Group, Doc. No. D6-23204 TN, 1968.

[15]McDonnell Douglas Aircraft Company, Detailed Weight Statement for MD-11 Transport Aircraft, June 1987.

[16]McDonnell Douglas Aircraft Company, Detailed Weight Statement for MD-80 Transport Aircraft, July 1991.

Appendix B

Designing Composite Transport Aircraft

by

L. Hornberger, M. Ardema, and F. Dickerson

DESIGNING COMPOSITE TRANSPORT AIRCRAFT

by
Mark Ardema, Frank Dickerson and Lee Hornberger
Mechanical Engineering Department
Santa Clara University

ADDING COMPOSITES TO PDCYL

Light weight materials such as fiber reinforced plastics (composites) and bonded honeycomb sandwiches have become more and more common in airplanes in the last two decades (1). Designers value the unique properties of these materials, particularly their high stiffness to weight ratios. They must, however, balance these assets against the additional cost of these materials and their manufacture. To aid designers with this analysis, a composites subroutine has been added to the PDCYL structures weight calculation code. This subroutine sizes the thickness of a particular composite necessary to withstand the required aircraft loads, and provides this information to PDCYL which calculates the resultant weight of the aircraft.

TYPICAL AIRCRAFT COMPOSITES

The selection and use of composites on transport aircraft is an evolving process. A variety of composites have been tested in both military and commercial aircraft in the last 25 years (1). These composites typically consist of a strong, stiff fiber such as glass, graphite or kevlar, and a protective, adhering, inexpensive plastic matrix such as polyester or epoxy.

Glass fibers embedded in a polyester matrix have been the dominate composite for military and civil aircraft in the past. Currently, the aircraft industry prefers the stiffer and higher temperature composites made from carbon fiber in an epoxy matrix. However, the grade of carbon fiber and epoxy seems to change from year to year and from airplane manufacturer to airplane manufacturer. The current favored carbon fibers are AS4 (Hercules/Hexcel), IM6 and IM7 (Hercules/Hexcel) . The AS4 is an economical, high-strength carbon fiber and the IM6 &7 are high-modulus expensive fibers. These three carbon fibers have been used on military

aircraft and in research, but are not on commercial vehicles. The T-800 fiber (a Toray equivalent to IM7) has recently been used in some commercial applications (1-6).

Epoxies, particularly the 350°F curing systems, are the least expensive high temperature options for matrix materials. Several epoxy systems have been developed and tested for use with specific fibers. There is a current trend to use rubber modified epoxies such as 8552 and 3900 to increase the toughness of the composite system and its resistance to impact. Fiber-resin combinations currently in use by airplane designers and researchers are:

AS4/938 (ICI Fiberite) -Boeing Advanced Composites Program Door Panel(2)
AS4/8552 (Hexcel/Hercules), -Boeing Adv. Comp Fuselage (6-7)
AS4/8551 (Hexcel/Hercules) (6)
AS4/3501-6 (Hercules) -McDonnell Douglas Adv. Technology Composite Wing program (8)
AS4/3502 (Hercules) Military Aircraft (6)

COMPOSITE STRUCTURAL ANALYSIS

Composite materials were originally added to the options in the PDCYL program in 1995. This was done by simulating these materials by homogeneous structures with uniform mechanical properties (strength and modulus of elasticity) in every direction. This approach limits the code to evaluation of only the simplest and weakest type of composites called random mat[1]. Random mat composites are made by stacking the reinforcing fiber in all direction throughout the thickness of the material. In this type of composite the elastic properties and strength of the layup are roughly the same in every direction but the fiber density and reinforcement is low in any specific direction.

Random mat composites are not favored by aircraft designers because of their low strength to weight ratios. The preferred type of composite for these applications are ones in which the properties of the material are customized to meet the specific directions and magnitudes of the structural loads. This yields the minimum weight composite for the job. To accomplish this, composite designers specify a layup pattern for a composite laminate relative to a major axis of loading.

---

[1] See Appendix A for definition of composite terms

A typical composite laminate is made of a stack of 4-16 plys. A ply is a single layer of parallel reinforcing fibers embedded in a partially cured matrix of plastic. The location of each ply in the stack is defined relative to the angle its fibers makes with a major axis, such as the x-axis. For instance. a 0/90/90/45/0 layup is one in which the fibers of the outer and inner layers are parallel to the x-axis, the next two plies have fibers perpendicular to this axis and the fibers of the third layer are at an angle 45° clockwise to the x axis. This type of composite would have reinforcing fibers to sustain tensile and compressive loads in the x and y directions but would be weakest in the 45° direction. Composites walls for structural parts such as aircraft are often made from stacks of these laminates.

Analysis of a multilayer stack is more complex than that of homogeneous materials such as aluminum or random mat and requires the use of a macromechanics approach to determine elastic properties and strength. The macromechanics approach used in the COMPOS part of the PDCYL code is that presented in most textbooks on composite design (9-11) . In this approach the stiffness of a particular laminate is calculated by summing the contributions of each layer (ply) in the stack to the stiffness of the laminate in a particular direction. The composite stiffness in each major direction is then used to calculate the net strain of the composite in that direction due to the applied loads. From the net strain, the strain on each layer (ply) parallel and transverse to its fiber is derived. The resulting strains are then compared to the failure strains of the ply material and from this the potential for the failure of the stack is determined. The details of implementing this approach in PDCYL are described in the following section describing the COMPOS (composites) code addition.

COMPOS CODE

COMPOS is a section of code which has been added to PDCYL program to calculate the minimum laminate thickness required to withstand the forces imposed at each section of the airplane.

Assumptions within COMPOS

•The laminate is symmetric and orthotropic. (This type of layup is commonly used in aircraft design to minimize warpage of the layup).

• Every ply in the stack is composed of the same resin- fiber material.

• The stack is a minimum of 3 plys. (A ply is usually .003-.007 inches thick depending on the material.)

• The modulus of the material is the same in compression and tension. (if the compression modulus is different than its tensile modulus, the smaller of the two values is selected for all calculations.)
• Failure of the composite laminate occurs when any single ply fails.
• Failure of a ply occurs when it reaches the maximum strain transverse or parallel to the fiber direction in tension, compression or shear (11) Maximum strain theory is invoked in this analysis because it is currently believed to be the most predictive failure theory for composites (3,4,8) .
•The minimum gage thickness for the composite material is assumed to be the thickness of the initial laminate (a stack of plies).
•All loads are applied in the plane of the ply. This means that there are no z direction loads in tension, compression or shear.
• The buckling equations used in PDCYL to analyze the frames and stringers made from homogeneous materials apply to these heterogeneous materials. For buckling analysis the modulus of the laminate in the direction of load is used. This is a very course assumption and may*be somewhat optimistic for quasi isotropic composites manufactured with adhesive joints but seems highly unlikely for symmetric orthotropic laminates with heterogeneous properties. However, buckling analysis of complex composites structures is still in the developmental stage.(12)*

Calculation Procedure

•Calculations for Compressive and Tensile Loads

Once the maximum tensile and/or compressive loads per unit width (Nx and Ny) at any given aircraft section are determined in the PDCYL code, they are transferred to the COMPOS subroutine. The effect of these normalized forces on the composite laminate strain is calculated using the following relationship for an orthotropic symmetric laminate (9) :

$$[N] = [A] \times [\varepsilon^0] \qquad (1)$$

Where:

[N] = Matrix of forces on the composite section (Nx, Ny and Nxy)
[A] = Stiffness matrix of the composite
$[\varepsilon^0]$ = strain matrix of the composite (ex, ey, exy)

The components of the stiffness matrix [A] are determined in the code through the following relationship (9):

$$A_{ij} = \Sigma^{n}_{\kappa=1} (QB_{ij})_k (h_k) \qquad (2)$$

Where:

QB_{ij} = component of each ply's stiffness in the i and j's directions
h = thickness of k ply
k= ply number in the laminate

The stiffness contributions, QB values, of each ply are determined from the initial ply properties, E1, E2, ν_{12} and the ply angles, θ, specified by the user in the input file for a particular laminate construction. (Here, the "1" direction is taken parallel to the fiber and the "2" direction transverse to the fiber).

Once the average laminate strain is determined from equation (1), this strain is then transferred to each ply and transformed into strain parallel and transverse to each fiber as well as shear strain. These strains are then divided by the mating failure strains for the material (supplied by the user in the input file) to determine the R value of the layup.

$R_{ij} = alle_{ij} / e_{ij}$

Where:
$alle_{ij}$=allowable components of strain in principle ply direction
e_{ij} = components of strain in principle ply directions

If the R value for all plys in all the principle directions is more than 1, the laminate thickness is adequate to support the load and is left unaltered. If R is less than one on any ply in any of the principle directions, the thickness of the laminate is increased by giving it the value of it initial thickness divided by R.

Calculations for Buckling
PDCYL currently determines critical buckling loads from the modulus of elasticity of the material. COMPOS calculates the modulus of the laminate in the direction parallel to the buckling force and passes this value back to PDCYL. As mentioned in the assumptions portion of this report, the buckling calculation of PDCYL may not be valid for composites as they were developed for isotropic materials. *Little research has been done on composites in buckling so the authors advise caution in interpreting this result particularly with non-isotropic layups.*

NON-OPTIMUM FACTORS

Unfortunately, few all composite planes have been built so it is difficult to find planes to use as checks for the composite section of the code (8). The all composite planes listed in the literature (8) are:

- Windecker Eagle in 1967 which was glass fiber reinforced
- Learfan in 1981 which used glass, carbon and kevlar fibers
- Piaggio Avanti in 1986 with carbon fiber parts
- Beech Starship in 1986 with carbon fiber
- Grob GF-200- all composite
- Slingsby T-3A Firefly -all composite

A literature search and personal interviews failed to turn up much information directly useful in determining non-optimum factors. (These factors are used to multiply the results of theoretical calculations to get weights of practical structures.)

One reference was found which had this type of data (12). In this reference, a theoretical analysis gave 8640 pounds as the weight of a composite wing box whereas the actual wing was estimated to weigh 11,284 pounds giving a non-optimum factor of 1.306. Using the non-optimum factors for aluminum structures (13) this number can be used to estimate non optimum factors for carbon fiber-epoxy structures. If it is assumed that the non-optimum factors for the fuselage primary structure increase in the same proportion as wing structure relative to aluminum, and that the increments for secondary structure and non-structural are the same for graphite-epoxy composites and aluminum, then the following non-optimum factors for the composite result:

	Primary Structure	*Primary &Secondary Structure*	*Total Assembly*
Fuselage	1.792	2.329	3.010
Wing	1.306	1.666	2.059

There are many composite components in commercial and military structure as well as some from research on advanced composites. It may be possible to compare these components to predictions of the code.

REFERENCES

1. Vosten, L. F., "Composite Chronicles: Past Performance and Future Prospects," Fourth NASA/DoD Advanced Composites Technology Conference, 1993, Salt Lake City, Utah, vol 1. p 1

2. Russell, S., Vastava, R., Ley, R., Polland, D and Mabson, G., "Design Cost Modeling of Fuselage Door Cutout Structure," Fifth NASA /DoD Advanced Composites Technology Conference August 22-25 1994. NASA Conference Publication 3294 Volume I, Part I. p 127.

3. Personal communication from Professor. Steve Swanson, Univ of Utah, Mechanical Engineering Department

4. Personal communication from Professor Mark Tuttle, Univ of Washington, Mechanical Engineering Department

5. Personal communication from George Lallas of Hexcel/Hercules

6. Personal communication from Jim Stearns of NASA Langley

7. Scholz, D., et al, "Material and Processing Development for Composite Fuselage Sandwich Structure," Fifth NASA /DoD Advanced Composites Technology Conference August 22-25 1994. NASA Conference Publication 3294 Volume I, Part I. p 257.

8. Hawley, A.V., "Preliminary Design of a Transport Aircraft Composite Wing, " Fifth NASA /DoD Advanced Composites Technology Conference August 22-25 1994, proceedings of which are contained in NASA Conference Publication 3294 Volume I, Part I,p. 736

9. Jones, R., *Mechanics of Composite Materials,* McGraw-Hill, New York, 1975.

10. Tsai, S., *Composite Design*, 4th edition, THINK COMPOSITES, Dayton, 1988.

11. Agarwal, B., and Broutman, L., *Analysis and Performance of Fiber Composites*, 2nd ed., John Wiley and Sons, New York. 1990.

12. Swanson, G., Wishart, R and Eastland, C, "Compression Test Results for Stiffened Composite Fuselage Structure," Fourth NASA /DoD Advanced Composites Technology Conference June 7-11 1993, Salt Lake City, Utah NASA Conference Publication 3229 Volume I, Part I, p125.

13. Ardema, M.D. et al., "Analytical Fuselage and Wing Weight Estimation of Transport aircraft, NASA TM 110392, May 1996.

APPENDIX 1
COMPOSITES TERMINOLOGY

Random Mat- equal fibers in every direction
Balanced- equal fibers in orthotropic directions yield a composite with identical properties in 2 principal directions.
Symmetric-A symmetric laminate is one in which for each ply above the center of the stack there is and identical one at an equal distance below the center. For instance, a 0/-45/90/90/-45/0 is a symmetric layup but a 0/-45/90/ 0/-45/90 is not.
Quasi-Isotropic- Layups which are designed to have only two independent elastic constants, the modulus of elasticity and Poisson's ratio. These materials have the same values in every inplane direction. To meet this criteria fiber (ply) layups must have the following conditions:

- Total number of plies must be 3 or more
- Individual plies must have identical stiffness [Q] matrices and thickness
- Layers must be oriented at "equal" angles (if total number of layers is n, than each layer is pi/n relative to the next). If the laminate is constructed from several groups of laminates,. the condition must be satisfied for each laminate group

Typical laminates which satisfy these rules : [0/60/-60], [0/45/-45/90]

Appendix C

Weights of ASA 2150 With Aluminum and Graphite/Epoxy Fuselage

ALUMINUM

```
    Calling Module #   1
    Calling Module #   2
      TAKEOFF


  WGTO = 0.1521810E+06  WFTO1 = 0.3242445E+04  WFTO2 = 0.0000000E+00   WFTO = 0.3242445E+04      W = 0.1489386E+06
  HNTO = 0.1500000E+04    CLS = 0.1769708E+01     VS = 0.1337697E+03    V2 = 0.2259222E+03   SMN2 = 0.2034092E+00
   CL2 = 0.1758139E+01    TN2 = 0.0000000E+00   SFC2 = 0.1000000E+01   TN0 = 0.0000000E+00   SFC0 = 0.1000000E+01
 TNAVE = 0.0000000E+00 SFCAVE = 0.1000000E+01   FLTO =-0.1450002E+05



      LANDING


  WGTO = 0.1521810E+06 WFUSED = 0.6402882E+05  WFRES = 0.1176211E+05  WFTOT = 0.6430918E+05  WFUEL = 0.6430918E+05
   WPL = 0.3150000E+05      W = 0.8815213E+05  WLAND = 0.1246486E+06 XGRLAN = 0.1692168E+04 FLLAND = 0.5155803E+04
 WGCALC = 0.1524791E+06

    Calling Module #   6
 FROM geometry: body diameter    =   12.58000
                BODY VOLUME      =     9348.345
                BODY LENGTH      =     117.8300
                TAPER RATIO      =    0.2500000
                ASPECT RATIO     =     7.946000
                RATIO 1/4 CHORD  =    0.4040000
                WING SWEEP       =     23.72453
                HOR. TAIL / CL   =    0.9800000
                NOSE VOLUME      =     1811.579
                TAIL VOLUME      =     5780.107
                CL1A             =     24.74486
                CL1B             =     38.87792
                T/C AT ROOT      =    0.1460000
                T/C AT TIP       =    0.1100000
                ENTEMP           =     2.000000
                ENWINGTEMP       =     2.000000
                CLRW1            =    0.2500000
                CLRW2            =    0.0000000E+00
                CLRW3            =    0.0000000E+00
                CLRP1            =    0.0000000E+00
                CLRP2            =    0.0000000E+00
 FROM weights.acs SLFMTEMP        =     2.500000
                  FACSTEMP        =     1.500000
                  WFPTEMP         =   4.3013584E-02
                  WINGLTEMP       =     104.9524
                  UWWGTEMP        =     7.110270
                  ARTTEMP         =    0.1389904
```

ASA 2150 Aluminum

```
                UWTTEMP          =     14.79906
                WWING            =     10309.89
                KWING            =            6
                WGTO             =     152181.0
FROM stblcon.acs CLRG1TEMP   =   0.0000000E+00
                CLRG2TEMP    =   0.0000000E+00
                WFGR1TEMP    =   0.0000000E+00
                WFGR2TEMP    =   0.0000000E+00
From namelist   ICYL         =             1
                WTFF         =   0.2792000
                ISCHRENK     =             1
                ICOMND       =             1
                CLRG1        =   0.1060000
                CLRG2        =   0.0000000E+00
                WFGR1        =   1.2370000E-02
                WFGR2        =   2.8860001E-02
                IGEAR        =             2
                CWMAN        =    1.000000
                ITAIL        =             1
                ISTAMA       =             2
                TMGW         =   2.0000000E-02
                EC           =    2.360000
                KGC          =   0.3680000
                KGW          =   0.5050000
                WGNO         =    1.737200
                CS1          =   0.1500000
                CS2          =   0.3500000
                EFFW         =   0.6560000
                EFFC         =    1.030000
                ESW          =   1.0800000E+07
                FCSW         =    63500.00
                DSW          =   0.1010000
                TRATWR       =   0.1460000
                TRATWT       =   0.1100000
                XCLWNGR      =   0.3764853
                NWING        =           40
                FTST         =    58500.00        58500.00        58500.00
  58500.00      0.0000000E+00  0.0000000E+00  0.0000000E+00  0.0000000E+00
 0.0000000E+00  0.0000000E+00  0.0000000E+00  0.0000000E+00
                FTSB         =    58500.00        58500.00        58500.00
  58500.00      0.0000000E+00  0.0000000E+00  0.0000000E+00  0.0000000E+00
 0.0000000E+00  0.0000000E+00  0.0000000E+00  0.0000000E+00
                FCST         =    54000.00        54000.00        54000.00
  54000.00      0.0000000E+00  0.0000000E+00  0.0000000E+00  0.0000000E+00
 0.0000000E+00  0.0000000E+00  0.0000000E+00  0.0000000E+00
                FCSB         =    54000.00        54000.00        54000.00
  54000.00      0.0000000E+00  0.0000000E+00  0.0000000E+00  0.0000000E+00
 0.0000000E+00  0.0000000E+00  0.0000000E+00  0.0000000E+00
```

```
                EST         =   1.0700000E+07  1.0700000E+07  1.0700000E+07
1.0700000E+07   0.0000000E+00   0.0000000E+00  0.0000000E+00  0.0000000E+00
0.0000000E+00   0.0000000E+00   0.0000000E+00  0.0000000E+00
                ESB         =   1.0700000E+07  1.0700000E+07  1.0700000E+07
1.0700000E+07   0.0000000E+00   0.0000000E+00  0.0000000E+00  0.0000000E+00
0.0000000E+00   0.0000000E+00   0.0000000E+00  0.0000000E+00
                EFT         =   1.0700000E+07  1.0700000E+07  1.0700000E+07
1.0700000E+07   0.0000000E+00   0.0000000E+00  0.0000000E+00  0.0000000E+00
0.0000000E+00   0.0000000E+00   0.0000000E+00  0.0000000E+00
                EFB         =   1.0700000E+07  1.0700000E+07  1.0700000E+07
1.0700000E+07   0.0000000E+00   0.0000000E+00  0.0000000E+00  0.0000000E+00
0.0000000E+00   0.0000000E+00   0.0000000E+00  0.0000000E+00
                DST         =   0.1010000      0.1010000      0.1010000
0.1010000       0.0000000E+00   0.0000000E+00  0.0000000E+00  0.0000000E+00
0.0000000E+00   0.0000000E+00   0.0000000E+00  0.0000000E+00
                DSB         =   0.1010000      0.1010000      0.1010000
0.1010000       0.0000000E+00   0.0000000E+00  0.0000000E+00  0.0000000E+00
0.0000000E+00   0.0000000E+00   0.0000000E+00  0.0000000E+00
                DFT         =   0.1010000      0.1010000      0.1010000
0.1010000       0.0000000E+00   0.0000000E+00  0.0000000E+00  0.0000000E+00
0.0000000E+00   0.0000000E+00   0.0000000E+00  0.0000000E+00
                DFB         =   0.1010000      0.1010000      0.1010000
0.1010000       0.0000000E+00   0.0000000E+00  0.0000000E+00  0.0000000E+00
0.0000000E+00   0.0000000E+00   0.0000000E+00  0.0000000E+00
                PS          =    1.000000
                CF          =   6.2500003E-05
                PGT         =    11.25000       11.25000       11.25000
 11.25000        11.25000        11.25000       11.25000       11.25000
 11.25000        11.25000        11.25000       11.25000
                PGB         =    11.25000       11.25000       11.25000
 11.25000        11.25000        11.25000       11.25000       11.25000
 11.25000        11.25000        11.25000       11.25000
                TMGT        =   3.5999998E-02  3.5999998E-02  3.5999998E-02
3.5999998E-02   0.0000000E+00   0.0000000E+00  0.0000000E+00  0.0000000E+00
0.0000000E+00   0.0000000E+00   0.0000000E+00  0.0000000E+00
                TMGB        =   3.5999998E-02  3.5999998E-02  3.5999998E-02
3.5999998E-02   0.0000000E+00   0.0000000E+00  0.0000000E+00  0.0000000E+00
0.0000000E+00   0.0000000E+00   0.0000000E+00  0.0000000E+00
                CLAQR       =   1.0000000E-03
                CKF         =    5.240000
                WCW         =    2.568600
                WCA         =   0.0000000E+00
                AXAC        =   0.0000000E+00
                IFUEL       =              2
                WMIS        =   0.0000000E+00
                WSUR        =   0.0000000E+00
                KCONT       =              4              4              4              4
        4               4               4              4              4              4
```

```
4          4
      KCONB     =          4          4          4          4
4          4          4          4          4          4
4          4
      CLBR1     =   1.100000
      ILOAD     =          3
      CMAN      =   1.000000
      CLAN      =  0.7210000
      CBUM      =   1.000000
      WFLAND    =  0.9000000
      WFBUMP    =  1.0000000E-03
      VSINK     =   10.00000
      STROKE    =   1.167000
      GFRL      =  1.0000000E-03
      SLFMB     =   1.200000
      CLRGW1    =  0.2090000
      CLRGW2    =  0.0000000E+00
```

SPAN	BS	ROOTC	TIPC	TAPER	TRATWR	TRATWT	GAML	GAMT	GAMS	VWING	WFUEL	DENW
FT	FT	FT	FT				DEG.	DEG.	DEG.	FT3	LBS	LB/FT3
107.3392	50.764	19.8116	5.4034	0.250	0.146	0.110	23.72453	7.82576	20.000	1269.270	42488.93	41.598

WING STATION FT	CHORD FT	LENGTH FT	LENGTH PRIME FT	BEND MOM FT-LBS	WEB SPACE IN	COVER THICK IN	WEB THICK IN	CGAGE THICK IN	WGAGE THICK IN	UNITWT COVERS LB/FT2	UNITWT WEBS LB/FT2	NJW
50.764	5.4034	2.4504	2.4504	130.	0.1830	0.0543	0.03960	0.0200	0.02000	0.7904	0.5760	3
49.495	5.7636	2.6341	2.6341	1713.	0.3699	0.0543	0.03960	0.0200	0.02000	0.7904	0.5760	3
48.226	6.1238	2.8179	2.8179	5798.	0.5195	0.0543	0.03960	0.0200	0.02000	0.7904	0.5760	3
46.957	6.4840	3.0017	3.0017	12923.	0.6522	0.0543	0.03960	0.0200	0.02000	0.7904	0.5760	3
45.688	6.8442	3.1855	3.1855	23489.	0.7751	0.0543	0.03960	0.0200	0.02000	0.7904	0.5760	3
44.419	7.2044	3.3692	3.3692	37831.	0.8915	0.0543	0.03960	0.0200	0.02000	0.7904	0.5760	3
43.150	7.5646	3.5530	3.5530	56236.	1.0032	0.0543	0.03960	0.0200	0.02000	0.7904	0.5760	3
41.881	7.9249	3.7368	3.7368	78955.	1.1114	0.0543	0.03960	0.0200	0.02000	0.7904	0.5760	3
40.611	8.2851	3.9206	3.9206	106209.	1.2169	0.0543	0.03960	0.0200	0.02000	0.7904	0.5760	3
39.342	8.6453	4.1043	4.1043	138198.	1.3202	0.0543	0.03960	0.0200	0.02000	0.7904	0.5760	3
38.073	9.0055	4.2881	4.2881	175102.	1.4217	0.0543	0.03960	0.0200	0.02000	0.7904	0.5760	3
36.804	9.3657	4.4719	4.4719	217079.	1.5217	0.0567	0.03960	0.0209	0.02000	0.8251	0.5760	5
35.535	9.7259	4.6557	4.6557	264273.	1.6204	0.0634	0.03960	0.0233	0.02000	0.9222	0.5760	5
34.266	10.0861	4.8395	4.8395	316811.	1.7179	0.0700	0.03960	0.0258	0.02000	1.0179	0.5760	5
32.997	10.4463	5.0232	5.0232	374806.	1.8146	0.0765	0.03960	0.0281	0.02000	1.1120	0.5760	5
31.728	10.8065	5.2070	5.2070	438357.	1.9104	0.0828	0.03960	0.0305	0.02000	1.2040	0.5760	5
30.459	11.1667	5.3908	5.3908	507548.	2.0054	0.0889	0.03960	0.0327	0.02000	1.2936	0.5760	5
29.190	11.5269	5.5746	5.5746	582452.	2.0997	0.0949	0.03960	0.0349	0.02000	1.3808	0.5760	5
27.920	11.8871	5.7583	5.7583	663128.	2.1934	0.1007	0.03960	0.0371	0.02000	1.4652	0.5760	5
26.651	12.2473	5.9421	5.9421	749622.	2.2865	0.1064	0.03960	0.0391	0.02000	1.5468	0.5760	5
25.382	12.6075	6.1259	6.1259	841966.	2.3790	0.1118	0.03960	0.0411	0.02000	1.6256	0.5760	5
24.113	12.9677	6.3097	6.3097	940182.	2.4711	0.1170	0.03960	0.0431	0.02000	1.7014	0.5760	5
22.844	13.3279	6.4934	6.4934	1044280.	2.5626	0.1220	0.03960	0.0449	0.02000	1.7743	0.5760	5

21.575	13.6881	6.6772	6.6772	1154256.	2.6537	0.1268	0.03960	0.0467	0.02000	1.8442	0.5760	5
20.306	14.0483	6.8610	6.8610	1270092.	2.7444	0.1314	0.03960	0.0484	0.02000	1.9112	0.5760	5
19.037	14.4085	7.0448	7.0448	1391762.	2.8346	0.1358	0.03960	0.0500	0.02000	1.9751	0.5760	5
17.768	14.7687	7.2286	7.2286	1519224.	2.9243	0.1400	0.03960	0.0515	0.02000	2.0361	0.5760	5
16.498	15.1289	7.4123	7.4123	1652423.	3.0137	0.1440	0.03960	0.0530	0.02000	2.0942	0.5760	5
15.229	15.4891	7.5961	7.5961	1791295.	3.1026	0.1478	0.03960	0.0544	0.02000	2.1493	0.5760	5
13.960	15.8493	7.7799	7.7799	1935760.	3.1911	0.1514	0.03960	0.0557	0.02000	2.2016	0.5760	5
12.691	16.2095	7.9637	7.9637	2085725.	3.2792	0.1548	0.03960	0.0570	0.02000	2.2510	0.5760	5
11.422	16.5697	8.1474	8.1474	2241086.	3.3669	0.1580	0.03960	0.0581	0.02000	2.2977	0.5760	5
10.153	16.9299	8.3312	8.3312	2401725.	3.4541	0.1610	0.03960	0.0592	0.02000	2.3415	0.5760	5
8.884	17.2901	8.5150	8.5150	2567507.	3.5409	0.1638	0.03960	0.0603	0.02000	2.3827	0.5760	5
7.615	17.6503	8.6988	8.6988	2734436.	3.6259	0.1662	0.03960	0.0612	0.02000	2.4177	0.5760	5
6.346	18.0105	8.8825	8.8825	2894486.	3.7066	0.1678	0.03960	0.0618	0.02000	2.4405	0.5760	5
5.076	18.3707	9.0663	9.0582	3059202.	3.7871	0.1693	0.03960	0.0623	0.02000	2.4619	0.5760	5
3.807	18.7309	9.2501	7.3616	3227873.	3.8673	0.1706	0.03960	0.0628	0.02000	2.4814	0.5760	5
2.538	19.0911	9.4339	5.6651	3398988.	3.9467	0.1718	0.03960	0.0632	0.02000	2.4980	0.5760	5
1.269	19.4513	9.6177	3.9685	3571425.	4.0251	0.1727	0.03960	0.0635	0.02000	2.5112	0.5760	5
0.000	19.8115	9.8014	2.2720	3743631.	4.1021	0.1733	0.03960	0.0638	0.02000	2.5204	0.5760	5

CLBOX1	CLINT	CLINTP	LBOX	WBOX	TBOX	NJW	WEBSB	TORK	TTO	TBCOV
FT	FT	FT	FT	FT	FT		FT	FT-LBS	IN	IN
47.603	49.955	59.861	9.9058	11.9334	2.892	5	0.3353	586064.7	0.0134	0.0438

WSHEAR	WBEND	WWING	WSHBOX	WBDBOX	WTOBOX	WWBOX	WWINGT	WPOD	DELTIP
LBS	LBS	LBS	LBS	LBS	LBS	LBS	LBS	LBS	FT
71.50	2532.25	9046.48	31.93	1177.02	59.63	1268.58	10315.06	3272.93	3.849

CONTROL AREA	STRUCTURE AREA	SPLAN
FT2.	FT2.	FT2.
514.99	719.62	1450.

WEIGHTS	WTO	WBOD	WWING	WPROP	WTAIL	CG	RG
	152181.	83574.	52804.	6546.	2983.	53.255	0.000

BODY/PROP	VOLUME	DENSITY	CL1	FIN RAT	LENGTH	WIDTH	ABOD	ASUR	CLP1	CLP2
PARAMETERS	9348.	16.2789	58.915	9.3665	117.830	12.580	1144.9	3596.8	0.00	0.00

TAIL	ATAIL	CLT
PARAMETERS	202.	115.47

CRUISE	WEIGHT	ALPHA	DEFLEC	LIFTB	LIFTW	LIFTT	CLAQW	CLAQB	STAMA	CGM
PARAMETERS	152181.	7.00	-11.50	132.	166974.	-14925.	16.45	0.02	4.72	53.3

MANEUVER	SLFM	ALPHA	DEFLEC	LIFTB	LIFTW	LIFTT
PARAMETERS	2.50	17.50	-28.75	330.	417435.	-37312.

X	Y	BEND MOMENT	WSAV(I)	BMBW	BMBL	BMW	BMP	BMT	BMG	MAX MOMENT
1.96	2.60	-0.3974E+03	219.	-399.	2.	0.	0.	0.	0.	0.3974E+03

3.93	3.31	-0.2581E+04	712.	-2590.	9.	0.	0.	0.	0.	0.2581E+04
5.89	3.81	-0.7710E+04	1417.	-7734.	24.	0.	0.	0.	0.	0.7710E+04
7.86	4.21	-0.1676E+05	2309.	-16806.	47.	0.	0.	0.	0.	0.1676E+05
9.82	4.56	-0.3060E+05	3372.	-30683.	80.	0.	0.	0.	0.	0.3060E+05
11.78	4.86	-0.5006E+05	4595.	-50178.	123.	0.	0.	0.	0.	0.5006E+05
13.75	5.12	-0.8179E+05	5970.	-76054.	176.	0.	0.	0.	-5915.	0.8179E+05
15.71	5.37	-0.1240E+06	7489.	-109036.	241.	0.	0.	0.	-15157.	0.1240E+06
17.67	5.59	-0.1739E+06	9147.	-149820.	318.	0.	0.	0.	-24399.	0.1739E+06
19.64	5.80	-0.2323E+06	10939.	-199073.	407.	0.	0.	0.	-33642.	0.2323E+06
21.60	6.00	-0.2998E+06	12860.	-257442.	509.	0.	0.	0.	-42884.	0.2998E+06
23.57	6.18	-0.3771E+06	14907.	-325555.	624.	0.	0.	0.	-52126.	0.3771E+06
25.53	6.29	-0.4646E+06	17068.	-404015.	753.	0.	0.	0.	-61368.	0.4646E+06
27.49	6.29	-0.5629E+06	19250.	-493168.	896.	0.	0.	0.	-70610.	0.5629E+06
29.46	6.29	-0.6718E+06	21432.	-593034.	1053.	0.	0.	0.	-79852.	0.6718E+06
31.42	6.29	-0.7915E+06	23614.	-703614.	1224.	0.	0.	0.	-89095.	0.7915E+06
33.39	6.29	-0.9218E+06	25797.	-824907.	1409.	0.	0.	0.	-98337.	0.9218E+06
35.35	6.29	-0.1063E+07	27979.	-956914.	1608.	0.	0.	0.	-107579.	0.1063E+07
37.31	6.29	-0.1215E+07	30161.	-1099635.	1821.	0.	0.	0.	-116821.	0.1215E+07
39.28	6.28	-0.1374E+07	32342.	-1253067.	4895.	0.	0.	0.	-126063.	0.1374E+07
41.24	6.22	-0.1547E+07	34498.	-1417161.	5038.	0.	0.	0.	-135306.	0.1547E+07
43.20	6.17	-0.1731E+07	36615.	-1591746.	5176.	0.	0.	0.	-144548.	0.1731E+07
45.17	6.11	-0.1925E+07	38694.	-1776630.	5307.	0.	0.	0.	-153790.	0.1925E+07
47.13	6.05	-0.2129E+07	40734.	-1971622.	5432.	0.	0.	0.	-163032.	0.3277E+29
49.10	5.99	-0.2343E+07	42734.	-2176535.	5551.	0.	0.	0.	-172274.	0.2343E+07
51.06	5.93	-0.2611E+07	0.	-2391175.	5662.	-20922.	-1154.	0.	-203004.	0.2611E+07
53.02	5.87	-0.3071E+07	0.	-2615345.	5767.	-119059.	-8748.	0.	-333668.	0.3071E+07
54.99	5.81	-0.3595E+07	0.	-2848849.	5866.	-206138.	-23094.	0.	-522706.	0.3595E+07
56.95	5.74	-0.4021E+07	0.	-3091491.	5957.	-177886.	-43795.	0.	-713745.	0.4021E+07
58.91	5.68	-0.4188E+07	0.	-3343067.	6043.	69967.	-70454.	0.	-850414.	0.4188E+07
60.88	5.61	-0.4006E+07	32660.	-3603380.	6122.	589028.	-101961.	0.	-896168.	0.4006E+07
62.84	5.54	-0.3778E+07	30944.	-3872219.	6195.	1149554.	-134099.	0.	-926973.	0.3778E+07
64.81	5.47	-0.3557E+07	29269.	-4149384.	6262.	1710081.	-166236.	0.	-957778.	0.3557E+07
66.77	5.40	-0.3345E+07	27638.	-4434665.	6325.	2270608.	-198374.	0.	-988583.	0.3345E+07
68.73	5.33	-0.3140E+07	26050.	-4727849.	6382.	2831135.	-230511.	0.	-1019388.	0.3140E+07
70.70	5.25	-0.2943E+07	24505.	-5028724.	6435.	3391663.	-262649.	0.	-1050193.	0.2943E+07
72.66	5.18	-0.2754E+07	23005.	-5337075.	6484.	3952190.	-294786.	0.	-1080997.	0.2754E+07
74.63	5.10	-0.2572E+07	21549.	-5652680.	6529.	4512717.	-326923.	0.	-1111802.	0.1274E+30
76.59	5.01	-0.2397E+07	20139.	-5975320.	6571.	5073245.	-359061.	0.	-1142607.	0.2397E+07
78.55	4.93	-0.2229E+07	18775.	-6304769.	6610.	5633772.	-391198.	0.	-1173412.	0.2229E+07
80.52	4.84	-0.2067E+07	17458.	-6640800.	6647.	6194300.	-423336.	0.	-1204217.	0.2067E+07
82.48	4.75	-0.1912E+07	16189.	-6983183.	6683.	6754827.	-455473.	0.	-1235022.	0.1912E+07
84.44	4.66	-0.1763E+07	14967.	-7331679.	6718.	7315354.	-487611.	0.	-1265827.	0.1763E+07
86.41	4.56	-0.1620E+07	13795.	-7686053.	6752.	7875882.	-519748.	0.	-1296631.	0.1620E+07
88.37	4.46	-0.1482E+07	12673.	-8046055.	6787.	8436409.	-551886.	0.	-1327436.	0.1482E+07
90.34	4.35	-0.1350E+07	11602.	-8411446.	6822.	8996936.	-584023.	0.	-1358241.	0.1350E+07
92.30	4.24	-0.1223E+07	10583.	-8781966.	6860.	9557463.	-616160.	0.	-1389046.	0.1223E+07
94.26	4.13	-0.1101E+07	9617.	-9157360.	6900.	10117991.	-648298.	0.	-1419851.	0.1101E+07
96.23	4.00	-0.9830E+06	8706.	-9537363.	6944.	10678518.	-680435.	0.	-1450656.	0.9830E+06

98.19	3.87	-0.8697E+06	7851.	-9921700.	6993.	11239045.	-712573.	0.	-1481460.	0.8697E+06
100.16	3.73	-0.7604E+06	7053.	-10310093.	7047.	11799573.	-744710.	0.	-1512265.	0.7604E+06
102.12	3.58	-0.6550E+06	6316.	-10702260.	7109.	12360100.	-776848.	0.	-1543070.	0.6550E+06
104.08	3.42	-0.5530E+06	5640.	-11097895.	7178.	12920627.	-808985.	0.	-1573875.	0.5530E+06
106.05	3.24	-0.4541E+06	5028.	-11496694.	7258.	13481155.	-841123.	0.	-1604680.	0.4541E+06
108.01	3.04	-0.3580E+06	4483.	-11898332.	7349.	14041682.	-873260.	0.	-1635485.	0.3580E+06
109.97	2.81	-0.2645E+06	4010.	-12302474.	7454.	14602209.	-905398.	0.	-1666290.	0.2645E+06
111.94	2.54	-0.1731E+06	3613.	-12708749.	7575.	15162737.	-937535.	0.	-1697094.	0.1731E+06
113.90	2.21	-0.8337E+05	3299.	-13116777.	7716.	15723264.	-969672.	0.	-1727899.	0.8337E+05
115.87	1.73	-0.1254E+05	98.	-13526116.	7881.	16283791.	-1001810.	-17587.	-1758704.	0.1254E+05

LANDING	WEIGHT	ALPHA	DEFLEC	LIFTB	LIFTW	LIFTT	CLAQW	CLAQB	STAMA	CGM
PARAMETERS	109722.	7.00	-149.10	-43.	-54239.	153032.	16.45	0.02	6.55	51.1

LANDING	SLFM	ALPHA	DEFLEC	LIFTB	LIFTW	LIFTT	FGEAR
PARAMETERS	2.58	7.00	******	-43.	-54239.	153032.	184619.

X	Y	BEND MOMENT	WSAV(I)	BMBW	BMBL	BMW	BMP	BMT	BMG	MAX MOMENT
1.96	2.60	-0.4127E+03	219.	-412.	0.	0.	0.	0.	0.	0.4127E+03
3.93	3.31	-0.2677E+04	712.	-2676.	-1.	0.	0.	0.	0.	0.2677E+04
5.89	3.81	-0.7993E+04	1417.	-7990.	-3.	0.	0.	0.	0.	0.7993E+04
7.86	4.21	-0.1737E+05	2309.	-17361.	-6.	0.	0.	0.	0.	0.1737E+05
9.82	4.56	-0.3171E+05	3372.	-31697.	-10.	0.	0.	0.	0.	0.3171E+05
11.78	4.86	-0.5185E+05	4595.	-51836.	-16.	0.	0.	0.	0.	0.5185E+05
13.75	5.12	-0.8447E+05	5970.	-78567.	-23.	0.	0.	0.	-5878.	0.8447E+05
15.71	5.37	-0.1277E+06	7489.	-112639.	-31.	0.	0.	0.	-15063.	0.1277E+06
17.67	5.59	-0.1791E+06	9147.	-154770.	-41.	0.	0.	0.	-24248.	0.1791E+06
19.64	5.80	-0.2391E+06	10939.	-205650.	-53.	0.	0.	0.	-33433.	0.2391E+06
21.60	6.00	-0.3086E+06	12860.	-265948.	-66.	0.	0.	0.	-42618.	0.3086E+06
23.57	6.18	-0.3882E+06	14907.	-336311.	-81.	0.	0.	0.	-51803.	0.3882E+06
25.53	6.29	-0.4785E+06	17068.	-417364.	-98.	0.	0.	0.	-60988.	0.4785E+06
27.49	6.29	-0.5798E+06	19250.	-509462.	-116.	0.	0.	0.	-70173.	0.5798E+06
29.46	6.29	-0.6921E+06	21432.	-612628.	-137.	0.	0.	0.	-79358.	0.6921E+06
31.42	6.29	-0.8156E+06	23614.	-726861.	-159.	0.	0.	0.	-88543.	0.8156E+06
33.39	6.29	-0.9501E+06	25797.	-852162.	-183.	0.	0.	0.	-97728.	0.9501E+06
35.35	6.29	-0.1096E+07	27979.	-988530.	-209.	0.	0.	0.	-106913.	0.1096E+07
37.31	6.29	-0.1252E+07	30161.	-1135967.	-237.	0.	0.	0.	-116098.	0.1252E+07
39.28	6.28	-0.1420E+07	32342.	-1294469.	-636.	0.	0.	0.	-125283.	0.1420E+07
41.24	6.22	-0.1599E+07	34498.	-1463984.	-655.	0.	0.	0.	-134468.	0.1599E+07
43.20	6.17	-0.1789E+07	36615.	-1644337.	-672.	0.	0.	0.	-143653.	0.1789E+07
45.17	6.11	-0.1989E+07	38694.	-1835330.	-690.	0.	0.	0.	-152838.	0.1989E+07
47.13	6.05	-0.2199E+07	40734.	-2036764.	-706.	0.	0.	0.	-162023.	0.2199E+07
49.10	5.99	-0.2420E+07	42734.	-2248447.	-721.	0.	0.	0.	-171208.	0.2420E+07
51.06	5.93	-0.2308E+07	0.	-2470179.	-736.	5934.	-1192.	0.	158344.	0.2611E+07
53.02	5.87	-0.6145E+06	0.	-2701755.	-749.	33770.	-9037.	0.	2063313.	0.3071E+07
54.99	5.81	0.1979E+07	0.	-2942975.	-762.	58469.	-23857.	0.	4888512.	0.3595E+07
56.95	5.74	0.4556E+07	0.	-3193633.	-774.	50455.	-45242.	0.	7745263.	0.4556E+07
58.91	5.68	0.6198E+07	0.	-3453522.	-785.	-19845.	-72782.	0.	9744895.	0.6198E+07

60.88	5.61	0.6316E+07	32660.	-3722435.	-795.	-167071.	-105330.	0.	10311309.	0.6316E+07
62.84	5.54	0.6176E+07	30944.	-4000157.	-805.	-326058.	-138529.	0.	10642047.	0.6176E+07
64.81	5.47	0.6029E+07	29269.	-4286480.	-814.	-485045.	-171729.	0.	10972785.	0.6029E+07
66.77	5.40	0.5873E+07	27638.	-4581186.	-822.	-644032.	-204928.	0.	11303525.	0.5873E+07
68.73	5.33	0.5708E+07	26050.	-4884057.	-829.	-803020.	-238127.	0.	11634264.	0.5708E+07
70.70	5.25	0.5536E+07	24505.	-5194873.	-836.	-962007.	-271326.	0.	11965003.	0.5536E+07
72.66	5.18	0.5356E+07	23005.	-5513412.	-842.	-1120994.	-304526.	0.	12295742.	0.5356E+07
74.63	5.10	0.5168E+07	21549.	-5839444.	-848.	-1279982.	-337725.	0.	12626481.	0.5168E+07
76.59	5.01	0.4974E+07	20139.	-6172745.	-854.	-1438969.	-370924.	0.	12957220.	0.4974E+07
78.55	4.93	0.4772E+07	18775.	-6513078.	-859.	-1597956.	-404124.	0.	13287959.	0.4772E+07
80.52	4.84	0.4563E+07	17458.	-6860212.	-864.	-1756944.	-437323.	0.	13618698.	0.4563E+07
82.48	4.75	0.4348E+07	16189.	-7213907.	-868.	-1915931.	-470522.	0.	13949437.	0.4348E+07
84.44	4.66	0.4127E+07	14967.	-7573917.	-873.	-2074918.	-503721.	0.	14280176.	0.4127E+07
86.41	4.56	0.3899E+07	13795.	-7939999.	-877.	-2233906.	-536921.	0.	14610915.	0.3899E+07
88.37	4.46	0.3666E+07	12673.	-8311897.	-882.	-2392893.	-570120.	0.	14941654.	0.3666E+07
90.34	4.35	0.3427E+07	11602.	-8689360.	-886.	-2551880.	-603319.	0.	15272394.	0.3427E+07
92.30	4.24	0.3183E+07	10583.	-9072122.	-891.	-2710868.	-636518.	0.	15603133.	0.3183E+07
94.26	4.13	0.2933E+07	9617.	-9459920.	-897.	-2869855.	-669718.	0.	15933872.	0.2933E+07
96.23	4.00	0.2679E+07	8706.	-9852477.	-902.	-3028842.	-702917.	0.	16264611.	0.2679E+07
98.19	3.87	0.2421E+07	7851.	-10249512.	-909.	-3187830.	-736116.	0.	16595349.	0.2421E+07
100.16	3.73	0.2158E+07	7053.	-10650738.	-916.	-3346817.	-769316.	0.	16926088.	0.2158E+07
102.12	3.58	0.1892E+07	6316.	-11055862.	-924.	-3505804.	-802515.	0.	17256826.	0.1892E+07
104.08	3.42	0.1622E+07	5640.	-11464569.	-933.	-3664791.	-835714.	0.	17587568.	0.1622E+07
106.05	3.24	0.1348E+07	5028.	-11876544.	-943.	-3823779.	-868913.	0.	17918306.	0.1348E+07
108.01	3.04	0.1072E+07	4483.	-12291453.	-955.	-3982766.	-902113.	0.	18249046.	0.1072E+07
109.97	2.81	0.7928E+06	4010.	-12708947.	-968.	-4141753.	-935312.	0.	18579784.	0.7928E+06
111.94	2.54	0.5116E+06	3613.	-13128646.	-984.	-4300741.	-968511.	0.	18910524.	0.5116E+06
113.90	2.21	0.2287E+06	3299.	-13550155.	-1003.	-4459728.	-1001710.	0.	19241262.	0.2287E+06
115.87	1.73	0.1426E+04	98.	-13973018.	-1024.	-4618715.	-1034910.	57091.	19572002.	0.1254E+05

BUMP	WEIGHT	ALPHA	DEFLEC	LIFTB	LIFTW	LIFTT	CLAQW	CLAQB	STAMA	CGM
PARAMETERS	152181.	7.00	-57.45	-126.	-159141.	159419.	16.45	0.02	4.72	53.3

BUMP	SLFM	ALPHA	DEFLEC	LIFTB	DEFLTW	LIFTT	FGEAR
PARAMETERS	1.20	7.00	-57.45	-126.	-159141.	159419.	182465.

X	Y	BEND MOMENT	WSAV(I)	BMBW	BMBL	BMW	BMP	BMT	BMG	MAX MOMENT
1.96	2.60	-0.1923E+03	219.	-192.	-1.	0.	0.	0.	0.	0.4127E+03
3.93	3.31	-0.1247E+04	712.	-1243.	-4.	0.	0.	0.	0.	0.2677E+04
5.89	3.81	-0.3722E+04	1417.	-3712.	-9.	0.	0.	0.	0.	0.7993E+04
7.86	4.21	-0.8085E+04	2309.	-8067.	-18.	0.	0.	0.	0.	0.1737E+05
9.82	4.56	-0.1476E+05	3372.	-14728.	-30.	0.	0.	0.	0.	0.3171E+05
11.78	4.86	-0.2413E+05	4595.	-24086.	-47.	0.	0.	0.	0.	0.5185E+05
13.75	5.12	0.2939E+05	5970.	-36506.	-67.	0.	0.	0.	65966.	0.8447E+05
15.71	5.37	0.1166E+06	7489.	-52337.	-92.	0.	0.	0.	169037.	0.1277E+06
17.67	5.59	0.2001E+06	9147.	-71913.	-121.	0.	0.	0.	272109.	0.2001E+06
19.64	5.80	0.2795E+06	10939.	-95555.	-155.	0.	0.	0.	375181.	0.2795E+06
21.60	6.00	0.3545E+06	12860.	-123572.	-194.	0.	0.	0.	478253.	0.3545E+06

23.57	6.18	0.4248E+06	14907.	-156266.	-238.	0.	0.	0.	581324.	0.4248E+06
25.53	6.29	0.4902E+06	17068.	-193927.	-287.	0.	0.	0.	684396.	0.4902E+06
27.49	6.29	0.5504E+06	19250.	-236721.	-342.	0.	0.	0.	787468.	0.5798E+06
29.46	6.29	0.6055E+06	21432.	-284656.	-402.	0.	0.	0.	890539.	0.6921E+06
31.42	6.29	0.6554E+06	23614.	-337734.	-467.	0.	0.	0.	993611.	0.8156E+06
33.39	6.29	0.7002E+06	25797.	-395955.	-537.	0.	0.	0.	1096683.	0.9501E+06
35.35	6.29	0.7398E+06	27979.	-459319.	-613.	0.	0.	0.	1199754.	0.1096E+07
37.31	6.29	0.7743E+06	30161.	-527825.	-694.	0.	0.	0.	1302826.	0.1252E+07
39.28	6.28	0.8026E+06	32342.	-601472.	-1866.	0.	0.	0.	1405898.	0.1420E+07
41.24	6.22	0.8268E+06	34498.	-680237.	-1921.	0.	0.	0.	1508969.	0.1599E+07
43.20	6.17	0.8460E+06	36615.	-764038.	-1973.	0.	0.	0.	1612041.	0.1789E+07
45.17	6.11	0.8603E+06	38694.	-852782.	-2023.	0.	0.	0.	1715113.	0.1989E+07
47.13	6.05	0.8697E+06	40734.	-946379.	-2071.	0.	0.	0.	1818185.	0.2199E+07
49.10	5.99	0.8744E+06	42734.	-1044737.	-2116.	0.	0.	0.	1921256.	0.2420E+07
51.06	5.93	0.1130E+07	0.	-1147764.	-2159.	16310.	-554.	0.	2263961.	0.2611E+07
53.02	5.87	0.2552E+07	0.	-1255365.	-2199.	92814.	-4199.	0.	3721168.	0.3071E+07
54.99	5.81	0.4609E+07	0.	-1367448.	-2236.	160697.	-11085.	0.	5829373.	0.4609E+07
56.95	5.74	0.6591E+07	0.	-1483916.	-2271.	138673.	-21022.	0.	7959901.	0.6591E+07
58.91	5.68	0.7789E+07	0.	-1604672.	-2304.	-54543.	-33818.	0.	9484074.	0.7789E+07
60.88	5.61	0.7754E+07	32660.	-1729622.	-2334.	-459183.	-48941.	0.	9994344.	0.7754E+07
62.84	5.54	0.7516E+07	30944.	-1858665.	-2362.	-896147.	-64367.	0.	10337888.	0.7516E+07
64.81	5.47	0.7274E+07	29269.	-1991705.	-2387.	-1333112.	-79793.	0.	10681432.	0.7274E+07
66.77	5.40	0.7029E+07	27638.	-2128639.	-2411.	-1770077.	-95219.	0.	11024978.	0.7029E+07
68.73	5.33	0.6779E+07	26050.	-2269368.	-2433.	-2207042.	-110645.	0.	11368523.	0.6779E+07
70.70	5.25	0.6526E+07	24505.	-2413788.	-2453.	-2644007.	-126071.	0.	11712068.	0.6526E+07
72.66	5.18	0.6269E+07	23005.	-2561796.	-2472.	-3080972.	-141497.	0.	12055613.	0.6269E+07
74.63	5.10	0.6009E+07	21549.	-2713286.	-2489.	-3517937.	-156923.	0.	12399158.	0.6009E+07
76.59	5.01	0.5745E+07	20139.	-2868154.	-2505.	-3954902.	-172349.	0.	12742704.	0.5745E+07
78.55	4.93	0.5478E+07	18775.	-3026290.	-2520.	-4391868.	-187775.	0.	13086248.	0.5478E+07
80.52	4.84	0.5208E+07	17458.	-3187584.	-2534.	-4828833.	-203201.	0.	13429793.	0.5208E+07
82.48	4.75	0.4934E+07	16189.	-3351928.	-2548.	-5265798.	-218627.	0.	13773339.	0.4934E+07
84.44	4.66	0.4658E+07	14967.	-3519206.	-2561.	-5702763.	-234053.	0.	14116884.	0.4658E+07
86.41	4.56	0.4379E+07	13795.	-3689305.	-2574.	-6139728.	-249479.	0.	14460429.	0.4379E+07
88.37	4.46	0.4098E+07	12673.	-3862107.	-2587.	-6576693.	-264905.	0.	14803974.	0.4098E+07
90.34	4.35	0.3813E+07	11602.	-4037495.	-2601.	-7013658.	-280331.	0.	15147520.	0.3813E+07
92.30	4.24	0.3527E+07	10583.	-4215344.	-2615.	-7450623.	-295757.	0.	15491064.	0.3527E+07
94.26	4.13	0.3238E+07	9617.	-4395533.	-2631.	-7887588.	-311183.	0.	15834610.	0.3238E+07
96.23	4.00	0.2946E+07	8706.	-4577934.	-2647.	-8324554.	-326609.	0.	16178154.	0.2946E+07
98.19	3.87	0.2653E+07	7851.	-4762416.	-2666.	-8761518.	-342035.	0.	16521700.	0.2653E+07
100.16	3.73	0.2358E+07	7053.	-4948845.	-2687.	-9198483.	-357461.	0.	16865244.	0.2358E+07
102.12	3.58	0.2061E+07	6316.	-5137085.	-2710.	-9635449.	-372887.	0.	17208790.	0.2061E+07
104.08	3.42	0.1762E+07	5640.	-5326990.	-2737.	-10072414.	-388313.	0.	17552336.	0.1762E+07
106.05	3.24	0.1462E+07	5028.	-5518413.	-2767.	-10509379.	-403739.	0.	17895880.	0.1462E+07
108.01	3.04	0.1160E+07	4483.	-5711200.	-2802.	-10946344.	-419165.	0.	18239426.	0.1160E+07
109.97	2.81	0.8570E+06	4010.	-5905188.	-2842.	-11383309.	-434591.	0.	18582970.	0.8570E+06
111.94	2.54	0.5531E+06	3613.	-6100200.	-2888.	-11820274.	-450017.	0.	18926516.	0.5531E+06
113.90	2.21	0.2484E+06	3299.	-6296054.	-2942.	-12257239.	-465443.	0.	19270060.	0.2484E+06
115.87	1.73	0.4214E+04	98.	-6492536.	-3005.	-12694204.	-480869.	61220.	19613606.	0.1254E+05

0

STRUCTURAL PARAMETERS	CKF	FSK	EFF	CK	PG	CF	CTHIC	SAFEFAC	DEFL
	5.2400	0.04504	0.76000	2.0390	11.250	0.6250E-04	0.000	1.500	0.000

1

FUSE STAT FT	BENDING MOMENT FT LBS	THIC IN	SHELL STRESS PSI	EQUIV THICK IN	GAGE THICK IN	FRAME SPACE IN	NJ	SECTION AREA SQ FT	SHELL UNITWT LB/FT2	FRAME UNITWT	MAX BENDING
1.9638	619.015	0.0000	33.1421	0.0734	0.0360	18010.9727	3	21.2041	1.0676	0.0000	LAN
3.9277	4015.657	0.0000	132.5520	0.0734	0.0360	4503.2979	3	34.3929	1.0676	0.0000	LAN
5.8915	11989.037	0.0000	298.2244	0.0734	0.0360	2001.5850	3	45.6394	1.0676	0.0000	LAN
7.8553	26050.969	0.0000	530.1569	0.0734	0.0360	1125.9333	3	55.7851	1.0676	0.0000	LAN
9.8192	47561.238	0.0000	828.3481	0.0734	0.0360	720.6165	3	65.1837	1.0676	0.0001	LAN
11.7830	77778.055	0.0000	1192.7972	0.0734	0.0360	500.4382	3	74.0269	1.0676	0.0002	LAN
13.7468	126702.141	0.0000	1744.9386	0.0734	0.0360	342.0873	3	82.4333	1.0676	0.0004	LAN
15.7107	191600.266	0.0000	2403.9612	0.0734	0.0360	248.3074	3	90.4832	1.0676	0.0008	LAN
17.6745	300112.031	0.0000	3468.3428	0.0734	0.0360	172.1056	3	98.2337	1.0676	0.0017	BUM
19.6383	419206.312	0.0000	4501.3037	0.0734	0.0360	132.6108	3	105.7277	1.0676	0.0031	BUM
21.6022	531729.500	0.0000	5342.1821	0.0734	0.0360	111.7374	3	112.9981	1.0676	0.0047	BUM
23.5660	637229.750	0.0000	6024.9893	0.0734	0.0360	99.0743	3	120.0712	1.0676	0.0064	BUM
25.5298	735272.000	0.0000	6719.1787	0.0734	0.0360	88.8384	3	124.2313	1.0676	0.0082	BUM
27.4937	869627.625	0.0000	7946.9687	0.0734	0.0360	75.1131	3	124.2313	1.0676	0.0115	LAN
29.4575	1038184.313	0.0000	9487.2998	0.0734	0.0360	62.9179	3	124.2313	1.0676	0.0164	LAN
31.4213	1223344.750	0.0000	11179.3613	0.0734	0.0360	53.3949	3	124.2313	1.0676	0.0228	LAN
33.3852	1425109.750	0.0000	13023.1621	0.0734	0.0360	45.8354	3	124.2313	1.0676	0.0309	LAN
35.3490	1643478.750	0.0000	15018.6953	0.0734	0.0360	39.7452	3	124.2313	1.0676	0.0411	LAN
37.3128	1878452.250	0.0000	17165.9688	0.0734	0.0360	34.7735	3	124.2313	1.0676	0.0537	LAN
39.2767	2130582.000	0.0000	19538.9277	0.0734	0.0360	30.5504	3	123.7931	1.0676	0.0693	LAN
41.2405	2398660.500	0.0000	22389.4512	0.0734	0.0360	26.6608	3	121.6254	1.0676	0.0894	LAN
43.2043	2682994.000	0.0000	25501.5098	0.0734	0.0360	23.4073	3	119.4408	1.0676	0.1139	LAN
45.1682	2983286.250	0.0000	28888.3418	0.0734	0.0360	20.6631	3	117.2388	1.0676	0.1434	LAN
47.1320	3299240.000	0.0000	32564.5059	0.0734	0.0360	18.3304	3	115.0187	1.0676	0.1788	LAN
49.0958	3630565.000	0.0000	36546.1406	0.0734	0.0360	16.3334	3	112.7799	1.0676	0.2208	LAN
51.0597	3915888.750	0.0000	40223.6992	0.0734	0.0360	14.8400	3	110.5216	1.0676	0.2622	MAN
53.0235	4606577.500	0.0000	47831.5078	0.0741	0.0364	12.6057	4	108.2432	1.0784	0.3595	MAN
54.9873	6913951.500	0.0000	54000.0000	0.1007	0.0494	15.1663	5	105.9439	1.4647	0.3301	BUM
56.9512	9887048.000	0.0000	54000.0000	0.1472	0.0722	22.1738	5	103.6227	2.1415	0.2209	BUM
58.9150	11683106.000	0.0000	54000.0000	0.1780	0.0873	26.8083	5	101.2787	2.5891	0.1785	BUM
60.8788	11631395.000	0.0000	54000.0000	0.1815	0.0890	27.3285	5	98.9111	2.6393	0.1710	BUM
62.8427	11274519.000	0.0000	54000.0000	0.1803	0.0884	27.1466	5	96.5186	2.6218	0.1680	BUM
64.8065	10911652.000	0.0000	53999.9961	0.1789	0.0878	26.9482	5	94.1001	2.6026	0.1650	BUM
66.7703	10542948.000	0.0000	54000.0000	0.1775	0.0871	26.7324	5	91.6544	2.5818	0.1620	BUM
68.7342	10168552.000	0.0000	54000.0000	0.1760	0.0863	26.4984	5	89.1801	2.5592	0.1591	BUM
70.6980	9788623.000	0.0000	54000.0000	0.1743	0.0855	26.2454	5	86.6757	2.5347	0.1561	BUM
72.6618	9403313.000	0.0000	53999.9961	0.1725	0.0846	25.9722	5	84.1396	2.5084	0.1531	BUM
74.6257	9012783.000	0.0000	54000.0000	0.1705	0.0836	25.6778	5	81.5699	2.4799	0.1501	BUM
76.5895	8617191.000	0.0000	53999.9961	0.1684	0.0826	25.3607	5	78.9646	2.4493	0.1471	BUM
78.5533	8216694.000	0.0000	54000.0000	0.1661	0.0815	25.0195	5	76.3216	2.4163	0.1442	BUM

80.5172	7811461.500	0.0000	54000.0000	0.1637	0.0803	24.6523	5	73.6382	2.3809	0.1412	BUM
82.4810	7401658.500	0.0000	54000.0039	0.1611	0.0790	24.2571	5	70.9119	2.3427	0.1382	BUM
84.4449	6987453.000	0.0000	54000.0000	0.1583	0.0776	23.8314	5	68.1393	2.3016	0.1351	BUM
86.4087	6569014.500	0.0000	53999.9961	0.1552	0.0761	23.3724	5	65.3170	2.2573	0.1321	BUM
88.3725	6146523.000	0.0000	54000.0000	0.1519	0.0745	22.8765	5	62.4408	2.2094	0.1290	BUM
90.3364	5720152.500	0.0000	54000.0000	0.1483	0.0728	22.3396	5	59.5061	2.1575	0.1259	BUM
92.3002	5290087.500	0.0000	54000.0039	0.1445	0.0709	21.7564	5	56.5072	2.1012	0.1227	BUM
94.2640	4856512.500	0.0000	54000.0000	0.1402	0.0688	21.1206	5	53.4377	2.0398	0.1196	BUM
96.2279	4419615.000	0.0000	54000.0078	0.1356	0.0665	20.4236	5	50.2898	1.9725	0.1164	BUM
98.1917	3979597.500	0.0000	54000.0039	0.1305	0.0640	19.6549	5	47.0541	1.8982	0.1131	BUM
100.1555	3536653.500	0.0000	54000.0000	0.1248	0.0612	18.7997	5	43.7189	1.8157	0.1099	BUM
102.1194	3090988.500	0.0000	53999.9961	0.1185	0.0581	17.8381	5	40.2695	1.7228	0.1067	BUM
104.0832	2642824.500	0.0000	54000.0000	0.1112	0.0545	16.7412	5	36.6869	1.6168	0.1036	BUM
106.0471	2192373.000	0.0000	54000.0000	0.1027	0.0504	15.4648	5	32.9456	1.4936	0.1007	BUM
108.0109	1739874.000	0.0000	54000.0000	0.0926	0.0454	13.9380	5	29.0100	1.3461	0.0984	BUM
109.9747	1285563.000	0.0000	54000.0039	0.0799	0.0392	12.0336	5	24.8271	1.1622	0.0975	BUM
111.9386	829707.000	0.0000	46374.3086	0.0734	0.0360	12.8718	3	20.3117	1.0676	0.0640	BUM
113.9024	372576.000	0.0000	27633.7871	0.0734	0.0360	21.6011	3	15.3064	1.0676	0.0171	BUM
115.8662	18816.750	0.0000	2263.7334	0.0734	0.0360	263.6889	3	9.4367	1.0676	0.0001	MAN
115.8662	0.000	0.0000	0.0000	0.0734	0.0360	263.6889	3	9.4367	1.0676	0.0001	NONE

1 STRUCTURAL WEIGHT SUMMARY

	WEIGHT (LBS)	WEIGHT FRACTION	UNIT WEIGHT (LBS/FT*FT)
SHELL	5719.80	0.0376	1.5945
FRAMES	373.81	0.0025	0.1042
NONOP	9558.42	0.0628	2.6646
SEC	0.00	0.0000	0.0000
TOTAL	15652.02	0.1029	4.3634
VOLPEN	0.00	0.0000	0.0000
GRANTOT	15652.02	0.1029	4.3634

Surface Area, SQF 3587.15
Volume Ratio 1.00000000
BODY WEIGHT 15652.02441406

1

FUSE STAT FT	BENDING MOMENT FT LBS	THIC IN	SHELL STRESS PSI	EQUIV THICK IN	GAGE THICK IN	FRAME SPACE IN	NJ	SECTION AREA SQ FT	SHELL UNITWT LB/FT2	FRAME UNITWT	MAX BENDING
1.9638	619.015	0.0000	33.1421	0.0734	0.0360	18010.9727	3	21.2041	1.0676	0.0000	LAN
3.9277	4015.657	0.0000	132.5520	0.0734	0.0360	4503.2979	3	34.3929	1.0676	0.0000	LAN
5.8915	11989.037	0.0000	298.2244	0.0734	0.0360	2001.5850	3	45.6394	1.0676	0.0000	LAN
7.8553	26050.969	0.0000	530.1569	0.0734	0.0360	1125.9333	3	55.7851	1.0676	0.0000	LAN

9.8192	47561.238	0.0000	828.3481	0.0734	0.0360	720.6165	3	65.1837	1.0676	0.0001	LAN
11.7830	77778.055	0.0000	1192.7972	0.0734	0.0360	500.4382	3	74.0269	1.0676	0.0002	LAN
13.7468	126702.141	0.0000	1744.9386	0.0734	0.0360	342.0873	3	82.4333	1.0676	0.0004	LAN
15.7107	191600.266	0.0000	2403.9612	0.0734	0.0360	248.3074	3	90.4832	1.0676	0.0008	LAN
17.6745	300112.031	0.0000	3468.3428	0.0734	0.0360	172.1056	3	98.2337	1.0676	0.0017	BUM
19.6383	419206.312	0.0000	4501.3037	0.0734	0.0360	132.6108	3	105.7277	1.0676	0.0031	BUM
21.6022	531729.500	0.0000	5342.1821	0.0734	0.0360	111.7374	3	112.9981	1.0676	0.0047	BUM
23.5660	637229.750	0.0000	6024.9893	0.0734	0.0360	99.0743	3	120.0712	1.0676	0.0064	BUM
25.5298	735272.000	0.0000	6719.1787	0.0734	0.0360	88.8384	3	124.2313	1.0676	0.0082	BUM
27.4937	869627.625	0.0000	7946.9687	0.0734	0.0360	75.1131	3	124.2313	1.0676	0.0115	LAN
29.4575	1038184.313	0.0000	9487.2998	0.0734	0.0360	62.9179	3	124.2313	1.0676	0.0164	LAN
31.4213	1223344.750	0.0000	11179.3613	0.0734	0.0360	53.3949	3	124.2313	1.0676	0.0228	LAN
33.3852	1425109.750	0.0000	13023.1621	0.0734	0.0360	45.8354	3	124.2313	1.0676	0.0309	LAN
35.3490	1643478.750	0.0000	15018.6953	0.0734	0.0360	39.7452	3	124.2313	1.0676	0.0411	LAN
37.3128	1878452.250	0.0000	17165.9688	0.0734	0.0360	34.7735	3	124.2313	1.0676	0.0537	LAN
39.2767	2130582.000	0.0000	19538.9277	0.0734	0.0360	30.5504	3	123.7931	1.0676	0.0693	LAN
41.2405	2398660.500	0.0000	22389.4512	0.0734	0.0360	26.6608	3	121.6254	1.0676	0.0894	LAN
43.2043	2682994.000	0.0000	25501.5098	0.0734	0.0360	23.4073	3	119.4408	1.0676	0.1139	LAN
45.1682	2983286.250	0.0000	28888.3418	0.0734	0.0360	20.6631	3	117.2388	1.0676	0.1434	LAN
47.1320	3299240.000	0.0000	32564.5059	0.0734	0.0360	18.3304	3	115.0187	1.0676	0.1788	LAN
49.0958	3630565.000	0.0000	36546.1406	0.0734	0.0360	16.3334	3	112.7799	1.0676	0.2208	LAN
51.0597	3915888.750	0.0000	40223.6992	0.0734	0.0360	14.8400	3	110.5216	1.0676	0.2622	MAN
53.0235	4606577.500	0.0000	47831.5078	0.0741	0.0364	12.6057	4	108.2432	1.0784	0.3595	MAN
54.9873	6913951.500	0.0000	54000.0000	0.1007	0.0494	15.1663	5	105.9439	1.4647	0.3301	BUM
56.9512	9887048.000	0.0000	54000.0000	0.1472	0.0722	22.1738	5	103.6227	2.1415	0.2209	BUM
58.9150	11683106.000	0.0000	54000.0000	0.1780	0.0873	26.8083	5	101.2787	2.5891	0.1785	BUM
60.8788	11631395.000	0.0000	54000.0000	0.1815	0.0890	27.3285	5	98.9111	2.6393	0.1710	BUM
62.8427	11274519.000	0.0000	54000.0000	0.1803	0.0884	27.1466	5	96.5186	2.6218	0.1680	BUM
64.8065	10911652.000	0.0000	53999.9961	0.1789	0.0878	26.9482	5	94.1001	2.6026	0.1650	BUM
66.7703	10542948.000	0.0000	54000.0000	0.1775	0.0871	26.7324	5	91.6544	2.5818	0.1620	BUM
68.7342	10168552.000	0.0000	54000.0000	0.1760	0.0863	26.4984	5	89.1801	2.5592	0.1591	BUM
70.6980	9788623.000	0.0000	54000.0000	0.1743	0.0855	26.2454	5	86.6757	2.5347	0.1561	BUM
72.6618	9403313.000	0.0000	53999.9961	0.1725	0.0846	25.9722	5	84.1396	2.5084	0.1531	BUM
74.6257	9012783.000	0.0000	54000.0000	0.1705	0.0836	25.6778	5	81.5699	2.4799	0.1501	BUM
76.5895	8617191.000	0.0000	53999.9961	0.1684	0.0826	25.3607	5	78.9646	2.4493	0.1471	BUM
78.5533	8216694.000	0.0000	54000.0000	0.1661	0.0815	25.0195	5	76.3216	2.4163	0.1442	BUM
80.5172	7811461.500	0.0000	54000.0000	0.1637	0.0803	24.6523	5	73.6382	2.3809	0.1412	BUM
82.4810	7401658.500	0.0000	54000.0039	0.1611	0.0790	24.2571	5	70.9119	2.3427	0.1382	BUM
84.4449	6987453.000	0.0000	54000.0000	0.1583	0.0776	23.8314	5	68.1393	2.3016	0.1351	BUM
86.4087	6569014.500	0.0000	53999.9961	0.1552	0.0761	23.3724	5	65.3170	2.2573	0.1321	BUM
88.3725	6146523.000	0.0000	54000.0000	0.1519	0.0745	22.8765	5	62.4408	2.2094	0.1290	BUM
90.3364	5720152.500	0.0000	54000.0000	0.1483	0.0728	22.3396	5	59.5061	2.1575	0.1259	BUM
92.3002	5290087.500	0.0000	54000.0039	0.1445	0.0709	21.7564	5	56.5072	2.1012	0.1227	BUM
94.2640	4856512.500	0.0000	54000.0000	0.1402	0.0688	21.1206	5	53.4377	2.0398	0.1196	BUM
96.2279	4419615.000	0.0000	54000.0078	0.1356	0.0665	20.4236	5	50.2898	1.9725	0.1164	BUM
98.1917	3979597.500	0.0000	54000.0039	0.1305	0.0640	19.6549	5	47.0541	1.8982	0.1131	BUM
100.1555	3536653.500	0.0000	54000.0000	0.1248	0.0612	18.7997	5	43.7189	1.8157	0.1099	BUM
102.1194	3090988.500	0.0000	53999.9961	0.1185	0.0581	17.8381	5	40.2695	1.7228	0.1067	BUM

104.0832	2642824.500	0.0000	54000.0000	0.1112	0.0545	16.7412	5	36.6869	1.6168	0.1036	BUM
106.0471	2192373.000	0.0000	54000.0000	0.1027	0.0504	15.4648	5	32.9456	1.4936	0.1007	BUM
108.0109	1739874.000	0.0000	54000.0000	0.0926	0.0454	13.9380	5	29.0100	1.3461	0.0984	BUM
109.9747	1285563.000	0.0000	54000.0039	0.0799	0.0392	12.0336	5	24.8271	1.1622	0.0975	BUM
111.9386	829707.000	0.0000	46374.3086	0.0734	0.0360	12.8718	3	20.3117	1.0676	0.0640	BUM
113.9024	372576.000	0.0000	27633.7871	0.0734	0.0360	21.6011	3	15.3064	1.0676	0.0171	BUM
115.8662	18816.750	0.0000	2263.7334	0.0734	0.0360	263.6889	3	9.4367	1.0676	0.0001	MAN
115.8662	0.000	0.0000	0.0000	0.0734	0.0360	263.6889	3	9.4367	1.0676	0.0001	NONE

1 STRUCTURAL WEIGHT SUMMARY

	WEIGHT (LBS)	WEIGHT FRACTION	UNIT WEIGHT (LBS/FT*FT)
SHELL	5719.80	0.0376	1.5945
FRAMES	373.81	0.0025	0.1042
NONOP	9558.42	0.0628	2.6646
SEC	0.00	0.0000	0.0000
TOTAL	15652.02	0.1029	4.3634
VOLPEN	0.00	0.0000	0.0000
GRANTOT	15652.02	0.1029	4.3634

Surface Area, SQF	3587.15
Volume Ratio	1.00000000
BODY WEIGHT	15652.02441406

1 STRUCTURAL WEIGHT SUMMARY

	WEIGHT (LBS)	WEIGHT FRACTION	UNIT WEIGHT (LBS/FT*FT)
SHELL	5719.80	0.0376	1.5945
FRAMES	373.81	186.9042	0.1042
NONOP	9558.42	0.0628	2.6646
SEC	0.00	0.0000	0.0000
TOTAL	15652.02	0.1029	4.3634
VOLPEN	0.00	0.0000	0.0000
GRANTOT	15652.02	0.1029	4.3634

Surface Area, SQF	3587.15
Volume Ratio	1.00000000
BODY WEIGHT	15652.02441406

Output for Module # 1

****

Fuselage Definition			Nacelle Definition			Nacelle Location		
X	R	Area	X-Xnose	R	Area	X	Y	Z
0.00	0.00	0.00	0.00	0.70	1.53	39.31	13.42	-6.64
1.24	1.10	3.78	0.37	0.70	1.53	39.31	-13.42	-6.64
2.47	1.81	10.29	0.37	0.70	1.53			
3.71	2.40	18.17	1.76	0.70	1.53			
4.95	2.92	26.85						
6.19	3.38	35.97						
7.42	3.80	45.27						
8.66	4.17	54.55						
9.90	4.50	63.64						
11.14	4.80	72.40						
12.37	5.07	80.73						
13.61	5.31	88.52						
14.85	5.52	95.69						
16.08	5.70	102.17						
17.32	5.86	107.90						
18.56	5.99	112.83						
19.80	6.10	116.91						
21.03	6.18	120.12						
22.27	6.24	122.43						
23.51	6.28	123.83						
24.74	6.29	124.29						
26.16	6.29	124.29						
27.57	6.29	124.29						
28.98	6.29	124.29						
30.40	6.29	124.29						
31.81	6.29	124.29						
33.22	6.29	124.29						
34.64	6.29	124.29						
36.05	6.29	124.29						
37.46	6.29	124.29						
38.88	6.29	124.29						
42.83	6.28	123.83						
46.77	6.24	122.43						
50.72	6.18	120.12						
54.67	6.10	116.91						
58.62	5.99	112.83						
62.56	5.86	107.90						
66.51	5.70	102.17						
70.46	5.52	95.69						
74.41	5.31	88.52						

78.35	5.07	80.73
82.30	4.80	72.40
86.25	4.50	63.64
90.20	4.17	54.55
94.14	3.80	45.27
98.09	3.38	35.97
102.04	2.92	26.85
105.99	2.40	18.17
109.93	1.81	10.29
113.88	1.10	3.78
117.83	0.00	0.00

	Fuselage		Nacelles - 2
Max. Diameter.....	12.580	.....	1.397
Fineness Ratio.....	9.366		
Surface Area.....	3522.634	.....	7.743 (each)
Volume.....	9348.345		

Dimensions of Planar Surfaces (each)

	Wing	H.Tail	V.Tail	Canard	Units
NUMBER OF SURFACES.	1.0	1.0	1.0	1.0	
PLAN AREA.....	1450.0	277.5	203.5	0.0	(SQ.FT.)
SURFACE AREA.....	2923.7	403.1	408.6	0.0	(SQ.FT.)
VOLUME.....	2064.4	106.0	175.0	0.0	(CU.FT.)
SPAN.....	107.339	39.669	15.885	0.000	(FT.)
L.E. SWEEP.....	23.725	37.176	45.001	0.000	(DEG.)
C/4 SWEEP.....	20.000	33.400	39.400	0.000	(DEG.)
T.E. SWEEP.....	7.826	19.921	15.935	0.000	(DEG.)
ASPECT RATIO	7.946	5.670	1.240	0.000	
ROOT CHORD.....	21.614	10.923	18.485	0.000	(FT.)
ROOT THICKNESS.....	37.867	11.797	19.964	0.000	(IN.)
ROOT T/C	0.146	0.090	0.090	0.000	
TIP CHORD.....	5.403	3.069	7.135	0.000	(FT.)
TIP THICKNESS.....	7.133	3.315	7.706	0.000	(IN.)
TIP T/C	0.110	0.090	0.090	0.000	
TAPER RATIO	0.250	0.281	0.386	0.000	
MEAN AERO CHORD....	15.130	7.731	13.648	0.000	(FT.)
LE ROOT AT.....	42.200	104.550	99.345	0.000	(FT.)
C/4 ROOT AT.....	47.603	107.281	103.966	0.000	(FT.)
TE ROOT AT.....	63.814	115.473	117.830	0.000	(FT.)
LE M.A.C. AT.....	51.635	110.664	106.114	0.000	(FT.)
C/4 M.A.C. AT.....	55.417	112.597	109.527	0.000	(FT.)
TE M.A.C. AT.....	66.764	118.395	119.763	0.000	(FT.)
Y M.A.C. AT.....	21.468	8.062	0.000	0.000	
LE TIP AT.....	65.787	119.592	115.230	0.000	(FT.)
C/4 TIP AT.....	67.137	120.359	117.014	0.000	(FT.)
TE TIP AT.....	71.190	122.661	122.365	0.000	(FT.)
ELEVATION.....	-6.290	5.032	6.290	0.000	(FT.)
GEOMETRIC TOTAL VOLUME COEFF		0.771	0.076	0.000	
REQUESTED TOTAL VOLUME COEFF		0.771	0.076	0.000	
ACTUAL TOTAL VOLUME COEFF		0.771	0.076	0.000	

E X T E N S I O N S

	Strake	Rear Extension
Centroid location at.....	0.00	0.00
Area.....	0.00	0.00
Sweep Angle.....	0.00	0.00
Wetted Area.....	0.00	0.00
Volume.....	0.00	0.00

Total Wing Area..... 1450.00
Total Wetted Area..... 7273.48

F U E L T A N K S

Tank	Volume	Weight	Density
Wing	1101.	55033.	50.00
Fus#1	186.	9276.	50.00
Fus#2	0.	0.	50.00
Total		64309.	

Mission Fuel Required = 64309. lbs.
Extra Fuel Carrying Capability = -9276. lbs.
Available Fuel Volume in Wing = 1101. cu.ft.

Aircraft Weight = 152181.000 lbs.
Aircraft Volume = 11693.691 cu.ft.
Aircraft Density = 13.014 lbs./cu.ft.
Actual - Required Fuel Volume = -185.529 cu.ft.

ICASE = 4 (Fineness Ratio Method)

Output for Module # 6

****

Weight Statement - Transport
TRANSPORT

Qmax: 400.
Design Load Factor: 2.50
Ultimate Load Factor: 3.75
Structure and Material: Aluminum Skin, Stringer
Wing Equation: Ardema/Chambers WWING Analysis
Body Equation: Ardema/Chambers PDCYL Analysis

Component	Pounds	Kilograms	Percent	Slope	Tech	Fixed
Airframe Structure	35228.	15979.	21.15			No
Wing	10315.	4679.	6.19	1.20	1.00	No
Fuselage	15652.	7100.	9.40	0.90	1.00	No
Horizontal Tail (Low)	1503.	682.	0.90	1.00	1.00	No
Vertical Tail	1480.	671.	0.89	1.00	1.00	No
Nacelles	4.	2.	0.00	1.00	1.00	No
Landing Gear	6275.	2846.	3.77	1.00	1.00	No
Propulsion	6546.	2969.	3.93			No
Engines (2)	6546.	2969.	3.93	0.85	1.00	Yes
Fuel System	0.	0.	0.00	1.00	1.00	No
Thrust Reverser	0.	0.	0.00	1.00		No
Fixed Equipment	24555.	11138.	14.74		1.00	No
Hyd & Pneumatic	661.	300.	0.40	1.00		No
Electrical	3891.	1765.	2.34	1.00		No
Avionics	2390.	1084.	1.43	1.00		No
Instrumentation	780.	354.	0.47	1.00		No
De-ice & Air Cond	1634.	741.	0.98	1.00		No
Aux Power System	928.	421.	0.56	1.00		No
Furnish & Eqpt	12439.	5642.	7.47	1.00		No
Seats and Lavatories	6600.	2994.	3.96	1.00		No
Galley	1950.	885.	1.17	1.00		No
Misc Cockpit	234.	106.	0.14	1.00		No
Cabin Finishing	2900.	1315.	1.74	1.00		No
Cabin Emergency Equip	405.	184.	0.24	1.00		No
Cargo Handling	350.	159.	0.21	1.00		No
Flight Controls	1831.	831.	1.10	1.00		No
Empty Weight	66329.	30087.	39.82			

Operating Items	4707.	2135.	2.83	No
Flight Crew (2)	340.	154.	0.20	No
Crew Baggage and Provisions	175.	79.	0.11	No
Flight Attendents (4)	520.	236.	0.31	No
Unusable Fuel and Oil	542.	246.	0.33	No
Passenger Service	3130.	1420.	1.88	No
Cargo Containers	0.	0.	0.00	No
Operating Weight Empty	71036.	32222.	42.65	
Fuel	64029.	29043.	38.44	
Payload	31500.	14288.	18.91	No
Passengers (150)	27000.	12247.	16.21	No
Baggage	4500.	2041.	2.70	No
Cargo	0.	0.	0.00	No
Calculated Weight	166565.	75554.	100.00	No
Estimated Weight	152181.	69029.		
Percent Error			9.45	

```
   Calling Module #   1
    Calling Module #   2
      TAKEOFF


  WGTO = 0.1521810E+06  WFTO1 = 0.3242445E+04  WFTO2 = 0.0000000E+00   WFTO = 0.3242445E+04       W = 0.1489386E+06
  HNTO = 0.1500000E+04    CLS = 0.1769708E+01     VS = 0.1337697E+03    V2 = 0.2259222E+03    SMN2 = 0.2034092E+00
   CL2 = 0.1758139E+01    TN2 = 0.0000000E+00   SFC2 = 0.1000000E+01   TN0 = 0.0000000E+00    SFC0 = 0.1000000E+01
 TNAVE = 0.0000000E+00 SFCAVE = 0.1000000E+01   FLTO =-0.1450002E+05



      LANDING


  WGTO = 0.1521810E+06 WFUSED = 0.6402882E+05  WFRES = 0.1176211E+05  WFTOT = 0.6430918E+05  WFUEL = 0.6430918E+05
   WPL = 0.3150000E+05      W = 0.8815213E+05  WLAND = 0.1246486E+06 XGRLAN = 0.1692168E+04 FLLAND = 0.5155803E+04
WGCALC = 0.1524791E+06

    Calling Module #   6
 FROM geometry: body diameter    =   12.58000
                BODY VOLUME      =    9348.345
                BODY LENGTH      =    117.8300
                TAPER RATIO      =   0.2500000
                ASPECT RATIO     =    7.946000
                RATIO 1/4 CHORD  =   0.4040000
                WING SWEEP       =    23.72453
                HOR. TAIL / CL   =   0.9800000
                NOSE VOLUME      =    1811.579
                TAIL VOLUME      =    5780.107
                CL1A             =    24.74486
                CL1B             =    38.87792
                T/C AT ROOT      =   0.1460000
                T/C AT TIP       =   0.1100000
                ENTEMP           =    2.000000
                ENWINGTEMP       =    2.000000
                CLRW1            =   0.2500000
                CLRW2            =   0.0000000E+00
                CLRW3            =   0.0000000E+00
                CLRP1            =   0.0000000E+00
                CLRP2            =   0.0000000E+00
FROM weights.acs SLFMTEMP        =    2.500000
                 FACSTEMP        =    1.500000
                 WFPTEMP         =  4.3013584E-02
                 WINGLTEMP       =    104.9524
                 UWWGTEMP        =    7.110270
                 ARTTEMP         =   0.1389904
```

ASA 2150 Composite

```
                UWTTEMP          =    14.79906
                WWING            =    10309.89
                KWING            =           6
                WGTO             =    152181.0
FROM stblcon.acs CLRG1TEMP   =   0.0000000E+00
                CLRG2TEMP    =   0.0000000E+00
                WFGR1TEMP    =   0.0000000E+00
                WFGR2TEMP    =   0.0000000E+00
From namelist   ICYL         =            1
                WTFF         =   0.2792000
                ISCHRENK     =            1
                ICOMND       =            1
                CLRG1        =   0.1060000
                CLRG2        =   0.0000000E+00
                WFGR1        =   1.2370000E-02
                WFGR2        =   2.8860001E-02
                IGEAR        =            2
                CWMAN        =    1.000000
                ITAIL        =            1
                ISTAMA       =            2
                TMGW         =   2.0000000E-02
                EC           =    2.360000
                KGC          =   0.3680000
                KGW          =   0.5050000
                WGNO         =    1.737200
                CS1          =   0.1500000
                CS2          =   0.3500000
                EFFW         =   0.6560000
                EFFC         =    1.030000
                ESW          =   1.0800000E+07
                FCSW         =    63500.00
                DSW          =   0.1010000
                TRATWR       =   0.1460000
                TRATWT       =   0.1100000
                XCLWNGR      =   0.3764853
                NWING        =           40
                FTST         =    50689.80       50689.80       50689.80
   50689.80      0.0000000E+00  0.0000000E+00  0.0000000E+00  0.0000000E+00
 0.0000000E+00  0.0000000E+00  0.0000000E+00  0.0000000E+00
                FTSB         =    50689.80       50689.80       50689.80
   50689.80      0.0000000E+00  0.0000000E+00  0.0000000E+00  0.0000000E+00
 0.0000000E+00  0.0000000E+00  0.0000000E+00  0.0000000E+00
                FCST         =    47036.48       47036.48       47036.48
   47036.48      0.0000000E+00  0.0000000E+00  0.0000000E+00  0.0000000E+00
 0.0000000E+00  0.0000000E+00  0.0000000E+00  0.0000000E+00
                FCSB         =    47036.48       47036.48       47036.48
   47036.48      0.0000000E+00  0.0000000E+00  0.0000000E+00  0.0000000E+00
 0.0000000E+00  0.0000000E+00  0.0000000E+00  0.0000000E+00
```

```
                EST         =    8160000.        8160000.        8160000.
 8160000.       0.0000000E+00  0.0000000E+00  0.0000000E+00  0.0000000E+00
0.0000000E+00   0.0000000E+00  0.0000000E+00  0.0000000E+00
                ESB         =    8160000.        8160000.        8160000.
 8160000.       0.0000000E+00  0.0000000E+00  0.0000000E+00  0.0000000E+00
0.0000000E+00   0.0000000E+00  0.0000000E+00  0.0000000E+00
                EFT         =    8160000.        8160000.        8160000.
 8160000.       0.0000000E+00  0.0000000E+00  0.0000000E+00  0.0000000E+00
0.0000000E+00   0.0000000E+00  0.0000000E+00  0.0000000E+00
                EFB         =    8160000.        8160000.        8160000.
 8160000.       0.0000000E+00  0.0000000E+00  0.0000000E+00  0.0000000E+00
0.0000000E+00   0.0000000E+00  0.0000000E+00  0.0000000E+00
                DST         =   5.6000002E-02  5.6000002E-02  5.6000002E-02
5.6000002E-02   0.0000000E+00  0.0000000E+00  0.0000000E+00  0.0000000E+00
0.0000000E+00   0.0000000E+00  0.0000000E+00  0.0000000E+00
                DSB         =   5.6000002E-02  5.6000002E-02  5.6000002E-02
5.6000002E-02   0.0000000E+00  0.0000000E+00  0.0000000E+00  0.0000000E+00
0.0000000E+00   0.0000000E+00  0.0000000E+00  0.0000000E+00
                DFT         =   5.6000002E-02  5.6000002E-02  5.6000002E-02
5.6000002E-02   0.0000000E+00  0.0000000E+00  0.0000000E+00  0.0000000E+00
0.0000000E+00   0.0000000E+00  0.0000000E+00  0.0000000E+00
                DFB         =   5.6000002E-02  5.6000002E-02  5.6000002E-02
5.6000002E-02   0.0000000E+00  0.0000000E+00  0.0000000E+00  0.0000000E+00
0.0000000E+00   0.0000000E+00  0.0000000E+00  0.0000000E+00
                PS          =    1.000000
                CF          =   6.2500003E-05
                PGT         =    11.25000        11.25000        11.25000
 11.25000        11.25000        11.25000        11.25000        11.25000
 11.25000        11.25000        11.25000        11.25000
                PGB         =    11.25000        11.25000        11.25000
 11.25000        11.25000        11.25000        11.25000        11.25000
 11.25000        11.25000        11.25000        11.25000
                TMGT        =   3.2000002E-02  3.2000002E-02  3.2000002E-02
3.2000002E-02   0.0000000E+00  0.0000000E+00  0.0000000E+00  0.0000000E+00
0.0000000E+00   0.0000000E+00  0.0000000E+00  0.0000000E+00
                TMGB        =   3.2000002E-02  3.2000002E-02  3.2000002E-02
3.2000002E-02   0.0000000E+00  0.0000000E+00  0.0000000E+00  0.0000000E+00
0.0000000E+00   0.0000000E+00  0.0000000E+00  0.0000000E+00
                CLAQR       =   1.0000000E-03
                CKF         =    5.240000
                WCW         =    3.010000
                WCA         =   0.0000000E+00
                AXAC        =   0.0000000E+00
                IFUEL       =            2
                WMIS        =   0.0000000E+00
                WSUR        =   0.0000000E+00
                KCONT       =            4           4           4           4
        4           4           4           4           4           4
```

4 4

KCONB = 4 4 4 4

4 4 4 4 4 4

4 4

CLBR1 = 1.100000
ILOAD = 3
CMAN = 1.000000
CLAN = 0.7210000
CBUM = 1.000000
WFLAND = 0.9000000
WFBUMP = 1.0000000E-03
VSINK = 10.00000
STROKE = 1.167000
GFRL = 1.0000000E-03
SLFMB = 1.200000
CLRGW1 = 0.2090000
CLRGW2 = 0.0000000E+00

SPAN	BS	ROOTC	TIPC	TAPER	TRATWR	TRATWT	GAML	GAMT	GAMS	VWING	WFUEL	DENW
FT	FT	FT	FT				DEG.	DEG.	DEG.	FT3	LBS	LB/FT3
107.3392	50.764	19.8116	5.4034	0.250	0.146	0.110	23.72453	7.82576	20.000	1269.270	42488.93	41.598

WING STATION FT	CHORD FT	LENGTH FT	LENGTH PRIME FT	BEND MOM FT-LBS	WEB SPACE IN	COVER THICK IN	WEB THICK IN	CGAGE THICK IN	WGAGE THICK IN	UNITWT COVERS LB/FT2	UNITWT WEBS LB/FT2	NJW
50.764	5.4034	2.4504	2.4504	130.	0.1830	0.0543	0.03960	0.0200	0.02000	0.7904	0.5760	3
49.495	5.7636	2.6341	2.6341	1713.	0.3699	0.0543	0.03960	0.0200	0.02000	0.7904	0.5760	3
48.226	6.1238	2.8179	2.8179	5798.	0.5195	0.0543	0.03960	0.0200	0.02000	0.7904	0.5760	3
46.957	6.4840	3.0017	3.0017	12923.	0.6522	0.0543	0.03960	0.0200	0.02000	0.7904	0.5760	3
45.688	6.8442	3.1855	3.1855	23489.	0.7751	0.0543	0.03960	0.0200	0.02000	0.7904	0.5760	3
44.419	7.2044	3.3692	3.3692	37831.	0.8915	0.0543	0.03960	0.0200	0.02000	0.7904	0.5760	3
43.150	7.5646	3.5530	3.5530	56236.	1.0032	0.0543	0.03960	0.0200	0.02000	0.7904	0.5760	3
41.881	7.9249	3.7368	3.7368	78955.	1.1114	0.0543	0.03960	0.0200	0.02000	0.7904	0.5760	3
40.611	8.2851	3.9206	3.9206	106209.	1.2169	0.0543	0.03960	0.0200	0.02000	0.7904	0.5760	3
39.342	8.6453	4.1043	4.1043	138198.	1.3202	0.0543	0.03960	0.0200	0.02000	0.7904	0.5760	3
38.073	9.0055	4.2881	4.2881	175102.	1.4217	0.0543	0.03960	0.0200	0.02000	0.7904	0.5760	3
36.804	9.3657	4.4719	4.4719	217079.	1.5217	0.0567	0.03960	0.0209	0.02000	0.8251	0.5760	5
35.535	9.7259	4.6557	4.6557	264273.	1.6204	0.0634	0.03960	0.0233	0.02000	0.9222	0.5760	5
34.266	10.0861	4.8395	4.8395	316811.	1.7179	0.0700	0.03960	0.0258	0.02000	1.0179	0.5760	5
32.997	10.4463	5.0232	5.0232	374806.	1.8146	0.0765	0.03960	0.0281	0.02000	1.1120	0.5760	5
31.728	10.8065	5.2070	5.2070	438357.	1.9104	0.0828	0.03960	0.0305	0.02000	1.2040	0.5760	5
30.459	11.1667	5.3908	5.3908	507548.	2.0054	0.0889	0.03960	0.0327	0.02000	1.2936	0.5760	5
29.190	11.5269	5.5746	5.5746	582452.	2.0997	0.0949	0.03960	0.0349	0.02000	1.3808	0.5760	5
27.920	11.8871	5.7583	5.7583	663128.	2.1934	0.1007	0.03960	0.0371	0.02000	1.4652	0.5760	5
26.651	12.2473	5.9421	5.9421	749622.	2.2865	0.1064	0.03960	0.0391	0.02000	1.5468	0.5760	5
25.382	12.6075	6.1259	6.1259	841966.	2.3790	0.1118	0.03960	0.0411	0.02000	1.6256	0.5760	5
24.113	12.9677	6.3097	6.3097	940182.	2.4711	0.1170	0.03960	0.0431	0.02000	1.7014	0.5760	5
22.844	13.3279	6.4934	6.4934	1044280.	2.5626	0.1220	0.03960	0.0449	0.02000	1.7743	0.5760	5

21.575	13.6881	6.6772	6.6772	1154256.	2.6537	0.1268	0.03960	0.0467	0.02000	1.8442	0.5760	5
20.306	14.0483	6.8610	6.8610	1270092.	2.7444	0.1314	0.03960	0.0484	0.02000	1.9112	0.5760	5
19.037	14.4085	7.0448	7.0448	1391762.	2.8346	0.1358	0.03960	0.0500	0.02000	1.9751	0.5760	5
17.768	14.7687	7.2286	7.2286	1519224.	2.9243	0.1400	0.03960	0.0515	0.02000	2.0361	0.5760	5
16.498	15.1289	7.4123	7.4123	1652423.	3.0137	0.1440	0.03960	0.0530	0.02000	2.0942	0.5760	5
15.229	15.4891	7.5961	7.5961	1791295.	3.1026	0.1478	0.03960	0.0544	0.02000	2.1493	0.5760	5
13.960	15.8493	7.7799	7.7799	1935760.	3.1911	0.1514	0.03960	0.0557	0.02000	2.2016	0.5760	5
12.691	16.2095	7.9637	7.9637	2085725.	3.2792	0.1548	0.03960	0.0570	0.02000	2.2510	0.5760	5
11.422	16.5697	8.1474	8.1474	2241086.	3.3669	0.1580	0.03960	0.0581	0.02000	2.2977	0.5760	5
10.153	16.9299	8.3312	8.3312	2401725.	3.4541	0.1610	0.03960	0.0592	0.02000	2.3415	0.5760	5
8.884	17.2901	8.5150	8.5150	2567507.	3.5409	0.1638	0.03960	0.0603	0.02000	2.3827	0.5760	5
7.615	17.6503	8.6988	8.6988	2734436.	3.6259	0.1662	0.03960	0.0612	0.02000	2.4177	0.5760	5
6.346	18.0105	8.8825	8.8825	2894486.	3.7066	0.1678	0.03960	0.0618	0.02000	2.4405	0.5760	5
5.076	18.3707	9.0663	9.0582	3059202.	3.7871	0.1693	0.03960	0.0623	0.02000	2.4619	0.5760	5
3.807	18.7309	9.2501	7.3616	3227873.	3.8673	0.1706	0.03960	0.0628	0.02000	2.4814	0.5760	5
2.538	19.0911	9.4339	5.6651	3398988.	3.9467	0.1718	0.03960	0.0632	0.02000	2.4980	0.5760	5
1.269	19.4513	9.6177	3.9685	3571425.	4.0251	0.1727	0.03960	0.0635	0.02000	2.5112	0.5760	5
0.000	19.8115	9.8014	2.2720	3743631.	4.1021	0.1733	0.03960	0.0638	0.02000	2.5204	0.5760	5

CLBOX1	CLINT	CLINTP	LBOX	WBOX	TBOX	NJW	WEBSB	TORK	TTO	TBCOV
FT	FT	FT	FT	FT	FT		FT	FT-LBS	IN	IN
47.603	49.955	59.861	9.9058	11.9334	2.892	5	0.3353	586064.7	0.0134	0.0438

WSHEAR	WBEND	WWING	WSHBOX	WBDBOX	WTOBOX	WWBOX	WWINGT	WPOD	DELTIP
LBS	LBS	LBS	LBS	LBS	LBS	LBS	LBS	LBS	FT
71.50	2532.25	9046.48	31.93	1177.02	59.63	1268.58	10315.06	3272.93	3.849

CONTROL AREA	STRUCTURE AREA	SPLAN
FT2.	FT2.	FT2.
514.99	719.62	1450.

WEIGHTS	WTO	WBOD	WWING	WPROP	WTAIL	CG	RG
	152181.	83574.	52804.	6546.	2983.	53.255	0.000

BODY/PROP	VOLUME	DENSITY	CL1	FIN RAT	LENGTH	WIDTH	ABOD	ASUR	CLP1	CLP2
PARAMETERS	9348.	16.2789	58.915	9.3665	117.830	12.580	1144.9	3596.8	0.00	0.00

TAIL	ATAIL	CLT
PARAMETERS	202.	115.47

CRUISE	WEIGHT	ALPHA	DEFLEC	LIFTB	LIFTW	LIFTT	CLAQW	CLAQB	STAMA	CGM
PARAMETERS	152181.	7.00	-11.50	132.	166974.	-14925.	16.45	0.02	4.72	53.3

MANEUVER	SLFM	ALPHA	DEFLEC	LIFTB	LIFTW	LIFTT
PARAMETERS	2.50	17.50	-28.75	330.	417435.	-37312.

X	Y	BEND MOMENT	WSAV(I)	BMBW	BMBL	BMW	BMP	BMT	BMG	MAX MOMENT
1.96	2.60	-0.3974E+03	219.	-399.	2.	0.	0.	0.	0.	0.3974E+03

3.93	3.31	-0.2581E+04	712.	-2590.	9.	0.	0.	0.	0.	0.2581E+04
5.89	3.81	-0.7710E+04	1417.	-7734.	24.	0.	0.	0.	0.	0.7710E+04
7.86	4.21	-0.1676E+05	2309.	-16806.	47.	0.	0.	0.	0.	0.1676E+05
9.82	4.56	-0.3060E+05	3372.	-30683.	80.	0.	0.	0.	0.	0.3060E+05
11.78	4.86	-0.5006E+05	4595.	-50178.	123.	0.	0.	0.	0.	0.5006E+05
13.75	5.12	-0.8179E+05	5970.	-76054.	176.	0.	0.	0.	-5915.	0.8179E+05
15.71	5.37	-0.1240E+06	7489.	-109036.	241.	0.	0.	0.	-15157.	0.1240E+06
17.67	5.59	-0.1739E+06	9147.	-149820.	318.	0.	0.	0.	-24399.	0.1739E+06
19.64	5.80	-0.2323E+06	10939.	-199073.	407.	0.	0.	0.	-33642.	0.2323E+06
21.60	6.00	-0.2998E+06	12860.	-257442.	509.	0.	0.	0.	-42884.	0.2998E+06
23.57	6.18	-0.3771E+06	14907.	-325555.	624.	0.	0.	0.	-52126.	0.3771E+06
25.53	6.29	-0.4646E+06	17068.	-404015.	753.	0.	0.	0.	-61368.	0.4646E+06
27.49	6.29	-0.5629E+06	19250.	-493168.	896.	0.	0.	0.	-70610.	0.5629E+06
29.46	6.29	-0.6718E+06	21432.	-593034.	1053.	0.	0.	0.	-79852.	0.6718E+06
31.42	6.29	-0.7915E+06	23614.	-703614.	1224.	0.	0.	0.	-89095.	0.7915E+06
33.39	6.29	-0.9218E+06	25797.	-824907.	1409.	0.	0.	0.	-98337.	0.9218E+06
35.35	6.29	-0.1063E+07	27979.	-956914.	1608.	0.	0.	0.	-107579.	0.1063E+07
37.31	6.29	-0.1215E+07	30161.	-1099635.	1821.	0.	0.	0.	-116821.	0.1215E+07
39.28	6.28	-0.1374E+07	32342.	-1253067.	4895.	0.	0.	0.	-126063.	0.1374E+07
41.24	6.22	-0.1547E+07	34498.	-1417161.	5038.	0.	0.	0.	-135306.	0.1547E+07
43.20	6.17	-0.1731E+07	36615.	-1591746.	5176.	0.	0.	0.	-144548.	0.1731E+07
45.17	6.11	-0.1925E+07	38694.	-1776630.	5307.	0.	0.	0.	-153790.	0.1925E+07
47.13	6.05	-0.2129E+07	40734.	-1971622.	5432.	0.	0.	0.	-163032.	0.3277E+29
49.10	5.99	-0.2343E+07	42734.	-2176535.	5551.	0.	0.	0.	-172274.	0.2343E+07
51.06	5.93	-0.2611E+07	0.	-2391175.	5662.	-20922.	-1154.	0.	-203004.	0.2611E+07
53.02	5.87	-0.3071E+07	0.	-2615345.	5767.	-119059.	-8748.	0.	-333668.	0.3071E+07
54.99	5.81	-0.3595E+07	0.	-2848849.	5866.	-206138.	-23094.	0.	-522706.	0.3595E+07
56.95	5.74	-0.4021E+07	0.	-3091491.	5957.	-177886.	-43795.	0.	-713745.	0.4021E+07
58.91	5.68	-0.4188E+07	0.	-3343067.	6043.	69967.	-70454.	0.	-850414.	0.4188E+07
60.88	5.61	-0.4006E+07	32660.	-3603380.	6122.	589028.	-101961.	0.	-896168.	0.4006E+07
62.84	5.54	-0.3778E+07	30944.	-3872219.	6195.	1149554.	-134099.	0.	-926973.	0.3778E+07
64.81	5.47	-0.3557E+07	29269.	-4149384.	6262.	1710081.	-166236.	0.	-957778.	0.3557E+07
66.77	5.40	-0.3345E+07	27638.	-4434665.	6325.	2270608.	-198374.	0.	-988583.	0.3345E+07
68.73	5.33	-0.3140E+07	26050.	-4727849.	6382.	2831135.	-230511.	0.	-1019388.	0.3140E+07
70.70	5.25	-0.2943E+07	24505.	-5028724.	6435.	3391663.	-262649.	0.	-1050193.	0.2943E+07
72.66	5.18	-0.2754E+07	23005.	-5337075.	6484.	3952190.	-294786.	0.	-1080997.	0.2754E+07
74.63	5.10	-0.2572E+07	21549.	-5652680.	6529.	4512717.	-326923.	0.	-1111802.	0.1274E+30
76.59	5.01	-0.2397E+07	20139.	-5975320.	6571.	5073245.	-359061.	0.	-1142607.	0.2397E+07
78.55	4.93	-0.2229E+07	18775.	-6304769.	6610.	5633772.	-391198.	0.	-1173412.	0.2229E+07
80.52	4.84	-0.2067E+07	17458.	-6640800.	6647.	6194300.	-423336.	0.	-1204217.	0.2067E+07
82.48	4.75	-0.1912E+07	16189.	-6983183.	6683.	6754827.	-455473.	0.	-1235022.	0.1912E+07
84.44	4.66	-0.1763E+07	14967.	-7331679.	6718.	7315354.	-487611.	0.	-1265827.	0.1763E+07
86.41	4.56	-0.1620E+07	13795.	-7686053.	6752.	7875882.	-519748.	0.	-1296631.	0.1620E+07
88.37	4.46	-0.1482E+07	12673.	-8046055.	6787.	8436409.	-551886.	0.	-1327436.	0.1482E+07
90.34	4.35	-0.1350E+07	11602.	-8411446.	6822.	8996936.	-584023.	0.	-1358241.	0.1350E+07
92.30	4.24	-0.1223E+07	10583.	-8781966.	6860.	9557463.	-616160.	0.	-1389046.	0.1223E+07
94.26	4.13	-0.1101E+07	9617.	-9157360.	6900.	10117991.	-648298.	0.	-1419851.	0.1101E+07
96.23	4.00	-0.9830E+06	8706.	-9537363.	6944.	10678518.	-680435.	0.	-1450656.	0.9830E+06

98.19	3.87	-0.8697E+06	7851.	-9921700.	6993.	11239045.	-712573.	0.	-1481460.	0.8697E+06
100.16	3.73	-0.7604E+06	7053.	-10310093.	7047.	11799573.	-744710.	0.	-1512265.	0.7604E+06
102.12	3.58	-0.6550E+06	6316.	-10702260.	7109.	12360100.	-776848.	0.	-1543070.	0.6550E+06
104.08	3.42	-0.5530E+06	5640.	-11097895.	7178.	12920627.	-808985.	0.	-1573875.	0.5530E+06
106.05	3.24	-0.4541E+06	5028.	-11496694.	7258.	13481155.	-841123.	0.	-1604680.	0.4541E+06
108.01	3.04	-0.3580E+06	4483.	-11898332.	7349.	14041682.	-873260.	0.	-1635485.	0.3580E+06
109.97	2.81	-0.2645E+06	4010.	-12302474.	7454.	14602209.	-905398.	0.	-1666290.	0.2645E+06
111.94	2.54	-0.1731E+06	3613.	-12708749.	7575.	15162737.	-937535.	0.	-1697094.	0.1731E+06
113.90	2.21	-0.8337E+05	3299.	-13116777.	7716.	15723264.	-969672.	0.	-1727899.	0.8337E+05
115.87	1.73	-0.1254E+05	98.	-13526116.	7881.	16283791.	-1001810.	-17587.	-1758704.	0.1254E+05

LANDING	WEIGHT	ALPHA	DEFLEC	LIFTB	LIFTW	LIFTT	CLAQW	CLAQB	STAMA	CGM
PARAMETERS	109722.	7.00	-149.10	-43.	-54239.	153032.	16.45	0.02	6.55	51.1

LANDING	SLFM	ALPHA	DEFLEC	LIFTB	LIFTW	LIFTT	FGEAR
PARAMETERS	2.58	7.00	******	-43.	-54239.	153032.	184619.

X	Y	BEND MOMENT	WSAV(I)	BMBW	BMBL	BMW	BMP	BMT	BMG	MAX MOMENT
1.96	2.60	-0.4127E+03	219.	-412.	0.	0.	0.	0.	0.	0.4127E+03
3.93	3.31	-0.2677E+04	712.	-2676.	-1.	0.	0.	0.	0.	0.2677E+04
5.89	3.81	-0.7993E+04	1417.	-7990.	-3.	0.	0.	0.	0.	0.7993E+04
7.86	4.21	-0.1737E+05	2309.	-17361.	-6.	0.	0.	0.	0.	0.1737E+05
9.82	4.56	-0.3171E+05	3372.	-31697.	-10.	0.	0.	0.	0.	0.3171E+05
11.78	4.86	-0.5185E+05	4595.	-51836.	-16.	0.	0.	0.	0.	0.5185E+05
13.75	5.12	-0.8447E+05	5970.	-78567.	-23.	0.	0.	0.	-5878.	0.8447E+05
15.71	5.37	-0.1277E+06	7489.	-112639.	-31.	0.	0.	0.	-15063.	0.1277E+06
17.67	5.59	-0.1791E+06	9147.	-154770.	-41.	0.	0.	0.	-24248.	0.1791E+06
19.64	5.80	-0.2391E+06	10939.	-205650.	-53.	0.	0.	0.	-33433.	0.2391E+06
21.60	6.00	-0.3086E+06	12860.	-265948.	-66.	0.	0.	0.	-42618.	0.3086E+06
23.57	6.18	-0.3882E+06	14907.	-336311.	-81.	0.	0.	0.	-51803.	0.3882E+06
25.53	6.29	-0.4785E+06	17068.	-417364.	-98.	0.	0.	0.	-60988.	0.4785E+06
27.49	6.29	-0.5798E+06	19250.	-509462.	-116.	0.	0.	0.	-70173.	0.5798E+06
29.46	6.29	-0.6921E+06	21432.	-612628.	-137.	0.	0.	0.	-79358.	0.6921E+06
31.42	6.29	-0.8156E+06	23614.	-726861.	-159.	0.	0.	0.	-88543.	0.8156E+06
33.39	6.29	-0.9501E+06	25797.	-852162.	-183.	0.	0.	0.	-97728.	0.9501E+06
35.35	6.29	-0.1096E+07	27979.	-988530.	-209.	0.	0.	0.	-106913.	0.1096E+07
37.31	6.29	-0.1252E+07	30161.	-1135967.	-237.	0.	0.	0.	-116098.	0.1252E+07
39.28	6.28	-0.1420E+07	32342.	-1294469.	-636.	0.	0.	0.	-125283.	0.1420E+07
41.24	6.22	-0.1599E+07	34498.	-1463984.	-655.	0.	0.	0.	-134468.	0.1599E+07
43.20	6.17	-0.1789E+07	36615.	-1644337.	-672.	0.	0.	0.	-143653.	0.1789E+07
45.17	6.11	-0.1989E+07	38694.	-1835330.	-690.	0.	0.	0.	-152838.	0.1989E+07
47.13	6.05	-0.2199E+07	40734.	-2036764.	-706.	0.	0.	0.	-162023.	0.2199E+07
49.10	5.99	-0.2420E+07	42734.	-2248447.	-721.	0.	0.	0.	-171208.	0.2420E+07
51.06	5.93	-0.2308E+07	0.	-2470179.	-736.	5934.	-1192.	0.	158344.	0.2611E+07
53.02	5.87	-0.6145E+06	0.	-2701755.	-749.	33770.	-9037.	0.	2063313.	0.3071E+07
54.99	5.81	0.1979E+07	0.	-2942975.	-762.	58469.	-23857.	0.	4888512.	0.3595E+07
56.95	5.74	0.4556E+07	0.	-3193633.	-774.	50455.	-45242.	0.	7745263.	0.4556E+07
58.91	5.68	0.6198E+07	0.	-3453522.	-785.	-19845.	-72782.	0.	9744895.	0.6198E+07

60.88	5.61	0.6316E+07	32660.	-3722435.	-795.	-167071.	-105330.	0.	10311309.	0.6316E+07
62.84	5.54	0.6176E+07	30944.	-4000157.	-805.	-326058.	-138529.	0.	10642047.	0.6176E+07
64.81	5.47	0.6029E+07	29269.	-4286480.	-814.	-485045.	-171729.	0.	10972785.	0.6029E+07
66.77	5.40	0.5873E+07	27638.	-4581186.	-822.	-644032.	-204928.	0.	11303525.	0.5873E+07
68.73	5.33	0.5708E+07	26050.	-4884057.	-829.	-803020.	-238127.	0.	11634264.	0.5708E+07
70.70	5.25	0.5536E+07	24505.	-5194873.	-836.	-962007.	-271326.	0.	11965003.	0.5536E+07
72.66	5.18	0.5356E+07	23005.	-5513412.	-842.	-1120994.	-304526.	0.	12295742.	0.5356E+07
74.63	5.10	0.5168E+07	21549.	-5839444.	-848.	-1279982.	-337725.	0.	12626481.	0.5168E+07
76.59	5.01	0.4974E+07	20139.	-6172745.	-854.	-1438969.	-370924.	0.	12957220.	0.4974E+07
78.55	4.93	0.4772E+07	18775.	-6513078.	-859.	-1597956.	-404124.	0.	13287959.	0.4772E+07
80.52	4.84	0.4563E+07	17458.	-6860212.	-864.	-1756944.	-437323.	0.	13618698.	0.4563E+07
82.48	4.75	0.4348E+07	16189.	-7213907.	-868.	-1915931.	-470522.	0.	13949437.	0.4348E+07
84.44	4.66	0.4127E+07	14967.	-7573917.	-873.	-2074918.	-503721.	0.	14280176.	0.4127E+07
86.41	4.56	0.3899E+07	13795.	-7939999.	-877.	-2233906.	-536921.	0.	14610915.	0.3899E+07
88.37	4.46	0.3666E+07	12673.	-8311897.	-882.	-2392893.	-570120.	0.	14941654.	0.3666E+07
90.34	4.35	0.3427E+07	11602.	-8689360.	-886.	-2551880.	-603319.	0.	15272394.	0.3427E+07
92.30	4.24	0.3183E+07	10583.	-9072122.	-891.	-2710868.	-636518.	0.	15603133.	0.3183E+07
94.26	4.13	0.2933E+07	9617.	-9459920.	-897.	-2869855.	-669718.	0.	15933872.	0.2933E+07
96.23	4.00	0.2679E+07	8706.	-9852477.	-902.	-3028842.	-702917.	0.	16264611.	0.2679E+07
98.19	3.87	0.2421E+07	7851.	-10249512.	-909.	-3187830.	-736116.	0.	16595349.	0.2421E+07
100.16	3.73	0.2158E+07	7053.	-10650738.	-916.	-3346817.	-769316.	0.	16926088.	0.2158E+07
102.12	3.58	0.1892E+07	6316.	-11055862.	-924.	-3505804.	-802515.	0.	17256826.	0.1892E+07
104.08	3.42	0.1622E+07	5640.	-11464569.	-933.	-3664791.	-835714.	0.	17587568.	0.1622E+07
106.05	3.24	0.1348E+07	5028.	-11876544.	-943.	-3823779.	-868913.	0.	17918306.	0.1348E+07
108.01	3.04	0.1072E+07	4483.	-12291453.	-955.	-3982766.	-902113.	0.	18249046.	0.1072E+07
109.97	2.81	0.7928E+06	4010.	-12708947.	-968.	-4141753.	-935312.	0.	18579784.	0.7928E+06
111.94	2.54	0.5116E+06	3613.	-13128646.	-984.	-4300741.	-968511.	0.	18910524.	0.5116E+06
113.90	2.21	0.2287E+06	3299.	-13550155.	-1003.	-4459728.	-1001710.	0.	19241262.	0.2287E+06
115.87	1.73	0.1426E+04	98.	-13973018.	-1024.	-4618715.	-1034910.	57091.	19572002.	0.1254E+05

BUMP	WEIGHT	ALPHA	DEFLEC	LIFTB	LIFTW	LIFTT	CLAQW	CLAQB	STAMA	CGM
PARAMETERS	152181.	7.00	-57.45	-126.	-159141.	159419.	16.45	0.02	4.72	53.3

BUMP	SLFM	ALPHA	DEFLEC	LIFTB	DEFLTW	LIFTT	FGEAR
PARAMETERS	1.20	7.00	-57.45	-126.	-159141.	159419.	182465.

X	Y	BEND MOMENT	WSAV(I)	BMBW	BMBL	BMW	BMP	BMT	BMG	MAX MOMENT
1.96	2.60	-0.1923E+03	219.	-192.	-1.	0.	0.	0.	0.	0.4127E+03
3.93	3.31	-0.1247E+04	712.	-1243.	-4.	0.	0.	0.	0.	0.2677E+04
5.89	3.81	-0.3722E+04	1417.	-3712.	-9.	0.	0.	0.	0.	0.7993E+04
7.86	4.21	-0.8085E+04	2309.	-8067.	-18.	0.	0.	0.	0.	0.1737E+05
9.82	4.56	-0.1476E+05	3372.	-14728.	-30.	0.	0.	0.	0.	0.3171E+05
11.78	4.86	-0.2413E+05	4595.	-24086.	-47.	0.	0.	0.	0.	0.5185E+05
13.75	5.12	0.2939E+05	5970.	-36506.	-67.	0.	0.	0.	65966.	0.8447E+05
15.71	5.37	0.1166E+06	7489.	-52337.	-92.	0.	0.	0.	169037.	0.1277E+06
17.67	5.59	0.2001E+06	9147.	-71913.	-121.	0.	0.	0.	272109.	0.2001E+06
19.64	5.80	0.2795E+06	10939.	-95555.	-155.	0.	0.	0.	375181.	0.2795E+06
21.60	6.00	0.3545E+06	12860.	-123572.	-194.	0.	0.	0.	478253.	0.3545E+06

23.57	6.18	0.4248E+06	14907.	-156266.	-238.	0.	0.	0.	581324.	0.4248E+06
25.53	6.29	0.4902E+06	17068.	-193927.	-287.	0.	0.	0.	684396.	0.4902E+06
27.49	6.29	0.5504E+06	19250.	-236721.	-342.	0.	0.	0.	787468.	0.5798E+06
29.46	6.29	0.6055E+06	21432.	-284656.	-402.	0.	0.	0.	890539.	0.6921E+06
31.42	6.29	0.6554E+06	23614.	-337734.	-467.	0.	0.	0.	993611.	0.8156E+06
33.39	6.29	0.7002E+06	25797.	-395955.	-537.	0.	0.	0.	1096683.	0.9501E+06
35.35	6.29	0.7398E+06	27979.	-459319.	-613.	0.	0.	0.	1199754.	0.1096E+07
37.31	6.29	0.7743E+06	30161.	-527825.	-694.	0.	0.	0.	1302826.	0.1252E+07
39.28	6.28	0.8026E+06	32342.	-601472.	-1866.	0.	0.	0.	1405898.	0.1420E+07
41.24	6.22	0.8268E+06	34498.	-680237.	-1921.	0.	0.	0.	1508969.	0.1599E+07
43.20	6.17	0.8460E+06	36615.	-764038.	-1973.	0.	0.	0.	1612041.	0.1789E+07
45.17	6.11	0.8603E+06	38694.	-852782.	-2023.	0.	0.	0.	1715113.	0.1989E+07
47.13	6.05	0.8697E+06	40734.	-946379.	-2071.	0.	0.	0.	1818185.	0.2199E+07
49.10	5.99	0.8744E+06	42734.	-1044737.	-2116.	0.	0.	0.	1921256.	0.2420E+07
51.06	5.93	0.1130E+07	0.	-1147764.	-2159.	16310.	-554.	0.	2263961.	0.2611E+07
53.02	5.87	0.2552E+07	0.	-1255365.	-2199.	92814.	-4199.	0.	3721168.	0.3071E+07
54.99	5.81	0.4609E+07	0.	-1367448.	-2236.	160697.	-11085.	0.	5829373.	0.4609E+07
56.95	5.74	0.6591E+07	0.	-1483916.	-2271.	138673.	-21022.	0.	7959901.	0.6591E+07
58.91	5.68	0.7789E+07	0.	-1604672.	-2304.	-54543.	-33818.	0.	9484074.	0.7789E+07
60.88	5.61	0.7754E+07	32660.	-1729622.	-2334.	-459183.	-48941.	0.	9994344.	0.7754E+07
62.84	5.54	0.7516E+07	30944.	-1858665.	-2362.	-896147.	-64367.	0.	10337888.	0.7516E+07
64.81	5.47	0.7274E+07	29269.	-1991705.	-2387.	-1333112.	-79793.	0.	10681432.	0.7274E+07
66.77	5.40	0.7029E+07	27638.	-2128639.	-2411.	-1770077.	-95219.	0.	11024978.	0.7029E+07
68.73	5.33	0.6779E+07	26050.	-2269368.	-2433.	-2207042.	-110645.	0.	11368523.	0.6779E+07
70.70	5.25	0.6526E+07	24505.	-2413788.	-2453.	-2644007.	-126071.	0.	11712068.	0.6526E+07
72.66	5.18	0.6269E+07	23005.	-2561796.	-2472.	-3080972.	-141497.	0.	12055613.	0.6269E+07
74.63	5.10	0.6009E+07	21549.	-2713286.	-2489.	-3517937.	-156923.	0.	12399158.	0.6009E+07
76.59	5.01	0.5745E+07	20139.	-2868154.	-2505.	-3954902.	-172349.	0.	12742704.	0.5745E+07
78.55	4.93	0.5478E+07	18775.	-3026290.	-2520.	-4391868.	-187775.	0.	13086248.	0.5478E+07
80.52	4.84	0.5208E+07	17458.	-3187584.	-2534.	-4828833.	-203201.	0.	13429793.	0.5208E+07
82.48	4.75	0.4934E+07	16189.	-3351928.	-2548.	-5265798.	-218627.	0.	13773339.	0.4934E+07
84.44	4.66	0.4658E+07	14967.	-3519206.	-2561.	-5702763.	-234053.	0.	14116884.	0.4658E+07
86.41	4.56	0.4379E+07	13795.	-3689305.	-2574.	-6139728.	-249479.	0.	14460429.	0.4379E+07
88.37	4.46	0.4098E+07	12673.	-3862107.	-2587.	-6576693.	-264905.	0.	14803974.	0.4098E+07
90.34	4.35	0.3813E+07	11602.	-4037495.	-2601.	-7013658.	-280331.	0.	15147520.	0.3813E+07
92.30	4.24	0.3527E+07	10583.	-4215344.	-2615.	-7450623.	-295757.	0.	15491064.	0.3527E+07
94.26	4.13	0.3238E+07	9617.	-4395533.	-2631.	-7887588.	-311183.	0.	15834610.	0.3238E+07
96.23	4.00	0.2946E+07	8706.	-4577934.	-2647.	-8324554.	-326609.	0.	16178154.	0.2946E+07
98.19	3.87	0.2653E+07	7851.	-4762416.	-2666.	-8761518.	-342035.	0.	16521700.	0.2653E+07
100.16	3.73	0.2358E+07	7053.	-4948845.	-2687.	-9198483.	-357461.	0.	16865244.	0.2358E+07
102.12	3.58	0.2061E+07	6316.	-5137085.	-2710.	-9635449.	-372887.	0.	17208790.	0.2061E+07
104.08	3.42	0.1762E+07	5640.	-5326990.	-2737.	-10072414.	-388313.	0.	17552336.	0.1762E+07
106.05	3.24	0.1462E+07	5028.	-5518413.	-2767.	-10509379.	-403739.	0.	17895880.	0.1462E+07
108.01	3.04	0.1160E+07	4483.	-5711200.	-2802.	-10946344.	-419165.	0.	18239426.	0.1160E+07
109.97	2.81	0.8570E+06	4010.	-5905188.	-2842.	-11383309.	-434591.	0.	18582970.	0.8570E+06
111.94	2.54	0.5531E+06	3613.	-6100200.	-2888.	-11820274.	-450017.	0.	18926516.	0.5531E+06
113.90	2.21	0.2484E+06	3299.	-6296054.	-2942.	-12257239.	-465443.	0.	19270060.	0.2484E+06
115.87	1.73	0.4214E+04	98.	-6492536.	-3005.	-12694204.	-480869.	61220.	19613606.	0.1254E+05

0

STRUCTURAL PARAMETERS	CKF	FSK	EFF	CK	PG	CF	CTHIC	SAFEFAC	DEFL
	5.2400	0.04504	0.76000	2.0390	11.250	0.6250E-04	0.000	1.500	0.000

1

FUSE STAT FT	BENDING MOMENT FT LBS	THIC IN	SHELL STRESS PSI	EQUIV THICK IN	GAGE THICK IN	FRAME SPACE IN	NJ	SECTION AREA SQ FT	SHELL UNITWT LB/FT2	FRAME UNITWT	MAX BENDING
1.9638	619.015	0.0000	60.8191	0.0400	0.0157	3966.2410	3	21.2041	0.3226	0.0000	LAN
3.9277	4015.657	0.0000	243.2463	0.0400	0.0157	991.6824	3	34.3929	0.3226	0.0000	LAN
5.8915	11989.037	0.0000	547.2716	0.0400	0.0157	440.7740	3	45.6394	0.3226	0.0000	LAN
7.8553	26050.969	0.0000	972.8910	0.0400	0.0157	247.9446	3	55.7851	0.3226	0.0001	LAN
9.8192	47561.238	0.0000	1520.1018	0.0400	0.0157	158.6888	3	65.1837	0.3226	0.0004	LAN
11.7830	77778.055	0.0000	2188.9026	0.0400	0.0157	110.2027	3	74.0269	0.3226	0.0010	LAN
13.7468	126702.141	0.0000	3202.1372	0.0400	0.0157	75.3319	3	82.4333	0.3226	0.0023	LAN
15.7107	191600.266	0.0000	4411.5093	0.0400	0.0157	54.6804	3	90.4832	0.3226	0.0048	LAN
17.6745	300112.031	0.0000	6364.7568	0.0400	0.0157	37.8998	3	98.2337	0.3226	0.0108	BUM
19.6383	419206.312	0.0000	8260.3418	0.0400	0.0157	29.2025	3	105.7277	0.3226	0.0196	BUM
21.6022	531729.500	0.0000	9803.4395	0.0400	0.0157	24.6060	3	112.9981	0.3226	0.0295	BUM
23.5660	637229.750	0.0000	11056.4580	0.0400	0.0157	21.8174	3	120.0712	0.3226	0.0398	BUM
25.5298	735272.000	0.0000	12330.3652	0.0400	0.0157	19.5633	3	124.2313	0.3226	0.0512	BUM
27.4937	869627.625	0.0000	14583.4834	0.0400	0.0157	16.5408	3	124.2313	0.3226	0.0717	LAN
29.4575	1038184.313	0.0000	17410.1465	0.0400	0.0157	13.8553	3	124.2313	0.3226	0.1021	LAN
31.4213	1223344.750	0.0000	20515.2480	0.0400	0.0157	11.7582	3	124.2313	0.3226	0.1418	LAN
33.3852	1425109.750	0.0000	23898.8066	0.0400	0.0157	10.0935	3	124.2313	0.3226	0.1925	LAN
35.3490	1643478.750	0.0000	27560.8105	0.0400	0.0157	8.7524	3	124.2313	0.3226	0.2560	LAN
37.3128	1878452.250	0.0000	31501.2734	0.0400	0.0157	7.6576	3	124.2313	0.3226	0.3344	LAN
39.2767	2130582.000	0.0000	17927.9453	0.0800	0.0392	26.9103	5	123.7931	0.6451	0.0540	LAN
41.2405	2398660.500	0.0000	20543.4434	0.0800	0.0392	23.4842	5	121.6254	0.6451	0.0696	LAN
43.2043	2682994.000	0.0000	23398.9141	0.0800	0.0392	20.6183	5	119.4408	0.6451	0.0887	LAN
45.1682	2983286.250	0.0000	26506.5000	0.0800	0.0392	18.2010	5	117.2388	0.6451	0.1117	LAN
47.1320	3299240.000	0.0000	29879.5664	0.0800	0.0392	16.1464	5	115.0187	0.6451	0.1393	LAN
49.0958	3630565.000	0.0000	22355.2773	0.1200	0.0589	32.3713	5	112.7799	0.9677	0.0510	LAN
51.0597	3915888.750	0.0000	24604.8379	0.1200	0.0589	29.4117	5	110.5216	0.9677	0.0605	MAN
53.0235	4606577.500	0.0000	29553.9219	0.1200	0.0589	24.4864	5	108.2432	0.9677	0.0855	MAN
54.9873	6913951.500	0.0000	27191.8789	0.2000	0.0981	44.3557	5	105.9439	1.6128	0.0425	BUM
56.9512	9887048.000	0.0000	28397.0078	0.2800	0.1373	59.4627	5	103.6227	2.2579	0.0324	BUM
58.9150	11683106.000	0.0000	26702.7754	0.3600	0.1766	81.3027	5	101.2787	2.9030	0.0218	BUM
60.8788	11631395.000	0.0000	27220.9453	0.3600	0.1766	79.7550	5	98.9111	2.9030	0.0221	BUM
62.8427	11274519.000	0.0000	27039.7930	0.3600	0.1766	80.2894	5	96.5186	2.9030	0.0213	BUM
64.8065	10911652.000	0.0000	26842.1113	0.3600	0.1766	80.8807	5	94.1001	2.9030	0.0204	BUM
66.7703	10542948.000	0.0000	26627.1602	0.3600	0.1766	81.5336	5	91.6544	2.9030	0.0196	BUM
68.7342	10168552.000	0.0000	26394.1270	0.3600	0.1766	82.2534	5	89.1801	2.9030	0.0187	BUM
70.6980	9788623.000	0.0000	26142.0918	0.3600	0.1766	83.0464	5	86.6757	2.9030	0.0179	BUM
72.6618	9403313.000	0.0000	25870.0254	0.3600	0.1766	83.9198	5	84.1396	2.9030	0.0170	BUM
74.6257	9012783.000	0.0000	28773.8477	0.3200	0.1569	67.0673	6	81.5699	2.5805	0.0229	BUM
76.5895	8617191.000	0.0000	28418.5586	0.3200	0.1569	67.9058	5	78.9646	2.5805	0.0216	BUM
78.5533	8216694.000	0.0000	28036.1699	0.3200	0.1569	68.8320	5	76.3216	2.5805	0.0203	BUM

80.5172	7811461.500	0.0000	27624.7090	0.3200	0.1569	69.8572	5	73.6382	2.5805	0.0191	BUM
82.4810	7401658.500	0.0000	27181.8398	0.3200	0.1569	70.9954	5	70.9119	2.5805	0.0178	BUM
84.4449	6987453.000	0.0000	26704.8340	0.3200	0.1569	72.2635	5	68.1393	2.5805	0.0165	BUM
86.4087	6569014.500	0.0000	26190.4316	0.3200	0.1569	73.6828	5	65.3170	2.5805	0.0152	BUM
88.3725	6146523.000	0.0000	25634.7813	0.3200	0.1569	75.2799	5	62.4408	2.5805	0.0139	BUM
90.3364	5720152.500	0.0000	28609.2949	0.2800	0.1373	59.0214	6	59.5061	2.2579	0.0189	BUM
92.3002	5290087.500	0.0000	27862.4805	0.2800	0.1373	60.6034	5	56.5072	2.2579	0.0170	BUM
94.2640	4856512.500	0.0000	27048.1484	0.2800	0.1373	62.4280	5	53.4377	2.2579	0.0151	BUM
96.2279	4419615.000	0.0000	26155.6289	0.2800	0.1373	64.5583	5	50.2898	2.2579	0.0133	BUM
98.1917	3979597.500	0.0000	29366.3047	0.2400	0.1177	49.2857	6	47.0541	1.9354	0.0183	BUM
100.1555	3536653.500	0.0000	28088.6504	0.2400	0.1177	51.5275	5	43.7189	1.9354	0.0156	BUM
102.1194	3090988.500	0.0000	26651.9238	0.2400	0.1177	54.3052	5	40.2695	1.9354	0.0129	BUM
104.0832	2642824.500	0.0000	30015.5234	0.2000	0.0981	40.1830	6	36.6869	1.6128	0.0179	BUM
106.0471	2192373.000	0.0000	27727.1777	0.2000	0.0981	43.4994	5	32.9456	1.6128	0.0137	BUM
108.0109	1739874.000	0.0000	31237.0234	0.1600	0.0785	30.8894	6	29.0100	1.2902	0.0192	BUM
109.9747	1285563.000	0.0000	26969.1016	0.1600	0.0785	35.7777	5	24.8271	1.2902	0.0122	BUM
111.9386	829707.000	0.0000	28367.1660	0.1200	0.0589	25.5108	5	20.3117	0.9677	0.0148	BUM
113.9024	372576.000	0.0000	25355.3828	0.0800	0.0392	19.0274	5	15.3064	0.6451	0.0133	BUM
115.8662	18816.750	0.0000	4154.1777	0.0400	0.0157	58.0676	3	9.4367	0.3226	0.0004	MAN
115.8662	0.000	0.0000	0.0000	0.0400	0.0157	58.0676	3	9.4367	0.3226	0.0004	NONE

1 STRUCTURAL WEIGHT SUMMARY

	WEIGHT (LBS)	WEIGHT FRACTION	UNIT WEIGHT (LBS/FT*FT)
SHELL	4927.71	0.0324	1.3737
FRAMES	180.11	0.0012	0.0502
NONOP	10266.71	0.0675	2.8621
SEC	0.00	0.0000	0.0000
TOTAL	15374.53	0.1010	4.2860
VOLPEN	0.00	0.0000	0.0000
GRANTOT	15374.53	0.1010	4.2860

Surface Area, SQF 3587.15
Volume Ratio 1.00000000
BODY WEIGHT 15374.53222656

1

FUSE STAT FT	BENDING MOMENT FT LBS	THIC IN	SHELL STRESS PSI	EQUIV THICK IN	GAGE THICK IN	FRAME SPACE IN	NJ	SECTION AREA SQ FT	SHELL UNITWT LB/FT2	FRAME UNITWT	MAX BENDING
1.9638	619.015	0.0000	60.8191	0.0400	0.0157	3966.2410	3	21.2041	0.3226	0.0000	LAN
3.9277	4015.657	0.0000	243.2463	0.0400	0.0157	991.6824	3	34.3929	0.3226	0.0000	LAN
5.8915	11989.037	0.0000	547.2716	0.0400	0.0157	440.7740	3	45.6394	0.3226	0.0000	LAN
7.8553	26050.969	0.0000	972.8910	0.0400	0.0157	247.9446	3	55.7851	0.3226	0.0001	LAN

9.8192	47561.238	0.0000	1520.1018	0.0400	0.0157	158.6888	3	65.1837	0.3226	0.0004	LAN
11.7830	77778.055	0.0000	2188.9026	0.0400	0.0157	110.2027	3	74.0269	0.3226	0.0010	LAN
13.7468	126702.141	0.0000	3202.1372	0.0400	0.0157	75.3319	3	82.4333	0.3226	0.0023	LAN
15.7107	191600.266	0.0000	4411.5093	0.0400	0.0157	54.6804	3	90.4832	0.3226	0.0048	LAN
17.6745	300112.031	0.0000	6364.7568	0.0400	0.0157	37.8998	3	98.2337	0.3226	0.0108	BUM
19.6383	419206.312	0.0000	8260.3418	0.0400	0.0157	29.2025	3	105.7277	0.3226	0.0196	BUM
21.6022	531729.500	0.0000	9803.4395	0.0400	0.0157	24.6060	3	112.9981	0.3226	0.0295	BUM
23.5660	637229.750	0.0000	11056.4580	0.0400	0.0157	21.8174	3	120.0712	0.3226	0.0398	BUM
25.5298	735272.000	0.0000	12330.3652	0.0400	0.0157	19.5633	3	124.2313	0.3226	0.0512	BUM
27.4937	869627.625	0.0000	14583.4834	0.0400	0.0157	16.5408	3	124.2313	0.3226	0.0717	LAN
29.4575	1038184.313	0.0000	17410.1465	0.0400	0.0157	13.8553	3	124.2313	0.3226	0.1021	LAN
31.4213	1223344.750	0.0000	20515.2480	0.0400	0.0157	11.7582	3	124.2313	0.3226	0.1418	LAN
33.3852	1425109.750	0.0000	23898.8066	0.0400	0.0157	10.0935	3	124.2313	0.3226	0.1925	LAN
35.3490	1643478.750	0.0000	27560.8105	0.0400	0.0157	8.7524	3	124.2313	0.3226	0.2560	LAN
37.3128	1878452.250	0.0000	31501.2734	0.0400	0.0157	7.6576	3	124.2313	0.3226	0.3344	LAN
39.2767	2130582.000	0.0000	17927.9453	0.0800	0.0392	26.9103	5	123.7931	0.6451	0.0540	LAN
41.2405	2398660.500	0.0000	20543.4434	0.0800	0.0392	23.4842	5	121.6254	0.6451	0.0696	LAN
43.2043	2682994.000	0.0000	23398.9141	0.0800	0.0392	20.6183	5	119.4408	0.6451	0.0887	LAN
45.1682	2983286.250	0.0000	26506.5000	0.0800	0.0392	18.2010	5	117.2388	0.6451	0.1117	LAN
47.1320	3299240.000	0.0000	29879.5664	0.0800	0.0392	16.1464	5	115.0187	0.6451	0.1393	LAN
49.0958	3630565.000	0.0000	22355.2773	0.1200	0.0589	32.3713	5	112.7799	0.9677	0.0510	LAN
51.0597	3915888.750	0.0000	24604.8379	0.1200	0.0589	29.4117	5	110.5216	0.9677	0.0605	MAN
53.0235	4606577.500	0.0000	29553.9219	0.1200	0.0589	24.4864	5	108.2432	0.9677	0.0855	MAN
54.9873	6913951.500	0.0000	27191.8789	0.2000	0.0981	44.3557	5	105.9439	1.6128	0.0425	BUM
56.9512	9887048.000	0.0000	28397.0078	0.2800	0.1373	59.4627	5	103.6227	2.2579	0.0324	BUM
58.9150	11683106.000	0.0000	26702.7754	0.3600	0.1766	81.3027	5	101.2787	2.9030	0.0218	BUM
60.8788	11631395.000	0.0000	27220.9453	0.3600	0.1766	79.7550	5	98.9111	2.9030	0.0221	BUM
62.8427	11274519.000	0.0000	27039.7930	0.3600	0.1766	80.2894	5	96.5186	2.9030	0.0213	BUM
64.8065	10911652.000	0.0000	26842.1113	0.3600	0.1766	80.8807	5	94.1001	2.9030	0.0204	BUM
66.7703	10542948.000	0.0000	26627.1602	0.3600	0.1766	81.5336	5	91.6544	2.9030	0.0196	BUM
68.7342	10168552.000	0.0000	26394.1270	0.3600	0.1766	82.2534	5	89.1801	2.9030	0.0187	BUM
70.6980	9788623.000	0.0000	26142.0918	0.3600	0.1766	83.0464	5	86.6757	2.9030	0.0179	BUM
72.6618	9403313.000	0.0000	25870.0254	0.3600	0.1766	83.9198	5	84.1396	2.9030	0.0170	BUM
74.6257	9012783.000	0.0000	28773.8477	0.3200	0.1569	67.0673	6	81.5699	2.5805	0.0229	BUM
76.5895	8617191.000	0.0000	28418.5586	0.3200	0.1569	67.9058	5	78.9646	2.5805	0.0216	BUM
78.5533	8216694.000	0.0000	28036.1699	0.3200	0.1569	68.8320	5	76.3216	2.5805	0.0203	BUM
80.5172	7811461.500	0.0000	27624.7090	0.3200	0.1569	69.8572	5	73.6382	2.5805	0.0191	BUM
82.4810	7401658.500	0.0000	27181.8398	0.3200	0.1569	70.9954	5	70.9119	2.5805	0.0178	BUM
84.4449	6987453.000	0.0000	26704.8340	0.3200	0.1569	72.2635	5	68.1393	2.5805	0.0165	BUM
86.4087	6569014.500	0.0000	26190.4316	0.3200	0.1569	73.6828	5	65.3170	2.5805	0.0152	BUM
88.3725	6146523.000	0.0000	25634.7813	0.3200	0.1569	75.2799	5	62.4408	2.5805	0.0139	BUM
90.3364	5720152.500	0.0000	28609.2949	0.2800	0.1373	59.0214	6	59.5061	2.2579	0.0189	BUM
92.3002	5290087.500	0.0000	27862.4805	0.2800	0.1373	60.6034	5	56.5072	2.2579	0.0170	BUM
94.2640	4856512.500	0.0000	27048.1484	0.2800	0.1373	62.4280	5	53.4377	2.2579	0.0151	BUM
96.2279	4419615.000	0.0000	26155.6289	0.2800	0.1373	64.5583	5	50.2898	2.2579	0.0133	BUM
98.1917	3979597.500	0.0000	29366.3047	0.2400	0.1177	49.2857	6	47.0541	1.9354	0.0183	BUM
100.1555	3536653.500	0.0000	28088.6504	0.2400	0.1177	51.5275	5	43.7189	1.9354	0.0156	BUM
102.1194	3090988.500	0.0000	26651.9238	0.2400	0.1177	54.3052	5	40.2695	1.9354	0.0129	BUM

104.0832	2642824.500	0.0000	30015.5234	0.2000	0.0981	40.1830	6	36.6869	1.6128	0.0179	BUM
106.0471	2192373.000	0.0000	27727.1777	0.2000	0.0981	43.4994	5	32.9456	1.6128	0.0137	BUM
108.0109	1739874.000	0.0000	31237.0234	0.1600	0.0785	30.8894	6	29.0100	1.2902	0.0192	BUM
109.9747	1285563.000	0.0000	26969.1016	0.1600	0.0785	35.7777	5	24.8271	1.2902	0.0122	BUM
111.9386	829707.000	0.0000	28367.1660	0.1200	0.0589	25.5108	5	20.3117	0.9677	0.0148	BUM
113.9024	372576.000	0.0000	25355.3828	0.0800	0.0392	19.0274	5	15.3064	0.6451	0.0133	BUM
115.8662	18816.750	0.0000	4154.1777	0.0400	0.0157	58.0676	3	9.4367	0.3226	0.0004	MAN
115.8662	0.000	0.0000	0.0000	0.0400	0.0157	58.0676	3	9.4367	0.3226	0.0004	NONE

1 STRUCTURAL WEIGHT SUMMARY

	WEIGHT (LBS)	WEIGHT FRACTION	UNIT WEIGHT (LBS/FT*FT)
SHELL	4927.71	0.0324	1.3737
FRAMES	180.11	0.0012	0.0502
NONOP	10266.71	0.0675	2.8621
SEC	0.00	0.0000	0.0000
TOTAL	15374.53	0.1010	4.2860
VOLPEN	0.00	0.0000	0.0000
GRANTOT	15374.53	0.1010	4.2860

Surface Area, SQF	3587.15
Volume Ratio	1.00000000
BODY WEIGHT	15374.53222656

1 STRUCTURAL WEIGHT SUMMARY

	WEIGHT (LBS)	WEIGHT FRACTION	UNIT WEIGHT (LBS/FT*FT)
SHELL	4927.71	0.0324	1.3737
FRAMES	180.11	90.0563	0.0502
NONOP	10266.71	0.0675	2.8621
SEC	0.00	0.0000	0.0000
TOTAL	15374.53	0.1010	4.2860
VOLPEN	0.00	0.0000	0.0000
GRANTOT	15374.53	0.1010	4.2860

Surface Area, SQF	3587.15
Volume Ratio	1.00000000
BODY WEIGHT	15374.53222656

Output for Module # 1

****

Fuselage Definition			Nacelle Definition			Nacelle Location		
X	R	Area	X-Xnose	R	Area	X	Y	Z
0.00	0.00	0.00	0.00	0.70	1.53	39.31	13.42	-6.64
1.24	1.10	3.78	0.37	0.70	1.53	39.31	-13.42	-6.64
2.47	1.81	10.29	0.37	0.70	1.53			
3.71	2.40	18.17	1.76	0.70	1.53			
4.95	2.92	26.85						
6.19	3.38	35.97						
7.42	3.80	45.27						
8.66	4.17	54.55						
9.90	4.50	63.64						
11.14	4.80	72.40						
12.37	5.07	80.73						
13.61	5.31	88.52						
14.85	5.52	95.69						
16.08	5.70	102.17						
17.32	5.86	107.90						
18.56	5.99	112.83						
19.80	6.10	116.91						
21.03	6.18	120.12						
22.27	6.24	122.43						
23.51	6.28	123.83						
24.74	6.29	124.29						
26.16	6.29	124.29						
27.57	6.29	124.29						
28.98	6.29	124.29						
30.40	6.29	124.29						
31.81	6.29	124.29						
33.22	6.29	124.29						
34.64	6.29	124.29						
36.05	6.29	124.29						
37.46	6.29	124.29						
38.88	6.29	124.29						
42.83	6.28	123.83						
46.77	6.24	122.43						
50.72	6.18	120.12						
54.67	6.10	116.91						
58.62	5.99	112.83						
62.56	5.86	107.90						
66.51	5.70	102.17						
70.46	5.52	95.69						
74.41	5.31	88.52						

78.35	5.07	80.73
82.30	4.80	72.40
86.25	4.50	63.64
90.20	4.17	54.55
94.14	3.80	45.27
98.09	3.38	35.97
102.04	2.92	26.85
105.99	2.40	18.17
109.93	1.81	10.29
113.88	1.10	3.78
117.83	0.00	0.00

	Fuselage		Nacelles - 2
Max. Diameter.....	12.580	.....	1.397
Fineness Ratio.....	9.366		
Surface Area.....	3522.634	.....	7.743 (each)
Volume.....	9348.345		

Dimensions of Planar Surfaces (each)

	Wing	H.Tail	V.Tail	Canard	Units
NUMBER OF SURFACES.	1.0	1.0	1.0	1.0	
PLAN AREA.....	1450.0	277.5	203.5	0.0	(SQ.FT.)
SURFACE AREA.....	2923.7	403.1	408.6	0.0	(SQ.FT.)
VOLUME.....	2064.4	106.0	175.0	0.0	(CU.FT.)
SPAN.....	107.339	39.669	15.885	0.000	(FT.)
L.E. SWEEP.....	23.725	37.176	45.001	0.000	(DEG.)
C/4 SWEEP.....	20.000	33.400	39.400	0.000	(DEG.)
T.E. SWEEP.....	7.826	19.921	15.935	0.000	(DEG.)
ASPECT RATIO	7.946	5.670	1.240	0.000	
ROOT CHORD.....	21.614	10.923	18.485	0.000	(FT.)
ROOT THICKNESS.....	37.867	11.797	19.964	0.000	(IN.)
ROOT T/C	0.146	0.090	0.090	0.000	
TIP CHORD.....	5.403	3.069	7.135	0.000	(FT.)
TIP THICKNESS.....	7.133	3.315	7.706	0.000	(IN.)
TIP T/C	0.110	0.090	0.090	0.000	
TAPER RATIO	0.250	0.281	0.386	0.000	
MEAN AERO CHORD....	15.130	7.731	13.648	0.000	(FT.)
LE ROOT AT.....	42.200	104.550	99.345	0.000	(FT.)
C/4 ROOT AT.....	47.603	107.281	103.966	0.000	(FT.)
TE ROOT AT.....	63.814	115.473	117.830	0.000	(FT.)
LE M.A.C. AT.....	51.635	110.664	106.114	0.000	(FT.)
C/4 M.A.C. AT.....	55.417	112.597	109.527	0.000	(FT.)
TE M.A.C. AT.....	66.764	118.395	119.763	0.000	(FT.)
Y M.A.C. AT.....	21.468	8.062	0.000	0.000	
LE TIP AT.....	65.787	119.592	115.230	0.000	(FT.)
C/4 TIP AT.....	67.137	120.359	117.014	0.000	(FT.)
TE TIP AT.....	71.190	122.661	122.365	0.000	(FT.)
ELEVATION.....	-6.290	5.032	6.290	0.000	(FT.)
GEOMETRIC TOTAL VOLUME COEFF	0.771	0.076	0.000		
REQUESTED TOTAL VOLUME COEFF	0.771	0.076	0.000		
ACTUAL TOTAL VOLUME COEFF	0.771	0.076	0.000		

E X T E N S I O N S

	Strake	Rear Extension
Centroid location at.....	0.00	0.00
Area.....	0.00	0.00
Sweep Angle.....	0.00	0.00
Wetted Area.....	0.00	0.00
Volume.....	0.00	0.00

Total Wing Area..... 1450.00
Total Wetted Area..... 7273.48

F U E L T A N K S

Tank	Volume	Weight	Density
Wing	1101.	55033.	50.00
Fus#1	186.	9276.	50.00
Fus#2	0.	0.	50.00
Total		64309.	

Mission Fuel Required = 64309. lbs.
Extra Fuel Carrying Capability = -9276. lbs.
Available Fuel Volume in Wing = 1101. cu.ft.

Aircraft Weight = 152181.000 lbs.
Aircraft Volume = 11693.691 cu.ft.
Aircraft Density = 13.014 lbs./cu.ft.
Actual - Required Fuel Volume = -185.529 cu.ft.

ICASE = 4 (Fineness Ratio Method)

Output for Module # 6

****

Weight Statement - Transport
TRANSPORT

Qmax: 400.
Design Load Factor: 2.50
Ultimate Load Factor: 3.75
Structure and Material: Aluminum Skin, Stringer
Wing Equation: Ardema/Chambers WWING Analysis
Body Equation: Ardema/Chambers PDCYL Analysis

Component	Pounds	Kilograms	Percent	Slope	Tech	Fixed
Airframe Structure	34950.	15853.	21.02			No
Wing	10315.	4679.	6.20	1.20	1.00	No
Fuselage	15375.	6974.	9.25	0.90	1.00	No
Horizontal Tail (Low)	1503.	682.	0.90	1.00	1.00	No
Vertical Tail	1480.	671.	0.89	1.00	1.00	No
Nacelles	4.	2.	0.00	1.00	1.00	No
Landing Gear	6275.	2846.	3.77	1.00	1.00	No
Propulsion	6546.	2969.	3.94			No
Engines (2)	6546.	2969.	3.94	0.85	1.00	Yes
Fuel System	0.	0.	0.00	1.00	1.00	No
Thrust Reverser	0.	0.	0.00	1.00		No
Fixed Equipment	24555.	11138.	14.77		1.00	No
Hyd & Pneumatic	661.	300.	0.40	1.00		No
Electrical	3891.	1765.	2.34	1.00		No
Avionics	2390.	1084.	1.44	1.00		No
Instrumentation	780.	354.	0.47	1.00		No
De-ice & Air Cond	1634.	741.	0.98	1.00		No
Aux Power System	928.	421.	0.56	1.00		No
Furnish & Eqpt	12439.	5642.	7.48	1.00		No
Seats and Lavatories	6600.	2994.	3.97	1.00		No
Galley	1950.	885.	1.17	1.00		No
Misc Cockpit	234.	106.	0.14	1.00		No
Cabin Finishing	2900.	1315.	1.74	1.00		No
Cabin Emergency Equip	405.	184.	0.24	1.00		No
Cargo Handling	350.	159.	0.21	1.00		No
Flight Controls	1831.	831.	1.10	1.00		No
Empty Weight	66052.	29961.	39.72			

Operating Items	4707.	2135.	2.83	No
Flight Crew (2)	340.	154.	0.20	No
Crew Baggage and Provisions	175.	79.	0.11	No
Flight Attendents (4)	520.	236.	0.31	No
Unusable Fuel and Oil	542.	246.	0.33	No
Passenger Service	3130.	1420.	1.88	No
Cargo Containers	0.	0.	0.00	No
Operating Weight Empty	70759.	32096.	42.55	
Fuel	64029.	29043.	38.50	
Payload	31500.	14288.	18.94	No
Passengers (150)	27000.	12247.	16.24	No
Baggage	4500.	2041.	2.71	No
Cargo	0.	0.	0.00	No
Calculated Weight	166287.	75428.	100.00	No
Estimated Weight	152181.	69029.		
Percent Error			9.27	

Appendix D

Optimization of Supersonic Transport Trajectories

by

M. Ardema, R. Windhorst, and J. Phillips

NASA/TM-1998-112223

March, 1998

NASA/TM—1998-112223

Optimization of Supersonic Transport Trajectories

Mark D. Ardema and Robert Windhorst
Santa Clara University, Santa Clara, California

James Phillips
Ames Research Center, Moffett Field, California

National Aeronautics and
Space Administration

Ames Research Center
Moffett Field, California 93035-1000

March 1998

Available from:

NASA Center for AeroSpace Information
800 Elkridge Landing Road
Linthicum Heights, MD 21090-2934
Price Code: A 17

National Technical Information Service
5285 Port Royal Road
Springfield, VA 22161
Price Code: A10

CONTENTS

SUMMARY

This paper develops a near-optimal guidance law for generating minimum fuel, time, or cost fixed-range trajectories for supersonic transport aircraft. The approach uses a choice of new state variables along with singular perturbation techniques to time-scale decouple the dynamic equations into multiple equations of single order (second order for the fast dynamics). Application of the maximum principle to each of the decoupled equations, as opposed to application to the original coupled equations, avoids the two point boundary value problem and transforms the problem from one of a functional optimization to one of multiple function optimizations. It is shown that such an approach produces well known aircraft performance results such as minimizing the Brequet factor for minimum fuel consumption and the energy climb path. Furthermore, the new state variables produce a consistent calculation of flight path angle along the trajectory, eliminating one of the deficiencies in the traditional energy state approximation. In addition, jumps in the energy climb path are smoothed out by integration of the original dynamic equations at constant load factor. Numerical results performed for a supersonic transport design show that a pushover dive followed by a pullout at nominal load factors are sufficient maneuvers to smooth the jump.

INTRODUCTION

The purpose of this work is to develop and implement a near-optimal guidance law for use in an aircraft synthesis computer code, such as the ACSYNT code[1] developed at NASA Ames Research Center. Of primary interest is the optimization of supersonic transport trajectories. ACSYNT, like other such codes, models all aspects (aerodynamics, propulsion, structures, weights, etc.) of an aircraft design to produce consistent performance estimates. It is capable of computing "closed" vehicles, that is, designs that meet mission requirements, by iteratively adjusting vehicle parameters. It is also capable of optimizing design parameters, again by iteratively cycling through the code.

A key element of any vehicle synthesis code is the trajectory calculation. Because the trajectory routine is exercised repeatedly in the course of a design study, it must be efficient, robust, and user-friendly. "Exact" trajectory optimization, relying on optimal control theory, requires iterative solution of an unstable two-point boundary-value problem (2PBVP), and therefore is not suitable for this application. Thus simplifying approximations are required.

It has long been known that if there is but one state equation, then the functional optimization problem (2PBVP) reduces to a function one[2,3,4]. A natural and well-established way to effect the required order reduction is to time-scale the system state equations and then apply singular perturbation techniques (see for example refs. 2–9). If each state variable is put on its own time-scale then the problem is thereby reduced to a sequence of function optimizations.

The main problem with completely time-scaling the aircraft dynamics is that speed and altitude are not time-scale separable. This is usually resolved by replacing the speed by the total mechanical energy as a state variable (see for example refs. 2–12), and we adopt this approach here. In addition, another new state variable is introduced to replace the altitude, one which removes the inconsistency in flight path angle[11,13,14] that occurs in the energy dynamics with the usual formulation. This does not

directly impact the energy dynamics solution but increases the accuracy of the altitude/flight path angle dynamics solution.

The energy-state approximation (neglecting all dynamics except the energy dynamics) has been applied with success to a wide variety of aircraft, including high performance supersonic aircraft and launch vehicles. It is perhaps best suited, however, to transport aircraft because the benign maneuvers of these vehicles make the assumptions involved in the energy-state approximation (ESA) less questionable. The ESA has been applied most thoroughly to subsonic transport aircraft by Erzberger[15–17]. The results were so satisfactory that the resulting algorithms currently are being used for on-board guidance in commercial transports.

Applying the ESA to supersonic transports introduces some new features. First, these aircraft have higher speeds and usually longer ranges than do subsonic aircraft. More importantly, due to the rise in drag near transonic speeds, they typically have an instantaneous altitude change in their energy-climb paths. These altitude jumps have been investigated by various means in references 12, 18–22. In this paper, we use the approach of references 12 and 22 to address this problem.

Finally, some numerical results are presented to demonstrate the utility of the method.

DYNAMIC MODELING

Equations of Motion

The equations of vehicle motion in ACSYNT are:

$$\begin{aligned} \dot{m} &= -\beta = -\pi T_m C \\ \dot{x} &= v\cos\gamma \\ \dot{v} &= \frac{T\cos\alpha - D - mg\sin\gamma}{m} \\ \dot{h} &= v\sin\gamma \\ \dot{\gamma} &= \frac{T\sin\alpha + L - mg\cos\gamma}{mv} \end{aligned} \tag{1}$$

These equations assume no winds, thrust direction fixed with respect to the aircraft body, and a non-rotating flat earth. A linear throttle is not assumed; that is, specific fuel consumption, C, varies with thrust. The symbols used here and throughout this report are defined in Appendix A.

To simplify the terms, define the tangential and normal load factors as

$$\begin{aligned} F &= \frac{(T\cos\alpha - D)}{mg} \\ N &= \frac{(T\sin\alpha + L)}{mg} \end{aligned} \tag{2}$$

Then equations (1) become

$$\begin{aligned} \dot{m} &= -\beta \\ \dot{x} &= v\cos\gamma \\ \dot{v} &= g(F - \sin\gamma) \\ \dot{h} &= v\sin\gamma \\ \dot{\gamma} &= \frac{g}{v}(N - \cos\gamma) \end{aligned} \tag{3}$$

In ACSYNT, as in many other vehicle synthesis codes, equations (3) are numerically integrated, with the $\dot{\gamma}$ term set to zero, for a specified set of ordered pairs of altitude and Mach number (or speed). The methods used for this integration are given in Appendix B. The (h, M) points needed for the integration may come from any number of sources, for example a constant dynamic pressure (constant equivalent airspeed) path or an external trajectory optimization. It is our purpose to develop an algorithm that generates these points near-optimally for some prescribed cost functional "on the fly", that is, as the trajectory integration proceeds.

Transformation to New State Variables

Experience has shown that the state variables in equations (3) have a natural time-scale separation for most vehicles and most missions, except that h and v are on almost the same time scale. To time scale separate these variables, we seek a new variable, $E(h, v)$, to replace v, such that the state equation for E is independent of γ[11,13,14]. Taking the time derivative of E and using equations (3):

$$\dot{E} = E_h\,\dot{h} + E_v\,\dot{v} = E_h\,v\sin\gamma + E_v\,g(F - \sin\gamma) \tag{4}$$

Throughout, the following notation will be used: If Q is any function of h and v, then

$$Q_h = \left.\frac{\partial Q}{\partial h}\right|_v , \qquad Q_v = \left.\frac{\partial Q}{\partial v}\right|_h \tag{5}$$

If $\dot{E}$ is to be independent of γ, from equation (4):

$$E_h\,v - E_v\,g = 0$$

The solution of this equation is

$$E = h + \frac{1}{2g}v^2 \tag{6}$$

or any once-differentiable function of this. From equation (6) we see that E is just the total mechanical energy of the aircraft per unit weight. Substituting E for v as a state variable gives

$$\begin{aligned} \dot{m} &= -\beta \\ \dot{x} &= v\cos\gamma \\ \dot{E} &= vF \\ \dot{h} &= v\sin\gamma \\ \dot{\gamma} &= \frac{g}{v}(N - \cos\gamma) \end{aligned} \tag{7}$$

Numerous analyses have shown that there is a strong time-scale separation between E and h (see for example refs. 23, 24). In equations (8), v is to be regarded as a function of E and h, as given by equations (7):

$$v = \sqrt{2g(E-h)} \tag{8}$$

The product vF in the third of equations (7) is usually called the specific excess power.

Equations (7), along with a suitably defined cost functional, define an optimal control problem in the five states m, x, E, h, and γ, with control α (and possibly throttle if it is allowed to vary). The boundary conditions on these states are

$$\begin{aligned} m(0) &= m_0 & m(t_f) &\text{ free} \\ x(0) &= 0 & x(t_f) &= R \\ E(0) &= E_0 & E(t_f) &= E_f \\ h(0) &= h_0 & h(t_f) &= h_f \\ \gamma(0) &= \gamma_0 & \gamma(t_f) &= \gamma_f \end{aligned} \tag{9}$$

where t_f is free.

The following constraints are placed on the trajectory:

1. Maximum dynamic pressure, $q(h,v) \leq q_m$
2. Maximum Mach number, $M(h,v) \leq M_m$
3. Maximum lift coefficient, $c_L(h,v) \leq c_{L_m}$
4. Minimum terrain limit, $h \geq h_m$
5. Maximum loft ceiling (locus of flight conditions for which $F = 0$ for maximum throttle and $\gamma = 0$)

All of these constraints may be written as functions of h and M or of h and E; when drawn in the (h, M) plane (fig. 1) they define the flight envelope. In the context of equations (7) they are state inequality constraints of the form:

$$s_i(h, v) \leq 0 \ ; \qquad i = 1, \cdot\cdot, 5 \tag{10}$$

Optimal control problems with state inequality constraints are a difficult class of problems for several reasons[25,26].

The complete time-scale decoupling of equations (7) will be formulated later. At present, for the sake of dynamic modeling, it is instructive to consider the energy-state approximation (ESA) associated with equations (7); it is:

$$\begin{aligned} m &= \text{const} \\ x &= \text{const} \\ \dot{E} &= vF \\ 0 &= v \sin\gamma \\ 0 &= \frac{g}{v}(N - \cos\gamma) \end{aligned} \tag{11}$$

The fourth of these implies that $\gamma = 0$ and the fifth then gives α as a function of h and E. The problem thus reduces to a single state equation with h (and possibly throttle) as control and E as state. The solution, for a suitable cost functional, may be put into the form (see later)

$$f(h, v) = 0 \tag{12}$$

This will be called the energy-climb path, or ECP. This may be either one of the constraints equations (10) or an interior extremal. One of the main advantages of the ESA is that it converts the state variable inequality constraints, equations (10), into state-dependent control inequality constraints, a much simpler situation from an optimal control point of view.

Since equation (12) generally gives $\dot{h} \neq 0$, γ will not be zero on the ECP, giving a contradiction. What is needed is a new variable that is constant along the ECP. An obvious choice is f itself since by equation (12) $\dot{f} = 0$ along the ECP[11,13,14]. Since $df = f_h\, dh + f_v\, dv = 0$ we have

$$\frac{dv}{dh} = -\frac{f_h}{f_v} \tag{13}$$

But from equations (3)

$$\frac{dv}{dh} = \frac{g(F - \sin\gamma)}{v \sin\gamma} \tag{14}$$

so that

$$\gamma = \sin^{-1}\left(\frac{F}{1 - \frac{v}{g}\frac{f_h}{f_v}}\right) \tag{15}$$

This is the consistent value of γ along the ECP. Also, from equations (3)

$$\dot{f} = f_h\,\dot{h} + f_v\,\dot{v}$$

$$\dot{f} = f_h\,v\sin\gamma + f_v\,g(F - \sin\gamma) \tag{16}$$

Note that the choice of variable f actually depends on the nature of the ECP and may vary along the trajectory. The equations of motion in the new variables are now:

$$\begin{aligned}
\dot{m} &= -\beta \\
\dot{x} &= v\cos\gamma \\
\dot{E} &= vF \\
\dot{f} &= f_h\,v\sin\gamma + f_v\,g(F - \sin\gamma) \\
\dot{\gamma} &= \frac{g}{v}(N - \cos\gamma)
\end{aligned} \tag{17}$$

These equations are entirely equivalent to equations (1).

Some examples of the function f will now be given.

1. ECP on a terrain limit:

$$f(h, v) = h - h_m = 0$$

$$f_h = 1\ , \qquad f_v = 0$$

From equations (15) and (16):

$$\gamma = 0$$

$$\dot{f} = v\sin\gamma$$

2. ECP on a dynamic pressure limit:

$$f(h, v) = \frac{1}{2}\rho(h)v^2 - q_m = 0$$

$$f_h = \frac{1}{2}\rho_h v^2 \quad , \qquad f_v = \rho v$$

$$\gamma = \sin^{-1}\left(\frac{F}{1 - \frac{\rho_h v^2}{2g\rho}}\right)$$

$$\dot{f} = \frac{1}{2}\rho_h v^3 \sin\gamma + \rho v g(F - \sin\gamma)$$

3. ECP an interior unbounded extremal. In this case $(\partial(vF)/\partial h)_E = 0$ so that:

$$f(h,v) = F + vF_v - \frac{v^2}{g}F_h = 0$$

$$f_h = F_h + vF_{vh} - \frac{v^2}{g}F_{hh}$$

$$f_v = 2F_v + vF_{vv} - \frac{2v}{g}F_h - \frac{v^2}{g}F_{hv}$$

$$\gamma = \sin^{-1}\left(\frac{F}{1 - \frac{v(gF_h + gvF_{vh} - v^2F_{hh})}{g(2gF_v + gvF_{vv} - 2vF_h - v^2F_{vh}}}\right)$$

$$\dot{f} = v\left(F_h + vF_{vh} - \frac{v^2}{g}F_{hh}\right)\sin\gamma + g\left(2F_v + vF_{vv} - \frac{2v}{g}F_h - \frac{v^2}{g}F_{hv}\right)(F - \sin\gamma)$$

Since this latter case involves second derivatives of F, usually a severe problem when dealing with numerically defined functions as in the case here, for this case it is probably preferable to compute γ along the ECP directly from equation (14)

$$\gamma = \sin^{-1}\left(\frac{F}{1 + \frac{v}{g}\frac{dv}{dh}}\right) \tag{18}$$

where dv/dh is evaluated numerically along the ESA solution. These examples show that the usual choice of variable in the ESA, h, is only valid when the ECP is on a terrain limit.

Now consider the ESA associated with equations (17):

$$m = \text{const.}$$

$$x = \text{const.}$$

$$\dot{E} = vF$$

$$0 = f_h v \sin\gamma + f_v g(F - \sin\gamma)$$

$$0 = \frac{g}{v}(N - \cos\gamma)$$

The fourth and fifth of these are to be solved for α and γ as functions of E and f. Direct elimination of γ gives

$$0 = f_h v\left(\sqrt{1-N^2}\right) + f_v g\left(F - \sqrt{1-N^2}\right)$$

and thus the restriction $-1 \leq N \leq 1$ must be imposed. Since we will need to consider cases $N > 1$ later on, this restriction is unacceptable. The problem is resolved by making the small γ assumption ($\sin\gamma = \gamma$, $\cos\gamma = 1$), a very good approximation for transport aircraft whose flight path angles are at most a few degrees. Finally then, the equations of motion we shall be dealing with are

$$\begin{aligned}
\dot{m} &= -\beta \\
\dot{x} &= v \\
\dot{E} &= vF \\
\dot{f} &= f_h v\gamma + f_v g(F-\gamma) \\
\dot{\gamma} &= \frac{g}{v}(N-1)
\end{aligned} \tag{19}$$

with boundary conditions

$$\begin{aligned}
m(0) &= m_0 & m(t_f) &\text{ free} \\
x(0) &= 0 & x(t_f) &= R \\
E(0) &= E_0 & E(t_f) &= E_f \\
f(0) &= f_0 & f(t_f) &= f_f \\
\gamma(0) &= \gamma_0 & \gamma(t_f) &= \gamma_f
\end{aligned} \tag{20}$$

where the boundary conditions on E and f are determined by the boundary conditions on h and v, and t_f is free.

OPTIMAL CONTROL AND SINGULAR PERTURBATIONS

The Maximum Principle

All of the equations of motion of the previous section (see for example equations (19)) are of state variable form:

$$\dot{\underline{x}} = \underline{f}(\underline{x}, \underline{u}) \tag{21}$$

where $\underline{x} \in I\!R^n$ is the state and $\underline{u} \in U \subset I\!R^m$ is the control. Suitable boundary conditions on the state vector components are prescribed (see for example eqs. (20)). It is desired to find the components of $\underline{u}$ along the trajectory such that a cost functional

$$J = \int_0^{t_f} \phi(\underline{x}, \underline{u}) dt \tag{22}$$

is minimized. It is assumed that the final time, t_f, is free. Extensions of this basic problem such as for terminal cost or fixed final time are easily made, but are not of interest here.

Theorem (the maximum principle)[25,27,28]: Introduce the variational Hamiltonian function

$$H = \lambda_0 \phi + \sum_{i=1}^{n} \lambda_i \, f_i \tag{23}$$

where the components of the adjoint vector, $\underline{\lambda}$, satisfy the differential equations

$$\dot{\lambda}_i = -\frac{\partial H}{\partial x_i} \; ; \qquad i = 1, \cdot\cdot, n \tag{24}$$

Then, if $\underline{u}$ is an optimal control, there exists a nontrivial solution of equations (24) such that

(a) $\underline{u} = \underset{\underline{u} \in U}{\arg\max} \; H$

(b) $H = 0$

(c) Transversality conditions ("natural" boundary conditions on the λ_i) hold

(d) $\lambda_0 = \text{const.} \leq 0$

In the sequel it is assumed that $\lambda_0 = 0$ does not lead to a solution and therefore we may take $\lambda_0 = -1$ (this scales the adjoint variables λ_i).

The maximum principle gives the control as a function of time or of the state variables. When this function is substituted into equations (21) and (24), the result is a $2n$ dimension $2PBVP$ in the states and adjoints. Exactly n boundary conditions are provided at $t = 0$ and the other n at $t = t_f$ (due to

the transversality conditions). Further, the equations are unstable in the sense that if they are linearized about a nominal trajectory, one-half of the system matrix eigenvalues will have positive real parts and the other negative (unless some are zero). Although many approaches have been developed to solve this class of problem, they are all computationally expensive (requiring repetitive solution of the equations), non-robust (due to the instability), and not user-friendly (requiring extensive input by experts). Thus they are unsuitable for use in a vehicle synthesis code and approximations must be developed for this purpose.

Approximation Techniques

Our basic approach is to reduce the complexity of the trajectory optimization problem by seeking means of reducing the problem to sub-problems of lower order. There are two keys observations in this regard.

First, suppose there is a state variable, say x_j, such that x_j does not appear in the system functions $\underline{f}$ nor the cost function f_0, except for possibly f_j, and the final value of x_j is unspecified. Then from equation (24) and the transversality conditions, the differential equation for the corresponding λ_j and its boundary condition are

$$\dot{\lambda}_j = -\frac{\partial f_j}{\partial x_j}\,\lambda_j \ , \qquad \lambda_j(t_f) = 0$$

The only solution to this linear differential equation for a finite value of $\partial f_j/\partial x_j$ is $\lambda_j \equiv 0$. Thus, from equation (23), we see that the j^{th} state equation does not influence the optimal control; this equation has uncoupled from the problem and may be integrated after the optimal control problem has been solved. This is the reason, for example, that the range equation uncouples from the other equations in the minimum time-to-climb problem.

Second, suppose that there is only one state equation ($\underline{x}$ is a scalar) and one control variable:

$$\dot{x} = f(x,u) \tag{25}$$

with cost functional

$$J = \int_0^{t_f} \phi(x,u)dt \tag{26}$$

We have then, from equations (23) and (24)

$$H = -\phi + \lambda f$$

$$\dot{\lambda} = \frac{\partial \phi}{\partial x} - \lambda\,\frac{\partial f}{\partial x}$$

The maximum principle gives, assuming that unbounded optimal control exists,

$$H = -\phi + \lambda f = 0$$

$$\frac{\partial H}{\partial u} = -\frac{\partial \phi}{\partial u} + \lambda\,\frac{\partial f}{\partial u} = 0$$

Eliminating λ from these two equations gives

$$-\frac{\partial \phi}{\partial u} f + \frac{\partial f}{\partial u} \phi = 0 \tag{27}$$

This may be thought of as an equation for u as a function of x, i.e., a feedback control law.

Alternatively, a direct approach may be used. Combining equations (25) and (26) gives

$$J = \int_0^{t_f} \frac{\phi}{f} dx$$

Thus (ϕ/f) is to be minimized with respect to u holding x fixed. Carrying out this minimization for unbounded control results in exactly equation (27). Actually, a stronger result holds for the single state case; if $\underline{u}$ is a bounded control of several components, then the optimal control is given by[2,3]

$$\underline{u} = \underset{\underline{u} \in U}{\arg\min} \left(\frac{\phi}{f} \right)_{x=\text{const}} \tag{28}$$

Singular Perturbations and Time Scaling

We have just seen that if the dynamic system can be approximated by a single state equation, or by a series of such equations, then the solution may be obtained by elementary means, without solving the 2PBVP. Singular perturbation theory provides a framework for accomplishing this, and indeed many of the references cited in the Introduction use this approach.

The extensive literature on the application of singular perturbation theory to optimal control problems in general and flight path optimization in particular will only be reviewed briefly here.

Perturbation methods have a long history of application in applied mathematics. Noteworthy examples are viscous fluid flow, nonlinear oscillations, and orbital dynamics. Singular perturbation methods were put on a solid mathematical foundation for ordinary differential equations by Tikonov[29] and Vasileva[30]. Initial applications to control were by O'Malley[31] and Kokotovic[32]. The theory concerns differential equations which depend on a parameter in such a way that the solutions as the parameter tends to zero do not approach uniformly the solution with the parameter set to zero.

The regions of nonuniform convergence are modeled by "boundary-layer" equations, a term arising in fluid dynamics. Solutions in the outer regions (away from the boundary layers) and the inner regions (the boundary layers) are independently determined by expanding all system variables in asymptotic power series. These solutions are then "matched" to determine their constants of integration. The final step is to combine the solutions to give uniformly valid approximations to the solution of the original problem. Thus the procedure is termed the method of matched asymptotic expansion (MAE).

Experience has shown that for the highly dynamic maneuvers of high performance fighter/attack type aircraft, carrying out the expansions to first order is required for high accuracy (see refs. 7 and 8 for

example). For low performance aircraft, such as commercial transports, however, zero order analysis has been found to suffice (refs. 15–17 for example). The exception, for supersonic aircraft, is the rapid altitude transition typically occurring at transonic speeds; study of this transition is one of the main objectives of this report and will be taken up in detail later.

In this report, for the most part, we will consider only zero-order approximations and complete time-scale decoupling. For this simple case the elaborate procedures of the MAE method are trivial[8] and do not need to be further explained.

Reference 33 was the first to suggest complete time-scale decoupling and to recognize its advantages. In this approach, a "small" parameter ϵ is inserted into the equations of motion as follows:

$$\dot{x}_0 = f_0(\underline{x}, \underline{u})$$

$$\epsilon \dot{x}_1 = f_1(\underline{x}, \underline{u})$$

$$\vdots$$

$$\epsilon^n \dot{x}_n = f_n(\underline{x}, \underline{u})$$

or

$$\epsilon^i \dot{x}_i = f_i(\underline{x}, \underline{u}) \; ; \qquad i = 0, \cdot\cdot, n \tag{29}$$

where now $\underline{x} = (x_0, x_1, \cdot\cdot, x_n)$. The maximum principle for the system (29) is the same as before, but with (see Theorem 5.1 of ref. 8)

$$H = \lambda_0 \phi + \sum_{i=0}^{n} \lambda_i f_i \tag{30}$$

$$\epsilon^i \dot{\lambda}_i = -\frac{\partial H}{\partial x_i} \; ; \qquad i = 0, \cdot\cdot, n \tag{31}$$

The i^{th} dynamics are obtained by the stretching transformation $t_i = t/\epsilon^i$. Substituting and then setting $\epsilon = 0$ gives (where now the dot denotes differentiation with respect to t_i)

$$\begin{aligned}
&\dot{x}_0 = 0 \qquad \Longrightarrow x_0 = \text{const.} \\
&\quad \vdots \\
&\dot{x}_{i-1} = 0 \qquad \Longrightarrow x_{i-1} = \text{const.} \\
&\dot{x}_i = f_i \\
&0 = f_{i+1} \\
&\quad \vdots \\
&0 = f_n
\end{aligned} \tag{32}$$

Thus the variables on a slower time-scale than x_i are held constant and the variables on a faster time-scale than x_i have their system functions set to zero. In order to be able to apply the maximum principle to this single-state problem, the conditions of Theorem 5.3 of reference 8 must hold. Let $\underline{f}_f = (f_{i+1}, \cdots, f_n)$ and $\underline{x}_f = (x_{i+1}, \cdot\cdot, x_n)$. Then the key condition is that the matrix

$$\left[\frac{\partial \underline{f}_f}{\partial \underline{x}_f} \ , \ \frac{\partial \underline{f}_f}{\partial \underline{u}}\right] \tag{33}$$

have maximum rank evaluated along the solution.

If condition (33) is satisfied, then by the implicit function theorem the equations $\underline{0} = \underline{f}_f$ can be solved for $n - i$ of the components of $\underline{x}_f$ and $\underline{u}$ in terms of the remaining m. After substituting these solutions into $\dot{x}_i = f_i$, the optimal control may be determined directly from equation (28) with f_i replacing f. Alternatively, the equations $\underline{0} = \underline{f}_f$ may be adjoined with ordinary Lagrange multipliers to the Hamiltonian function and the maximum principle applied. This latter method has the advantage that it provides the values of these multipliers. This is of interest because these multipliers are the slow estimates of the adjoint variables associated with the fast states[8].

In the following section, transport aircraft guidance laws will be developed using the following time-scale dynamic model associated with equations (19):

$$\begin{aligned}
\dot{m} &= -\epsilon\beta \\
\dot{x} &= v \\
\epsilon\dot{E} &= vF \\
\epsilon^2\dot{f} &= f_h v\gamma + f_v g(F - \gamma) \\
\epsilon^2\dot{\gamma} &= \frac{g}{v}(N - 1)
\end{aligned} \tag{34}$$

Note that with this formulation the mass is constant on all time-scales to zero order. The implications of this will be discussed later.

Note also that the system is not completely time-scale decoupled because f and γ are on the same time-scale. This was the approach adopted by Ardema (with h replacing f)[7,8]. Calise, on the other hand, time-scale decoupled h and γ[2,3,4,33]. This will be discussed in more detail later.

As a cost functional, following Erzberger a weighted sum of flight time and fuel consumption is adopted[15–17].

$$J = \int_0^{t_f} (K_1 + K_2\beta)dt \tag{35}$$

Since some elements of transport airplane direct operating cost are time dependent and some are fuel consumption dependent, a proper weighting of these two effects by appropriate selection of the parameters K_1 and K_2 will give a close approximation of direct operating cost.

Finally, note that the system dynamics do not depend on state variable x and that therefore the state equation $\dot{x} = v$ would uncouple from the problem if its terminal condition were not specified.

GUIDANCE LAW DEVELOPMENT

Range Dynamics

Setting $\epsilon = 0$ in equations (34) gives the range dynamics:

$$\begin{aligned} \dot{m} &= 0 \\ \dot{x} &= v \\ 0 &= vF \\ 0 &= f_h v\gamma + f_v g(F - \gamma) \\ 0 &= \frac{g}{v}(N - 1) \end{aligned} \tag{36}$$

Thus the single state equation with its boundary conditions is

$$\dot{x} = v \ , \qquad x(0) = 0 \ , \qquad x(t_f) = R \tag{37}$$

subject to

$$\begin{aligned} m &= \text{const} \\ F &= 0 \\ \gamma &= 0 \\ N &= 1 \end{aligned} \tag{38}$$

The matrix (33) evaluated for conditions (38) is

$$\begin{bmatrix} vF_E & vF_f & 0 & vF_\alpha \\ f_v g F_E & f_v g F_f & f_h v - f_v g & f_v g F_\alpha \\ \frac{g}{v}N_E & \frac{g}{v}N_f & 0 & \frac{g}{v}N_\alpha \end{bmatrix} \tag{39}$$

where, if Q is any function of E, f, and α,

$$Q_E = \left.\frac{\partial Q}{\partial E}\right|_{f,\alpha} \ , \qquad Q_f = \left.\frac{\partial Q}{\partial f}\right|_{E,\alpha} \ , \qquad Q_\alpha = \left.\frac{\partial Q}{\partial \alpha}\right|_{f,E} \tag{40}$$

The rank of matrix (39) depends on the energy dynamics solution, which determines f. For example, if the energy dynamics solution is on a terrain limit, then $f = h - h_T$ so that $f_h = 1$ and $f_v = 0$. Thus

the matrix (39) becomes

$$\begin{bmatrix} vF_E & vF_f & 0 & vF_\alpha \\ 0 & 0 & v & 0 \\ \frac{g}{v}N_E & \frac{g}{v}N_f & 0 & \frac{g}{v}N_\alpha \end{bmatrix}$$

For the special case of thrust-aligned-with velocity, $N = L/W$ and N may be taken as the control; the matrix now becomes, with h replacing f,

$$\begin{bmatrix} vF_E & vF_h & 0 & vF_N \\ 0 & 0 & v & 0 \\ 0 & 0 & 0 & \frac{g}{v} \end{bmatrix}$$

Clearly this will have maximum rank if either $F_E \neq 0$ or $F_h \neq 0$.

Assuming that matrix (39) has maximum rank, we may apply the maximum principle to the single state problem defined in equation (37). Although equation (28) could be used to directly determine the optimal control, because the adjoint λ_x will be needed we proceed by forming the Hamiltonian. Note that the constraints (10) are now control constraints and do not need to be adjoined to the Hamiltonian.

Forming the Hamiltonian (see eqs. (23), (35), and (37)):

$$H = -K_1 - K_2\beta + \lambda_x v \tag{41}$$

subject to $F = 0$, $N = 1$ and equations (10). Applying the maximum principle gives the optimal control as

$$h_c, E_c = \underset{h,E}{\arg\min} \left(\frac{K_1 + K_2\beta}{v} \right) \begin{array}{l} F = 0 \\ N = 1 \\ \text{eqs. (11)} \end{array} \tag{42}$$

and the value of λ_x as

$$\lambda_x = \frac{K_1 + K_2\beta_c}{v_c} \tag{43}$$

Equation (42) defines the optimal cruise conditions.

There are two interesting special cases. First, if $K_1 = 1$ and $K_2 = 0$, the problem reduces to

$$v_c = \max(v) \tag{44}$$

as expected for minimum time. Second, if $K_1 = 0$ and $K_2 = 1$ and the fuel-flow varies linearly with throttle near the cruise point, equation (42) is equivalent to

$$h_c, E_c = \arg \max_{h,E} \left[\frac{v(L/D)}{C} \right] \tag{45}$$

where C is the thrust specific fuel consumption. That is, the Brequet factor is to be maximized.

The total range of a transport aircraft is the sum of the ranges covered during the ascent, cruise, and descent portions of the flight. In our analysis of the range dynamics, the ascent and descent portions of the flight occur on a faster time scale and thus do not appear in the determination of the cruise condition.

In Erzberger's analysis of this problem[15–17] he subtracts out the range covered in climb and descent in determining the cruise conditions. This is important in short range flight and in fact Erzberger was able to get good results for flight ranges short enough to be composed entirely of climb and descent. For the long range flights of supersonic transports, of primary interest here, this factor is of less importance. In the context of singular perturbation theory, climb and descent range may be expected to appear as first order corrections.

The range dynamics solution assumes constant mass. Variations in mass between take-off and cruise when determining the cruise point may be expected to be accounted for by first order corrections, not pursued here.

Energy Dynamics

Changing the independent variable to $t_1 = t/\epsilon$ in equations (34) and then setting $\epsilon = 0$ gives (the dot will denote differentiation with respect to t_1 in this section)

$$\begin{aligned} m &= \text{const} \\ x &= \text{const} \\ \dot{E} &= vF \\ \gamma &= \frac{F}{1 - \frac{v}{g}\frac{f_h}{f_v}} \\ N &= 1 \end{aligned} \tag{46}$$

The matrix (33) for this case is

$$\begin{bmatrix} A & f_h v - f_v g & f_v g F_\alpha \\ \frac{g}{v} N_f & 0 & \frac{g}{v} N_\alpha \end{bmatrix} \tag{47}$$

where

$$A = \frac{F}{f_v g - f_h v}\Big[v f_{hh}\, h_f\, f_v\, g + v g\, f_{hv}\, v_f\, f_v + f_h\, v_f\, f_v\, g$$
$$- f_{vh}\, h_f\, g\, f_h\, v - f_{vv}\, v_f\, g\, f_h\, v + \frac{f_v\, g\, (F_h\, h_f + F_v\, v_f)}{F}(f_v\, g - f_h\, v)\Big]$$

For the case of solution on a terrain limit, $f = h - h_T$, $f_h = 1$, $f_v = 0$, $f_{hh} = f_{vv} = f_{hv} = 0$ so that (47) becomes

$$\begin{bmatrix} 0 & v & 0 \\ \frac{g}{v} N_f & 0 & \frac{g}{v} N_\alpha \end{bmatrix}$$

For the special case of thrust-aligned with velocity vector and N replacing α as control, this reduces to

$$\begin{bmatrix} 0 & v & 0 \\ 0 & 0 & \frac{g}{v} \end{bmatrix}$$

which is in agreement with Section 6.2 of reference 8, and clearly has maximum rank if $v \neq 0$.

Forming the Hamiltonian associated with equations (46):

$$H = -K_1 - K_2\beta + \lambda_x v + \lambda_E v F \tag{48}$$

The constraints (10) are state-dependent control constraints for this problem. Maximizing H gives

$$h = \arg \max_h \Big(P \Big)_{\substack{N = 1 \\ E = \text{const}}} \tag{49}$$

where

$$P = \frac{vF}{K_1 + K_2\beta - \lambda_x v} \tag{50}$$

with the value of λ_E as

$$\lambda_E = \frac{1}{P} \tag{51}$$

Note that as h and v approach h_c and v_c, P becomes infinitely large. The three terms in the denominator of P have the following obvious interpretation. In climb, three factors are important: minimizing time (K_1 term), minimizing fuel consumption (K_2), and covering range ($-\lambda_x v$).

For the case of an unbounded local maximum, equation (49) implies

$$\left(\frac{\partial P}{\partial h}\right)_E = 0$$

or, in terms of v and h (see eqs. (5)),

$$P_v - \frac{v}{g}P_h = 0 \tag{52}$$

For this case,

$$f(v,h) = P_v - \frac{v}{g}P_h$$

$$f_h = P_{vh} - \frac{v}{g}P_{hh}$$

$$f_v = P_{vv} - \frac{1}{g}P_h - \frac{v}{g}P_{hv}$$

Substituting into the third of equations (46),

$$\gamma = \frac{F}{1 + \frac{v(gP_{vh} - vP_{hh})}{g(vP_{vh} + P_h - gP_{vv})}} \tag{53}$$

As mentioned earlier, it is probably best to avoid computing numerical second derivatives and use equation (18):

$$\gamma = \frac{F}{1 + \frac{v}{g}\frac{dv}{dh}}$$

instead for the value of γ along the energy dynamics solution.

Fast States Dynamics

Changing the independent variable to $t_2 = t/\epsilon^2$ in equations (34) and then setting $\epsilon = 0$ gives (dot denotes differentiation with respect to t_2):

$$\begin{aligned} m &= \text{const.} \\ x &= \text{const.} \\ E &= \text{const.} \\ \dot{f} &= f_h v\gamma + f_v g(F - \gamma) \\ \dot{\gamma} &= \frac{g}{v}(N - 1) \end{aligned} \tag{54}$$

Our main interest in this paper is to use these equations to model the altitude transition that typically occurs transonically in the energy dynamics solution for supersonic aircraft. There have been three approaches to the solution of equations (54).

Ardema[7,8] for the case of $f = h$, left h and γ on the same time scale and iteratively solved the associated 2PBVP. Although this is not the approach that will be used here, the problem is formulated in general in Appendix C as a starting point for future investigation. Calise[33,34] time-scaled decoupled h and γ and obtained non-iterative solutions for each. This required adding a penalty term on γ to the cost function and a "constrained matching" technique.

The approach used in this paper is a non-optimal one that assumes the fast state dynamics occur at constant load factor, N. This is motivated by reference 22 which showed that the transonic altitude transitions occurring in discontinuous energy dynamics solutions consisted of a push-over followed by a push-up (see fig. 2 which is reproduced from ref. 22). Reference 12 modeled this load factor history by two constant load factor segments and obtained good results. Using a non-optimal approach to the fast dynamics is partially justified by the fact that these altitude transitions take relatively little time and consume relatively little fuel.

One way to approximate the altitude transition is to begin flying a constant minimum load factor flight path when a jump is detected and then switch to a constant maximum load factor when the new branch is crossed; this is the dotted path in figure 3, from reference 12. This is undesirable for two reasons. First, the transition is initiated too late, and second, the transition path overshoots the new branch of the energy dynamics solution. In our approach, we use the fast state dynamics to determine $\overline{v}$, the optimum point for transition through $\overline{E}$ (see fig. 3).

Noting that $F = 0$ because $\dot{E} = 0$, consider the last two of equations (54)

$$\begin{aligned} \dot{f} &= f_h v\gamma - f_v g\gamma \\ \dot{\gamma} &= \frac{gK}{v} \end{aligned} \tag{55}$$

where $K = N - 1$ is a known constant.

Following reference 12, the first of these equations is divided by the second to give an equation in f and γ:

$$\frac{df}{d\gamma} = \frac{v}{gK}(f_h v - f_v g)\gamma$$

$$gK \int \frac{df}{v(vf_h - gf_v)} = \int \gamma d\gamma \tag{56}$$

From equation (9) for $E = \text{const.}$, $dh = -\frac{v}{g}dv$ so that

$$df = f_h dh + f_v dv = \left(f_v - f_h \frac{v}{g}\right) dv$$

Substituting into equation (56) and carrying out the integration gives

$$-K\int\frac{dv}{v}=\int\gamma d\gamma+\text{const.}$$

$$-K\ln v=\frac{1}{2}\gamma^2+\text{const.} \tag{57}$$

Now label the last point on the subsonic climb path as point 1, the first point on the supersonic climb path as point 2, and the load factor transition point by an overbar (see fig. 3). Then equation (57) must hold from point 1 to the transition point with $K_1=N_1-1$ and from the transition to point 2 with $K_2=N_2-1$:

$$-K_1\ln\frac{\overline{v}_A}{v_1}=\frac{1}{2}\left(\overline{\gamma}^2-\gamma_1^2\right)$$

$$-K_2\ln\frac{v_2}{\overline{v}_A}=\frac{1}{2}\left(\gamma_2^2-\overline{\gamma}^2\right)$$

Solving for $\overline{v}$ and $\overline{\gamma}$:

$$\overline{v}_A=\left[\frac{v_2^{K_2}}{v_1^{K_1}}e^{\left(\frac{\gamma_2^2-\gamma_1^2}{2}\right)}\right]^{\frac{1}{K_2-K_1}} \tag{58}$$

$$\overline{\gamma}_A=\sqrt{\frac{2(K_1\gamma_2^2-K_2\gamma_1^2)+4K_1K_2\ln\frac{v_2}{v_1}}{2(K_1-K_2)}}$$

This is the same solution as obtained in reference 12 except that now the values of γ_1 and γ_2 are to be determined according to equation (15).

The transition path is then determined as follows. Constant load factor solutions are generated with load factor N_1 (see Appendix B) which leave the lower energy branch of the climb path at different points. The solution that just achieves $v=\overline{v}$ when $E=\overline{E}$ is chosen and then the load factor is set to N_2 for the transition from $\overline{E}$ to the higher energy branch.

It is also possible to obtain an integrated solution if the small γ assumption is not made (this was not possible in reference 12 because of Coriolis and Earth curvature terms). This may be of importance because γ may become large in some altitude transitions. Now divide the last two of equations (17)

and integrate with $F = 0$:

$$\frac{df}{d\gamma} = \frac{v(f_h v - f_v g)\sin\gamma}{g(N - \cos\gamma)}$$

$$-\int \frac{dv}{v} = \int \frac{\sin\gamma}{N - \cos\gamma} d\gamma + \text{const.}$$

$$-\ln v = \ln(N - \cos\gamma) + \text{const.}$$

$$v(N - \cos\gamma) = \text{const.}$$

Applying this to both branches of the transition

$$\overline{v}_B(N_1 - \cos\overline{\gamma}) = v_1(N_1 - \cos\gamma_1)$$

$$\overline{v}_B(N_2 - \cos\overline{\gamma}) = v_2(N_2 - \cos\gamma_2)$$

or, solving for $\overline{v}$ and $\overline{\gamma}$,

$$\overline{v}_B = \frac{v_2(N_2 - \cos\gamma_2) - v_1(N_1 - \cos\gamma_1)}{N_2 - N_1} \tag{59}$$

$$\overline{\gamma}_B = \cos^{-1}\left[\frac{v_2 N_1(N_2 - \cos\gamma_2) - v_1 N_2(N_1 - \cos\gamma_1)}{v_2(N_2 - \cos\gamma_2) - v_1(N_1 - \cos\gamma_1)}\right]$$

Comparison of equations (58) and (59) shows that the non-small γ solution, $\overline{v}_B$, is just as easy to implement as the small γ solution, $\overline{v}_A$. Also note that, as a check,

$$\lim_{N_1 \to \infty} \overline{v}_A = \lim_{N_1 \to \infty} \overline{v}_B = v_1$$

$$\lim_{N_2 \to \infty} \overline{v}_A = \lim_{N_2 \to \infty} \overline{v}_B = v_2$$

NUMERICAL EXAMPLE

The guidance algorithm developed in the previous section has been implemented in the ACSYNT Computer Code and used to compute near-optimal trajectories for a supersonic transport design. The main characteristics of the design are listed in table 1.

Figure 4 shows maximum thrust of the aircraft as a function of Mach number for various energy levels (recall that a linear throttle is not assumed), and figure 5 shows the total drag for $N = 1$ as a function of Mach for various energy levels, in the region of Mach 1. The transonic drag rise is clearly shown in figure 5, and this raises the possibility that there may be an instantaneous altitude transition in the energy climb path near Mach 1.

The first step of the algorithm is to find the optimum cruise point, as given by equation (42). Figure 6 shows the optimal cruise point at each energy level throughout the flight envelope for minimum fuel ($K_1 = 0$ and $K_2 = 1$). The optimal cruise point is interior to the flight envelope except from about Mach 1.25 to Mach 1.75, for which it is on the loft ceiling bound.

Figure 7 shows the data of figure 6 plotted in a different way, as λ_x vs. Mach (see eq. (43)). This curve has three local minimums, each a locally optimal cruise point. One of these is a subsonic condition at Mach 0.95. The globally optimum point is at Mach 2.4, the highest Mach allowed. From figure 6, this Mach 2.4 cruise point is at an altitude of about 52,500 ft. The Mach 2.4 cruise condition has about a 15% higher cruise efficiency than the Mach 0.95 condition, as measured by λ_x; the Mach 0.95 cruise point would be used for over-land flight.

The next step in the algorithm is determining the climb path. This involves maximizing P (see eqs. (49) and (50)) with respect to h at energy levels from take-off to cruise. Figure 8 plots P as a function of Mach for various energy levels for maximum thrust and again minimum fuel. The maximum dynamic pressure constraint is not applied for this calculation. The value of λ_x used in equation (50) is given by equation (43) for the Mach 2.4 optimal cruise condition. It is seen that for many energy levels P has two or more local maxima in the vicinity of Mach 1; it is the jumping of the global maxima between these local maxima that causes the transonic altitude transition.

The resulting flight path in the Mach-altitude plane is shown in figure 9. The path starts along a terrain limit and then climbs at almost a constant high subsonic Mach. At about 32,500 ft, it instantaneously transitions to about 22,500 ft at Mach 1.25. It then continues up to the cruise point, with a jump to higher altitudes between Mach 1.6 and 1.8. Also shown in figure 9 is the path with the dynamic pressure constraint imposed. It is seen that the unconstrained path violates the constraint by only a small amount between Mach 1.3 and 1.7.

Figure 10 compares the minimum fuel flight path with λ_x included in P in equation (50) with the path with the λ_x term omitted. The latter case corresponds to minimum fuel to climb without regard to a range constraint. The paths are similar except at high speed where the path with λ_x omitted has much higher dynamic pressure (there is no dynamic pressure constraint imposed). A computation was made to verify that including the λ_x term gives better performance. Referring to figure 11, the path with the λ_x term included ended with an airplane weight of 657,310 lb and a range of 836 nm. The path without λ_x ended at 690,683 lb and 349 nm. By the Brequet formula, the range covered in a cruise condition

is (see eq. (45)):

$$R_{\text{cruise}} = \frac{v(L/D)}{C} \ln \frac{m_0}{m_f}$$

At the cruise condition, $v = 2323$ ft/sec, $(L/D) = 9.0$, and $C = 1.315$ lb_{fuel} per hour per $\text{lb}_{\text{thrust}}$. Thus for the same fuel consumed along the path with λ_x, the path without λ_x, has a range of

$$349 + \frac{(9.0)(2323)}{(1.315)} \left(\frac{3600}{6076}\right) \ln \frac{690,683}{657,310} = 815 \text{ nm}$$

Thus the case with λ_x gives 21 nm. more range for the same fuel than the case without λ_x.

Minimum fuel, minimum time ($K_1 = 0$, $K_2 = 1$), and "minimum direct operating cost" climb trajectories are compared in figure 12. For the minimum cost trajectory, $K_1 = \$500$/hr and $K_2 = \$0.0626$/lb; these are the values used in reference 15 for short range subsonic transports, and would likely need to be adjusted for supersonic long range transports. The minimum fuel and minimum time trajectories are quite different. The latter has no transonic altitude transition, whereas the former has a large one. Also, the minimum time path is much lower in altitude in the high supersonic range (the dynamic pressure constraint was relaxed for this calculation and would be violated by the minimum time path). As expected, the minimum cost path is intermediate between the other two, being more like the minimum time path.

One of the principal goals of this research has been to develop an algorithm for computing the trajectory segments connecting the branches of the energy climb path in the transonic region, that is, the altitude transitions. Specifically, equation (50) was used to determine $\overline{v}$, the value of v which is to be obtained when $E = \overline{E}$ (see fig. 3). An iteration is then made to determine where on the subsonic branch of the ECP the departure should be made to achieve this condition. The constant load factor integration as described in Appendix B is used to generate the flight paths.

Figure 13 shows the transition for $N_1 = 0.97$ and $N_2 = 1.05$ for the minimum fuel case in the altitude-Mach plane, and figure 14 shows the same path in the transonic region. The integration is terminated when the flight path angle is equal to the flight path angle on the supersonic branch of the ECP as given by equation (53). The dynamic pressure limit was ignored for this calculation. The figures show that there is a very close match between the altitude transition and the ECP at the termination of the former, and that even mild maneuvers (N_1 and N_2 close to 1) give adequate transition trajectories.

The transition trajectories for the same conditions, but using the linear estimate of $\overline{v}$ as given by equation (58), are shown in figure 15. Comparing figures 14 and 15 shows that the nonlinear solution gives a better match with the supersonic branch of the ECP than does the linear.

The transition trajectory for a more severe load factor maneuver, $N_1 = 0.5$ and $N_2 = 1.5$, is shown in figure 16 (these load factors would not be acceptable for a commercial transport). As compared with a more benign maneuver, as shown in figure 14, the transition through $\overline{E}$ occurs at a much higher altitude and the trajectory is much closer to $\overline{E}$, as expected.

Figure 17 shows the variation of energy rate, vF, as a function of Mach in the transonic region for the mild transition ($N_1 = 0.97$, $N_2 = 1.05$). As expected, the energy rate drops when the load factor is

switched from 0.97 to 1.05, but never gets near zero. Also as expected, the flight path angle, γ, at first decreases, and then increases when the load factor is switched as shown in figure 18; the magnitude of γ stays below 6 deg, making the small γ approximation extremely good.

The same plots are made for the more severe maneuver ($N_1 = 0.5$, $N_2 = 1.5$) in figures 19 and 20. In this case, the energy rate becomes negative after the load factor switch and the magnitude of γ reaches about 22 deg, meaning that equations (59) and not equations (58) should be used for the calculation of the transition point.

CONCLUDING REMARKS

An algorithm for optimizing supersonic transport trajectories suitable for use in an aircraft synthesis computer code has been developed. The algorithm has been implemented in the ACSYNT computer program and illustrated using a typical supersonic transport design.

The algorithm is based on singular perturbation theory and complete time-scale decoupling of the energy-state version of the equations of motion (except for the fast dynamics). This results in replacing the functional optimization problem by a series of function optimization problems.

The first problem is determining the optimal cruise condition. This involves a weighted sum of the importance of time and fuel consumption. The second problem is determining the energy-climb path (ECP) to the cruise condition, which involves a weighted sum of the importance of time, fuel consumption, and cruise efficiency.

For the fast dynamics, a variable is introduced such that the ECP gives a consistent value of the flight path angle. This variable is left on the same time scale as the flight path angle and a nonoptimal solution of the fast dynamics using constant load factor segments is obtained.

Numerical results for a nominal supersonic transport showed the following: (1) The optimal cruise point was at the highest and fastest point in the flight envelope, although there are local optimal cruise points at high subsonic and low supersonic speeds. (2) The ECP for the minimum fuel case had a large transonic altitude transition, the minimum time case had no transition, and the minimum direct operating cost case had a mild transition. (3) The altitude transition solutions gave good matches between the subsonic and supersonic branches of the ECP with operationally acceptable load factors.

There are two obvious shortcomings of the present state of the analysis. First, the weight is held constant during the search for the optimal cruise point. This weight is the gross take-off weight according to the time-scale assumptions, but in practice could be some empirical estimate of the weight at the start of cruise. Second, the range during climb and descent is ignored when optimizing the cruise point. This is obviously a more serious problem at short ranges than for the long ranges of a supersonic transport.

It is expected that both of these shortcomings could be eliminated by solving the time-scaled equations of motion to first order, that is, by expanding all the state variables to first order terms. This is the next obvious step in this research. In addition to solving these problems, the first order solutions will give better overall accuracy to the algorithm.

APPENDIX A – NOMENCLATURE

D = drag
E = mechanical energy
F = normalized tangential force
g = gravity
h = altitude
H = Hamiltonian
J = cost functional
L = lift
m = mass
M = Mach number
q = dynamic pressure
T = thrust
v = velocity
x = range

α = angle of attack
β = fuel flow rate
ϵ = small parameter
γ = flight path angle
λ = adjoint variable
ϕ = cost function
ρ = air density

APPENDIX B – NUMERICAL INTEGRATION OF STATE EQUATIONS

In this appendix we give the algorithms by which the state equations are integrated within ACSYNT. Two cases are of interest. First, the integration of the trajectory when pairs of altitude and energy (equivalently altitude and speed or Mach number) are given; (E_0, h_0), (E_1, h_1), $\cdots$, (E_f, h_f). This is sometimes called path following. Second, the integration of the trajectory when the normal load factor N is held constant.

Path Following

It is assumed that all variables are known at step $n-1$. These values are sought at step n, knowing only E_n and h_n. Of particular interest are the values of t_n, m_n, and x_n. We start with equations (7), with $\dot{\gamma} = 0$, written in finite difference form from step $n-1$ to step n:

$$\begin{aligned} \frac{\Delta m}{\Delta t} &= -\overline{\beta} \\ \frac{\Delta x}{\Delta t} &= \overline{v}\cos\overline{\gamma} \\ \frac{\Delta E}{\Delta t} &= \frac{\overline{v}\,\overline{F}'}{g\overline{m}} \\ \frac{\Delta h}{\Delta t} &= \overline{v}\sin\overline{\gamma} \\ 0 &= \frac{g}{\overline{v}}\left(\overline{N} - \cos\overline{\gamma}\right) \end{aligned} \tag{B1}$$

where $F' = T\cos\alpha - D$ and, if Q is any variable,

$$\Delta Q = Q_n - Q_{n-1}$$

$$\overline{Q} = \frac{Q_n + Q_{n-1}}{2}$$

From the first of equations (B1),

$$m_n = m_{n-1} - \overline{\beta}\Delta t \tag{B2}$$

so that

$$\overline{m} = m_{n-1} - \frac{\overline{\beta}}{2}\Delta t$$

Substituting this into the third of equations (B1) and solving for Δt,

$$\Delta t = \frac{m_{n-1}}{\frac{\overline{v}\,\overline{F}'}{g\Delta E} + \frac{\overline{\beta}}{2}} \tag{B3}$$

Note that $\overline{v}$, ΔE, $\overline{h}$, and $\overline{\beta}$ are all known (the latter if throttle is fixed). The only quantity not known in equation (B3) is $\overline{F}'$, which depends on α. If Δt were known, the fourth of equations (B1) gives $\overline{\gamma}$:

$$\overline{\gamma} = \sin^{-1}\left(\frac{\Delta h}{\overline{v}\Delta t}\right) \tag{B4}$$

The algorithm may now be stated as follows:

1. Guess α_n.

2. Compute Δt from equation (B3).

3. Compute $\overline{\gamma}$ from equation (B4).

4. Check to see if the fifth of equations (B1) is satisfied to a suitable degree of accuracy. If not, select a new α_n by a suitable one-dimensional search procedure and return to step (2). If satisfied, continue.

5. Compute m_n from equation (B2) and t_n and x_n from:

$$t_n = t_{n-1} + \Delta t$$

$$x_n = x_{n-1} + \overline{v}\Delta t \cos\overline{\gamma}$$

Phillips[35] has proposed an alternative integration scheme as follows. The third of equations (B1) is now averaged directly

$$\frac{\Delta E}{\Delta t} = \frac{1}{2g}\left(\frac{v_n F_n'}{m_n} + \frac{v_{n-1}F_{n-1}'}{m_{n-1}}\right)$$

This is then combined with equation (B2) to give

$$\left(\frac{\overline{\beta}F_{n-1}v_{n-1}}{gm_{n-1}}\right)\Delta t^2 - \left(F_n v_n + F_{n-1}v_{n-1} + 2\overline{\beta}\Delta E\right)\Delta t + 2gm_{n-1}\Delta E = 0$$

This is a quadratic equation to be solved for Δt, and replaces equation (B3) in the numerical procedure. As the integration step size tends to zero, these two integration schemes become equivalent.

Constant Normal Load Factor (N) Paths

In this case, ΔE is not a suitable integration variable because it may happen that $\Delta E \leq 0$, which causes serious numerical problems. Alternative choices are Δt and $\Delta\gamma$. Because the choice Δt results in an algorithm with three nested iterations, we follow Phillips[35] and choose $\Delta\gamma$. For this integration we do not neglect $\dot{\gamma}$.

Because N, $\Delta\gamma$, and γ_n are now known,

$$\overline{K} = g(N - \cos\overline{\gamma})$$

is a known constant. Thus the finite difference form of the last of equations (8) is

$$\frac{\Delta\gamma}{\Delta t} = \frac{\overline{K}}{\overline{v}}$$

Use this and equation (B2) to eliminate m_n and Δt from the rest of equations (B1). The result is

$$h_n = h_{n-1} + \left(\frac{\Delta\gamma \sin\overline{\gamma}}{\overline{K}}\right)\left(\frac{v_n + v_{n-1}}{2}\right)^2 \tag{B5}$$

$$\Delta E = \frac{\overline{v}^2 \overline{F}'^2}{\overline{K}\left(\frac{g m_{n-1}}{\Delta\gamma} - \frac{\overline{\beta}\,\overline{v}}{2\,\overline{K}}\right)} \tag{B6}$$

$$0 = N\left(g m_{n-1} - \frac{\overline{\beta}\overline{v}\Delta\gamma}{\overline{K}}\right) - \overline{T}\sin\overline{\alpha} - \overline{L} \tag{B7}$$

The algorithm is as follows:

(1) Guess v_n.

(2) Solve for h_n from equation (B5).

(3) Compute $E_n = h_n + \frac{1}{2g}v_n^2$ and $\Delta E = E_n - E_{n-1}$.

(4) Guess α_n.

(5) Check to see if equation (B7) is satisfied. If not, select a new α_n and repeat this step. If satisfied, continue.

(6) Check to see if equation (B6) is satisfied. If not, select a new v_n and return to step (2). If satisfied, continue.

(7) Compute all other quantities of interest.

Thus this algorithm requires a nested two parameter search, whereas the path following routine required a one parameter search. From equations (B5)–(B7) it is seen that $\overline{K} = 0$ ($N = \cos\overline{\gamma}$) is not allowed. Should this happen, one solution is a Δt integration but, as mentioned earlier, this involves a three parameter search.

Phillips[35] has proposed an alternative method of constant load factor integration with $\Delta\gamma$ as integration variable. This approach holds all variables constant at the previous step but does a second order integration of the altitude state equation. The increments Δt and Δv may be now directly computed from the third and fifth of equations (3):

$$\Delta t = \frac{v_{n-1}}{g(N - \cos\gamma_{n-1})}\Delta\gamma$$

$$\Delta v = g(F_{n-1} - \sin\gamma_{n-1})\Delta t$$

Differentiating the fourth of equations (3):

$$\ddot{h} = \dot{V}\sin\gamma + v\dot{\gamma}\cos\gamma$$

Using the third and fifth of equations (3) this becomes

$$\ddot{h} = g(F_{n-1} \sin \gamma_{n-1} + N \cos \gamma_{n-1} - 1) = C$$

Integrating twice:

$$h = \frac{1}{2} C t^2 + c_1 t$$

The constant of integration c_1 is determined from $\dot{h}_{n-1} = v_{n-1} \sin \gamma_{n-1} = c_1$ so that

$$h_n = v_{n-1} \Delta t \sin \gamma_{n-1} + \frac{1}{2} g \Delta t^2 \left(F_{n-1} \sin \gamma_{n-1} + N \cos \gamma_{n-1} - 1\right)$$

with Δt determined as above. Reference 35 shows that this gives good numerical results.

APPENDIX C – NECESSARY CONDITIONS FOR FAST DYNAMICS

The state equations of the fast dynamics are the last two of equations (54):

$$\begin{aligned} \dot{f} &= f_h\, v\gamma + f_v\, g(F-\gamma) \\ \dot{\gamma} &= \frac{g}{v}(N-1) \end{aligned} \tag{C1}$$

with m, x, and E (the slower states) all known constants; the control variable is α.

From equation (23) the Hamiltonian is

$$\begin{aligned} H = &-K_1 - K_2\beta + \lambda_x\, v + \lambda_E\, vF + \lambda_f\,[f_h\, v\gamma + f_v\, g(F-\gamma)] \\ &+\lambda_\gamma \frac{g}{v}(N-1) + \sum_{i=1}^{5} \nu_i s_i \end{aligned} \tag{C2}$$

where the constraints equations (11) are now state constraints and must be adjoined to H with multipliers ν_i ; the s_i are assumed to be written as functions of f and E, the latter a known constant. The adjoints λ_x and λ_E are known constants from the slower dynamics solutions, equations (43) and (51). From equation (24) the adjoint equations are

$$\begin{aligned} \dot{\lambda}_f = &K_2\beta_f - \lambda_x\, v_f - \lambda_E v_f F - \lambda_E\, vF_f - \lambda_f \Big[(f_h)_f\, v\gamma + f_h\, v_f\gamma + f_v\, gF_f \\ &+ (f_v)_f\, g(F-\gamma)\Big] + \lambda_\gamma \frac{g}{v^2} v_f (N-1) - \lambda_\gamma \frac{g}{v} N_f - \sum_{i=1}^{5} \nu_i s_{f_i} \\ \dot{\lambda}_\gamma = &-\lambda_f\, f_h v + \lambda_f\, f_v g \end{aligned} \tag{C3}$$

where the notations of equations (5) and (40) have been used. In these equations, if $Q(h,v)$ is any function then

$$Q_f = Q_h h_f + Q_v v_f \tag{C4}$$

Assuming an unbounded optimal control, conditions (a) and (b) of the maximum principle give

$$\begin{aligned} &\lambda_E\, vF_\alpha + \lambda_f\, f_v\, gF_\alpha + \lambda_\gamma \frac{g}{v} N_\alpha = 0 \\ &-K_1 - K_2\beta + \lambda_x\, v + \lambda_E vF + \lambda_f[f_h v\gamma + f_v g(F-\gamma)] + \lambda_\gamma \frac{g}{v}(N-1) = 0 \end{aligned} \tag{C5}$$

From equations (2) explicit forms for F_α and N_α are

$$\begin{aligned} F_\alpha &= \frac{1}{mg}\,(T_\alpha \cos\alpha - T\sin\alpha - D_\alpha) \\ N_\alpha &= \frac{1}{mg}\,(T_\alpha \sin\alpha + T\cos\alpha + L_\alpha) \end{aligned} \tag{C6}$$

Equations (C1), (C3), and (C5) are used to model transitions from an initial condition to the energy dynamics solution (energy climb path, or ECP), from the ECP to a terminal condition, and between different branches of the ECP if the ECP is discontinuous. In what follows, the first case, transition from an initial condition to the ECP will be considered for the purpose of illustration.

For this case, the boundary conditions on equations (C1) and (C3) are

$$
\begin{aligned}
& f(0) = f_0 \\
& \gamma(0) = \gamma_0 \\
& \lambda_f(0) = \frac{K_1 + K_2\beta_0 - \lambda_x v_0 - \lambda_E v_0 F_0 - \lambda_\gamma \frac{g}{v_0}(N_0 - 1)}{f_{h_0} v_0 \gamma_0 + f_{v_0}\, g(F_0 - \gamma_0)} \\
& \lambda_\gamma(0) = \lambda_{\gamma_0} \text{ selected to match with ECP}
\end{aligned}
\tag{C7}
$$

where the second of equations (5) was used and where all quantities are known except λ_{γ_0}. In summary, equations (C1) and (C3) are to be integrated with control given by the first of equations (C5) subject to initial conditions equations (C7).

The fast dynamics equations depend on the nature of the ECP solution because this solution determines the choice of variable f. If the ECP solution is an unbounded optimum, singular perturbation theory states that the ECP solution will be an equilibrium point of the fast dynamics,[7,8] and the goal is to find a solution of the fast dynamics such that the solution approaches the ECP as $t \to \infty$. If, on the other hand, the ECP is on a constraint, then the fast dynamics solution may reach the ECP in finite time.[36]

Some examples will now be given. If the ECP is on a terrain limit,

$$f = f(h, v) = h - h_m$$

In this case the transformation $(h, v) \to (E, f)$ and its inverse are given by

$$
\begin{aligned}
E &= h + \frac{1}{2g}v^2 \qquad & h &= f \\
f &= h - h_m \qquad & v &= \sqrt{2g(E - f)}
\end{aligned}
$$

so that

$$f_h = 1\,, \qquad f_v = 0\,, \quad h_f = 1\,, \qquad v_f = -\frac{g}{v}$$

and from equation (C4)

$$Q_f = Q_h - \frac{g}{v}Q_v$$

Putting these results into equations (C1) and (C3)

$$\dot{f} = v\gamma$$

$$\dot{\gamma} = \frac{g}{v}(N-1)$$

$$\dot{\lambda}_f = K_2\left(\beta_h - \frac{g}{v}\beta_v\right) + \lambda_x\frac{g}{v} + \lambda_E\frac{g}{v}F - \lambda_E v\left(F_h - \frac{g}{v}F_v\right) + \lambda_f\frac{g}{v}\gamma$$

$$-\lambda_\gamma\frac{g^2}{v^3}(N-1) - \lambda_\gamma\frac{g}{v}\left(N_h - \frac{g}{v}N_v\right) - \sum_{i=1}^{5}\nu_i\left(s_h - \frac{g}{v}s_v\right)_i$$

$$\dot{\lambda}_\gamma = -\lambda_f v$$

and into equations (C5)

$$\lambda_E v F_\alpha + \lambda_\gamma\frac{g}{v}N_\alpha = 0$$

$$-K_1 - K_2\beta + \lambda_x v + \lambda_E v F + \lambda_f v\gamma + \lambda_\gamma\frac{g}{v}(N-1) = 0$$

The initial conditions for the integration of equations (C7) are as follows:

$$f(0) = f_0$$

$$\gamma(0) = \gamma_0$$

$$\lambda_f(0) = \frac{K_1 + K_2\beta_0 - \lambda_x v_0 - \lambda_E v_0 F_0 - \lambda_{\gamma_0}\frac{g}{v}(N_0 - 1)}{v_0\gamma_0}$$

$\lambda_\gamma(0) = \lambda_{\gamma_0}$. selected to match with ECP

If the ECP is on a dynamic pressure limit, the transformation $(h, v) \rightarrow (E, f)$ is

$$E = h + \frac{1}{2g}v^2$$

$$f = \frac{1}{2}\rho v^2 - q_m$$

with $\rho = \rho(h)$ so that

$$f_h = \frac{1}{2}\rho_h v^2\,, \qquad f_v = \rho v$$

The inverse transformation is implicit. Taking differentials and using the fact that E = const.:

$$dE = dh + \frac{v}{g}dv = 0$$

$$df = \frac{1}{2}\rho_h v^2 dh + \rho v\, dv$$

Combining these equations gives

$$v_f = \frac{1}{v\left(\rho - \frac{\rho_h v^2}{2g}\right)}$$

$$h_f = \frac{1}{\frac{1}{2}\rho_h v^2 - \rho g}$$

Then from equation (C4)

$$Q_f = \frac{Q_h}{\frac{1}{2}\rho_h v^2 - \rho g} + \frac{Q_v}{v\left(\rho - \frac{\rho_h v^2}{2g}\right)}$$

This gives, for example,

$$\rho_f = \frac{\rho_h}{\frac{1}{2}\rho_h v^2 - \rho g}$$

$$(\rho_h)_f = \frac{\rho_{hh}}{\frac{1}{2}\rho_h v^2 - \rho g}$$

$$(f_h)_f = \frac{\frac{1}{2}\rho_{hh} v^2}{\frac{1}{2}\rho_h v^2 - \rho g} + \frac{\rho_h v}{v\left(\rho - \frac{\rho_h v^2}{2g}\right)}$$

$$(f_v)_f = \frac{\rho_h v}{\frac{1}{2}\rho_h v^2 - \rho g} + \frac{\rho}{v\left(\rho - \frac{\rho_h v^2}{2g}\right)}$$

$$F_f = \frac{F_h}{\frac{1}{2}\rho_h v^2 - \rho g} + \frac{F_v}{v\left(\rho - \frac{\rho_h v^2}{2g}\right)}$$

$$\beta_f = \frac{\beta_h}{\frac{1}{2}\rho_h v^2 - \rho g} + \frac{\beta_v}{v\left(\rho - \frac{\rho_h v^2}{2g}\right)}$$

Equations (C1) and (C3) become

$$\dot{f} = \frac{1}{2}\rho_h v^3 \gamma + \rho v g(F - \gamma)$$

$$\dot{\gamma} = \frac{g}{v}(N - 1)$$

$$\dot{\lambda}_f = K_2\beta_f - \lambda_x v_f - \lambda_E v_f F - \lambda_E v F_f - \lambda_f \left[(f_h)_f v\gamma + \frac{1}{2}\rho_h v^2 v_f \gamma + \rho v g\, F_f \right.$$
$$\left. + (f_v)_f g(F - \gamma)\right] + \lambda_\gamma \frac{g}{v^2} v_f (N - 1) - \lambda_\gamma \frac{g}{v} N_f - \sum_{i=1}^{5} \nu_i s_{f_i}$$

$$\dot{\lambda}_\gamma = -\lambda_f \frac{1}{2}\rho_h v^3 + \lambda_f \rho v g$$

and equations (C5) become

$$\lambda_E v F_\alpha + \lambda_v \rho v g F_\alpha + \lambda_\gamma \frac{g}{v} N_\alpha = 0$$

$$-K_1 - K_2\beta + \lambda_x v + \lambda_E v F + \lambda_f \left[\frac{1}{2}\rho_h v^3 \gamma + \rho v g(F - \gamma)\right] + \lambda_\gamma \frac{g}{v}(N - 1) = 0$$

Initial conditions equations (C7) become

$$f(0) = f_0$$

$$\gamma(0) = \gamma_0$$

$$\lambda_f(0) = \frac{K_1 + K_2\beta_0 - \lambda_x v_0 - \lambda_E v_0 F_0 - \lambda_{\gamma_0} \frac{g}{v_0}(N_0 - 1)}{\frac{1}{2}\rho_{h_0} v_0^3 \gamma_0 + \rho_0 v_0 g(F_0 - \gamma_0)}$$

$$\lambda_\gamma(0) = \lambda_{\gamma_0} \text{ selected to match with ECP}$$

In all of these equations, quantities such as v_f, F_f, and $(f_h)_f$ are to be determined from the equations derived above.

Finally, consider the case for which the ECP is an unbounded local optimum. From equation (52), f in this case is

$$f = P_v - \frac{v}{g} P_h$$

where P is given by equation (50). Thus

$$f_h = P_{vh} - \frac{v}{g} P_{hh}$$

$$f_v = P_{vv} - \frac{1}{g} P_h - \frac{v}{g} P_{hv}$$

Because E = const.,

$$dE = dh + \frac{v}{g} dv = 0$$

$$df = f_h dh + f_v dv$$

so that

$$h_f = \frac{1}{f_h - \frac{g f_v}{v}}$$

$$v_f = \frac{1}{f_v - \frac{v f_h}{g}}$$

Let $\phi = \phi(h, v)$ be defined as

$$\phi = f_v - \frac{v f_h}{g}$$

Then

$$\phi = P_{vv} - \frac{1}{g} P_h - \frac{2v}{g} P_{hv} + \frac{v^2}{g^2} P_{hh}$$

and equation (C4) becomes

$$Q_f = \frac{Q_v - \frac{v}{g} Q_h}{\phi}$$

This explains how to compute quantities such as β_f, F_f, and $(f_h)_f$ in equations (C3). Equations (C1), (C3), (C5), and (C7) will not be written out explicitly for this case.

REFERENCES

1. Myklebust, Arvid; and Gelhausen, P.: *Putting the ACSYNT on Aircraft Design.* Aerospace America, Sept. 1994, pp. 26–30.

2. Calise, A.: *Singular Perturbation Methods for Variational Problems in Aircraft Flight.* IEEE Transactions on Automatic Control, vol. AC-21, June 1976, pp. 345–353.

3. Calise, A.: *Extended Energy Management Methods for Flight Performance Optimization.* AIAA Journal, vol. 15, no. 3, Mar. 1977, pp. 314–321.

4. Calise, A.: *A New Boundary Layer Matching Procedure for Singularly Perturbed Systems.* IEEE Transaction on Automatic Control, vol. AC-23, no. 3, June 1978.

5. Kelley, H.: *Aircraft Maneuver Optimization by Reduced-Order Approximation.* Control and Dynamic Systems, vol. 10, Academic Press, New York, 1973, pp. 131–178.

6. Kelley, H.; and Edelbaum, T.: *Energy Climbs, Energy Turns, and Asymptotic Expansions.* Journal of Aircraft, vol. 7, Jan. 1970, pp. 93–95.

7. Ardema, M.: *Solution of the Minimum Time-to-Climb Problem by Matched Asymptotic Expansions.* AIAA Journal, vol. 14, no. 7, July 1976.

8. Ardema, M.: *Singular Perturbations in Flight Mechanics.* NASA TM X-62,380, Aug. 1974.

9. Shinar, J.: *On Applications of Singular Perturbation Techniques in Nonlinear Optimal Control.* Automatica, vol. 19, no. 2, 1983, pp. 203–211.

10. Bryson, A.; Desai, M.; and Hoffman, W.: *Energy-State Approximation in Performance Optimization of Supersonic Aircraft.* Journal of Aircraft, vol. 6, no. 6, Nov.–Dec. 1969.

11. Kelley, H.; Cliff, E.; and Weston, A.: *Energy State Revisited.* Optimal Control Applications & Methods, vol. 7, 1986, pp. 195–200.

12. Ardema, M.; Bowles, J.; Terjesen, E.; and Whittaker T.: *Approximate Altitude Transitions for High-Speed Aircraft.* Journal of Guidance, Control, and Dynamics, vol. 18, no. 3, May–June 1995, pp. 561–566.

13. Ardema, M.; and Rajan, N.: *Selection of Slow and Fast Variables in Three-Dimensional Flight Dynamics.* American Control Conference, WP7-3:30, June 1984.

14. Ardema, M.; and Rajan, N.: *Slow and Fast State Variables for Three-Dimensional Flight Dynamics.* Journal of Guidance, Control, and Dynamics, vol. 8, no. 4, July–Aug. 1985.

15. Erzberger, H.: *Automation of On-Board Flight path Management.* NASA TM 84212, Dec. 1981.

16. Erzberger, H.: *Theory and Applications of Optimal Control in Aerospace Systems.* AGARDograph No. 251, July 1981.

17. Erzberger, H.; and Lee, H.: *Algorithm for Fixed-Range Optimal Trajectories.* NASA TP 1565, July 1980.

18. Breakwell, J.: *Optimal Flight-Path-Angle Transitions in Minimum-Time Airplane Climbs.* Journal of Aircraft, vol. 14, no. 8, Aug. 1977.

19. Breakwell, J.: *More about Flight-Path-Angle Transitions in Optimal Airplane Climbs.* Journal of Guidance and Control, vol. 1, no. 3, May–June 1978.

20. Weston, A.; Cliff, E.; and Kelley, H.: *Altitude Transitions in Energy Climbs.* Automatica, vol. 19, Mar. 1983, pp. 199–202.

21. Shinar, J.; and Fainstein, V.: *Improved Feedback Algorithms for Optimal Maneuvers in Vertical Plane.* AIAA Paper 85-1976, 1985.

22. Ardema, M.; and Yang, L.: *Interior Transition Layers in Flight-Path Optimization.* Journal of Guidance, vol. 11, no. 1, Jan.–Feb. 1988.

23. Ardema, M.; and Rajan, N.: *Separation of Time Scales in Aircraft Trajectory Optimization.* Journal of Guidance, Control, and Dynamics, vol. 8, no. 2, Mar.–Apr. 1985.

24. Bharadwaj, S.; Wu, M.; and Mease, K.: *Identifying Time-Scale Structure for Simplified Guidance Law Development.* AIAA Guidance, Navigation, and Control Conference, AIAA Paper 97-3708, 1997.

25. Bryson, A.; and Ho, Y.: *Applied Optimal Control.* Hemisphere Publishing Co., 1975.

26. Jacobson, E.; Lele, M.; and Speyer, J.: *New Necessary Conditions of Optimality for Control Problems with State-Variable Inequality Constraints.* Journal of Mathematical Analysis and Applications, vol. 35, Aug. 1971, pp. 255–284.

27. Pontryagin, L.; Boltyanskii, U.; Gamkrelidze, R.; and Mishchenko, E.: *The Mathematical Theory of Optimal Processes.* Interscience, 1962.

28. Leitmann, G.: *The Calculus of Variations and Optimal Control.* Plenum Press, New York and London, 1981.

29. Tihonov, A.: *Systems of Differential Equations Containing Small Parameters Multiplying Some of the Derivatives.* Math. Sb., vol. 73, no. 3, N.S. (31), 1952 (in Russian).

30. Vasileva, A.: *Asymptotic Behavior of Solutions to Certain Problems Involving Nonlinear Differential Equations Containing a Small Parameter Multiplying the Highest Derivatives.* Russian Math Surveys, vol. 18, no. 3, 1963.

31. O'Malley, R.: *Introduction to Singular Perturbations*: Academic Press, New York and London, 1974.

32. Kokotovic, P.; and Sannuti, P.: *Singular Perturbation Method for Reducing the Model Order in Optimal Control Design.* IEEE Trans. on Automatic Control, vol. 13, no. 4, Aug. 1968.

33. Calise, A.; Aggarwal, R.; and Goldstein, F.: *Singular Perturbation Analysis of Optimal Flight Profiles for Transport Aircraft.* Joint Automatic Control Conference, June 1977.

34. Calise, A.: *Optimization of Aircraft Altitude and Flight-Path Angle Dynamics.* Journal of Guidance, Control and Dynamics, vol. 7, no. 1, Jan.–Feb. 1984.

35. Phillips, J.: *An Accurate and Flexible Trajectory Analysis.* Paper 975599, presented at the 1997 World Aviation Congress, Anaheim, CA, Oct. 1997.

36. Calise, A.; and Corban, J.: *Optimal Control of Two-Time-Scale Systems with State-Variable Inequality Constraints.* Journal of Guidance, Control, and Dynamics, vol. 15, no. 2, Mar.–Apr. 1992.

Table 1. Characteristics of supersonic transport

Gross take-off weight	753,500 lb
Wing planform area	5500 ft^2
Wing span	137.35 ft
Leading edge sweep	48 deg
Aspect ratio	3.43
Body length	314 ft
Payload	
first class passengers	30
coach class passengers	274
flight crew	2
flight attendants	9
Maximum Mach number	2.4
Maximum dynamic pressure	1000 psf

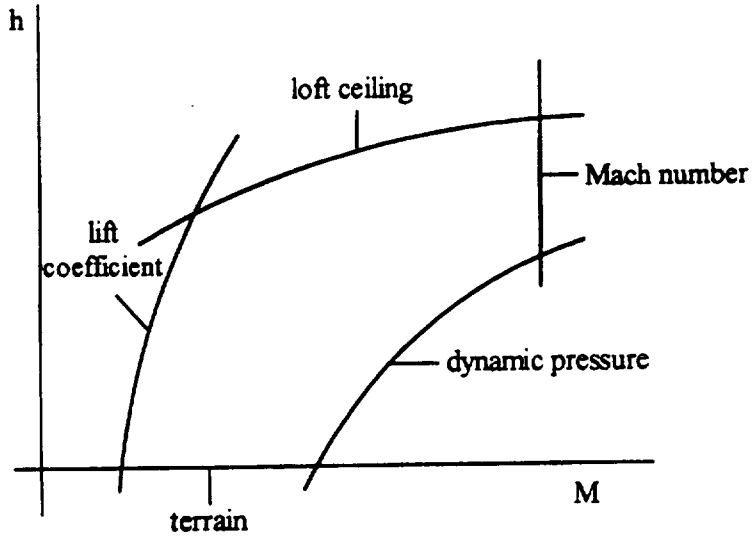

Figure 1. Sketch of constraints defining flight envelope.

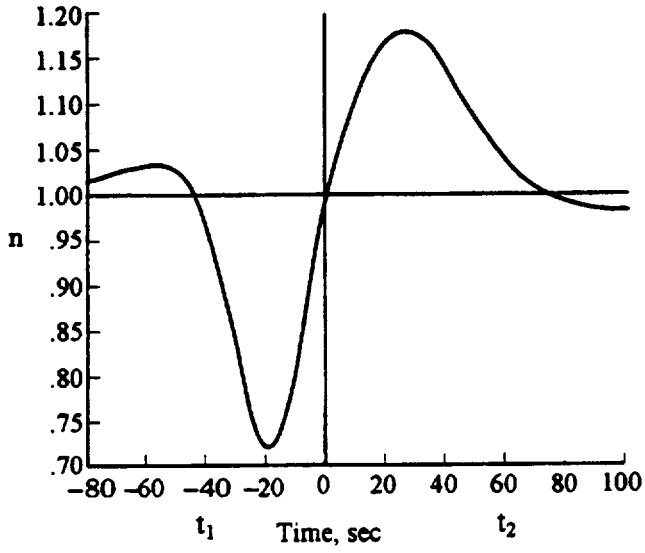

Figure 2. Load factor history during altitude transition for a high performance aircraft.

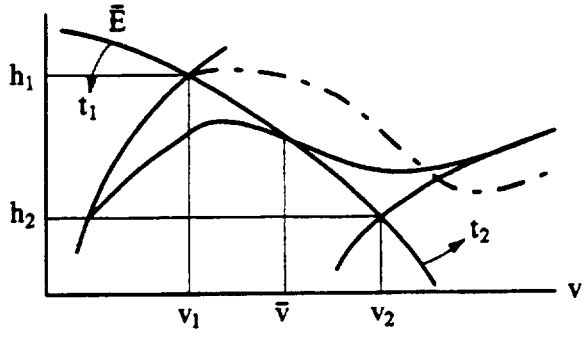

Figure 3. Sketch of an altitude transition.

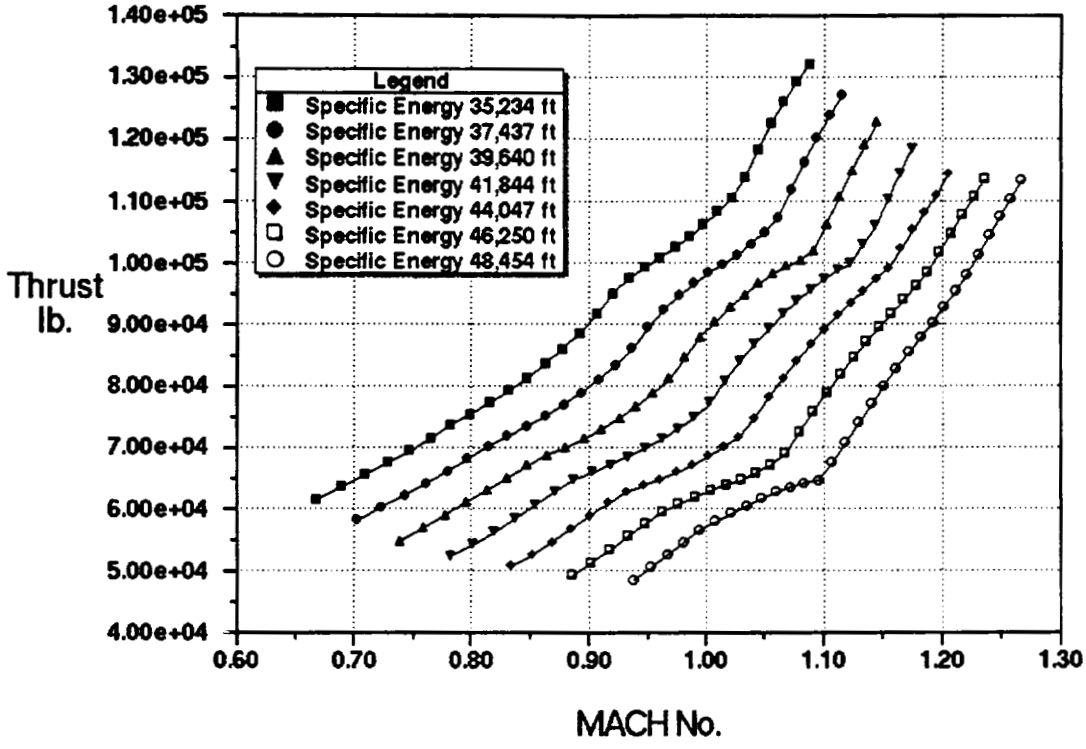

Figure 4. Thrust vs. Mach number in the transonic region.

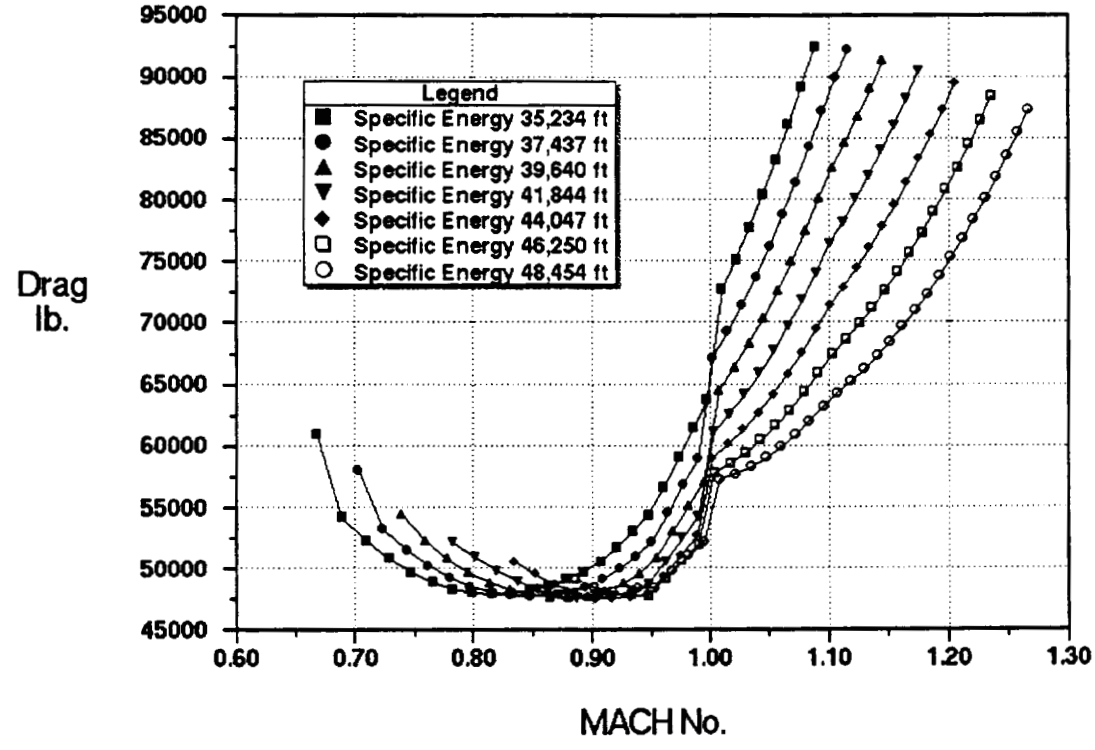

Figure 5. Drag for $N = 1$ vs. Mach number in the transonic region.

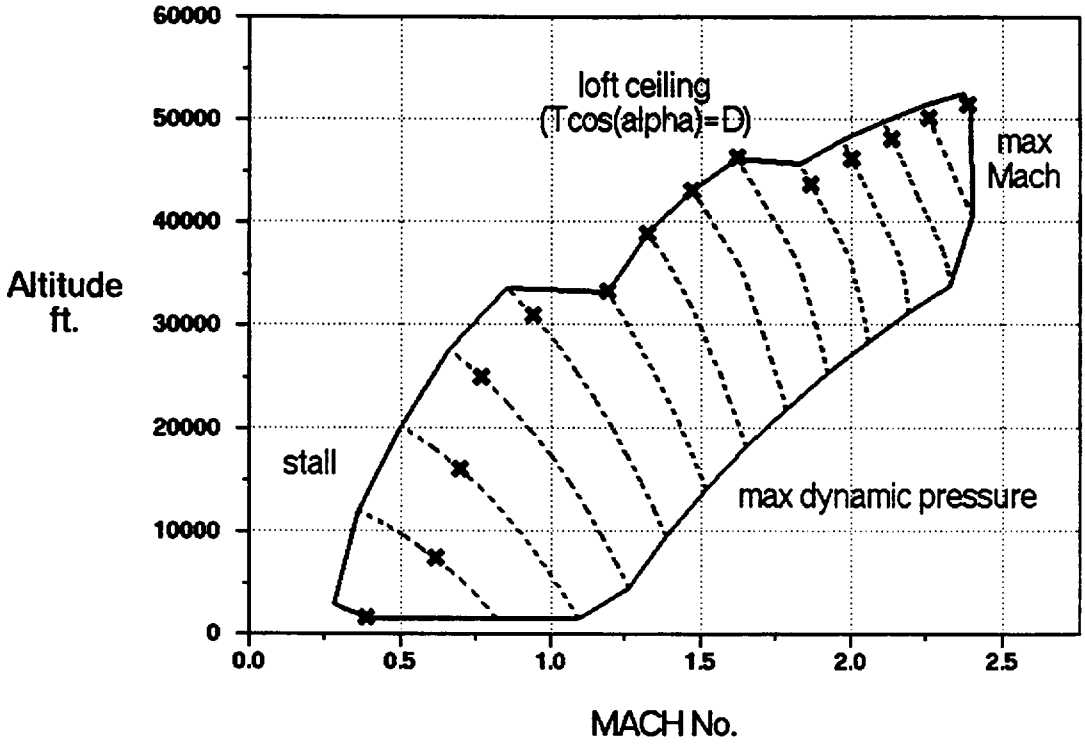

Figure 6. Optimum cruise points in the flight envelope for minimum fuel.

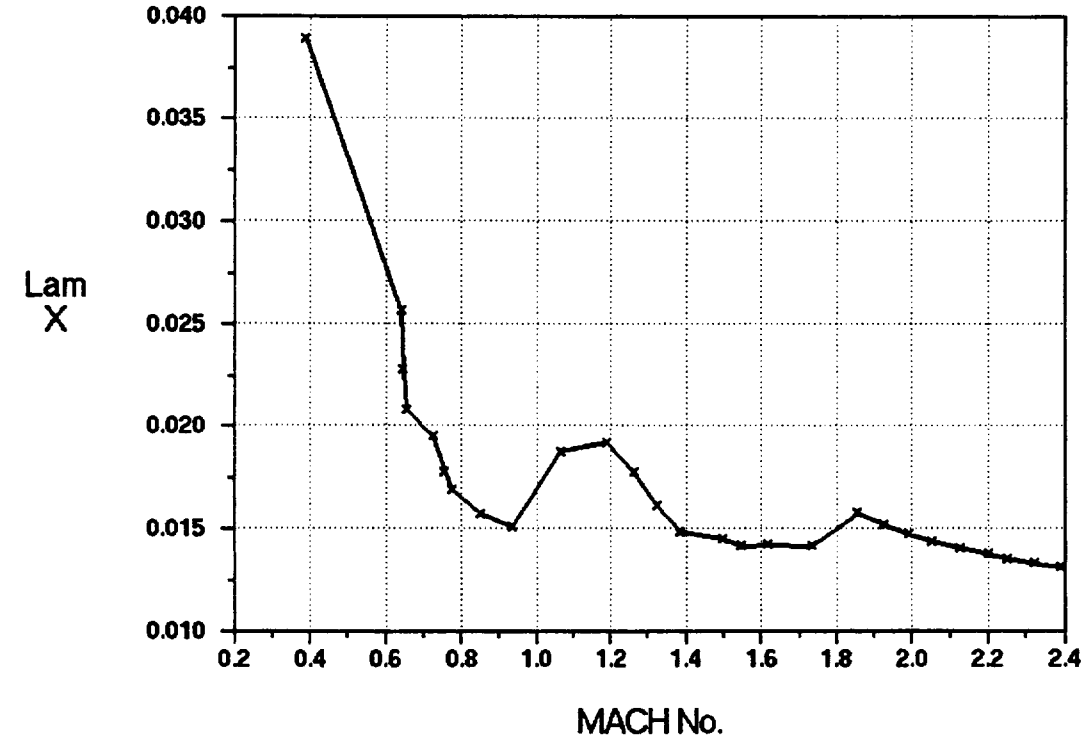

Figure 7. λ_x vs. Mach number.

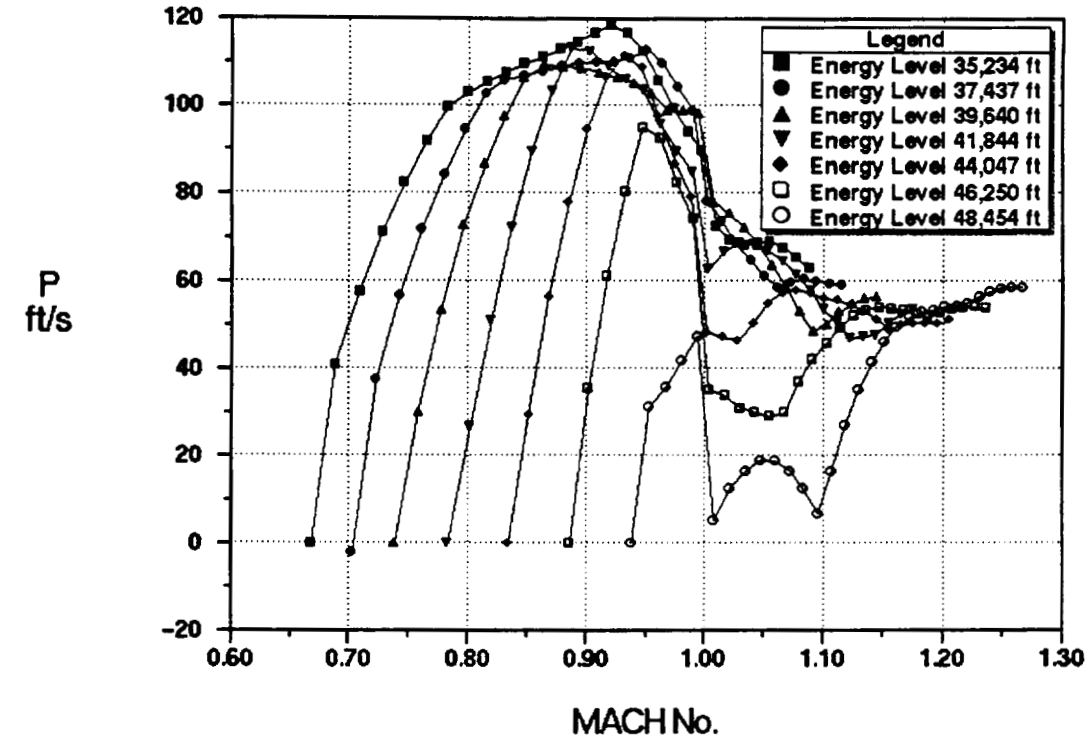

Figure 8. Energy rate vs. Mach number in the transonic region.

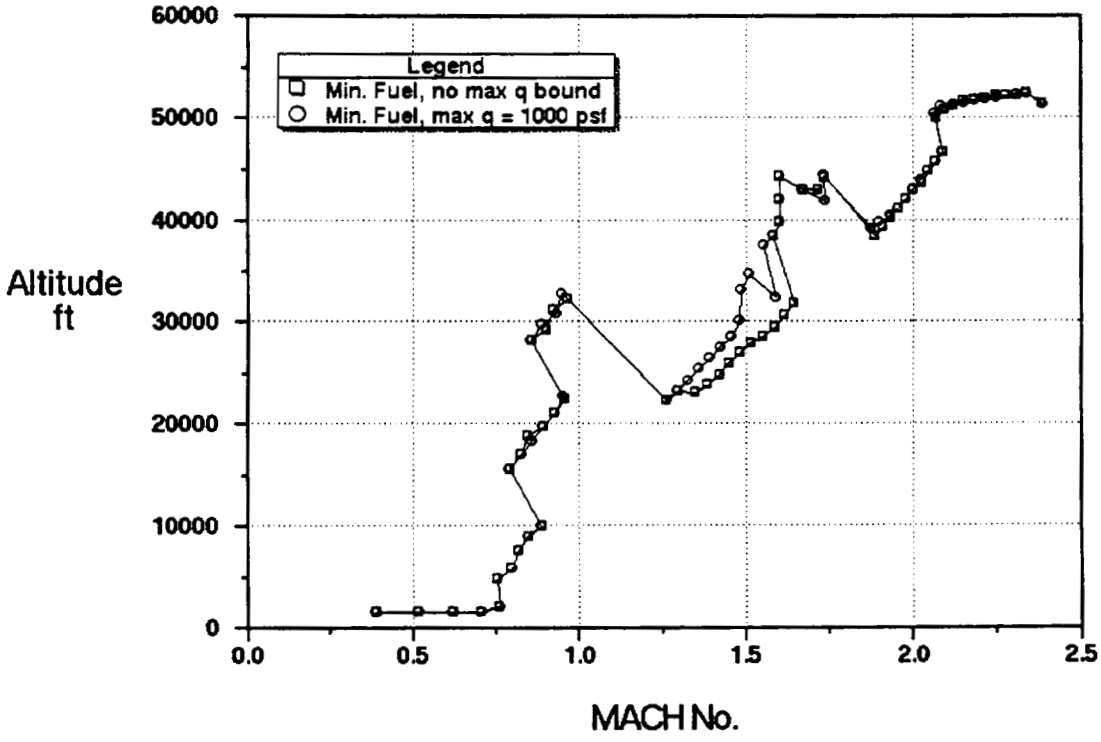

Figure 9. Energy climb path with and without dynamic pressure constraint.

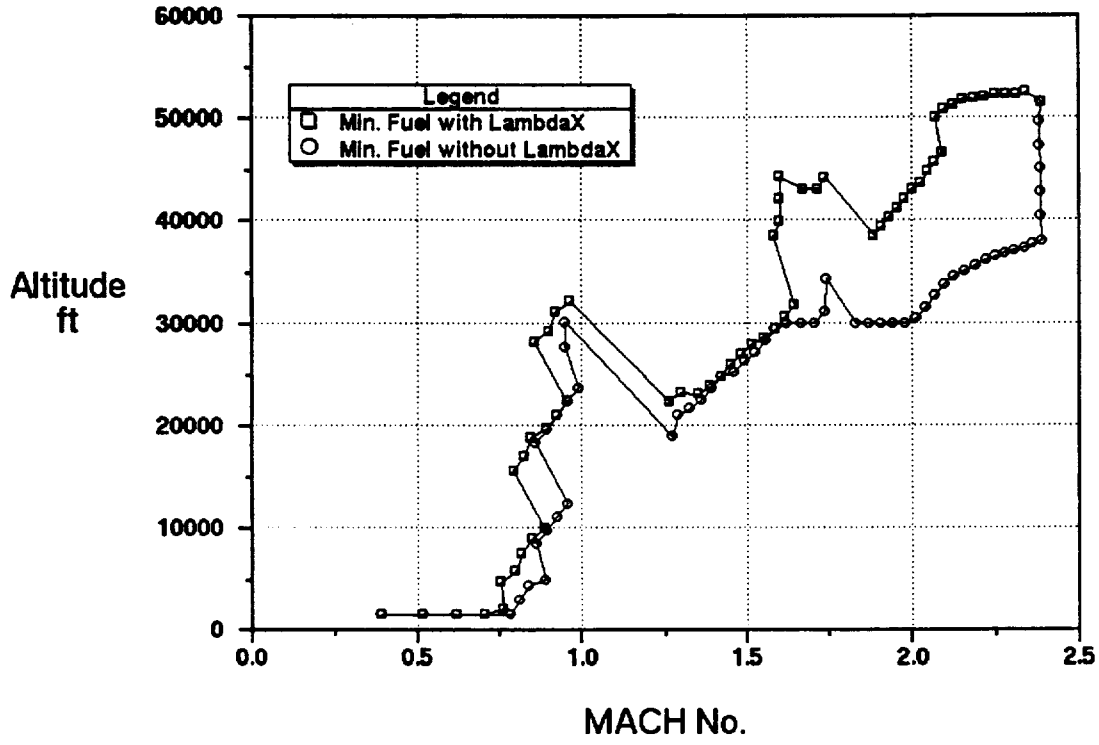

Figure 10. Energy climb path with and without λ_x.

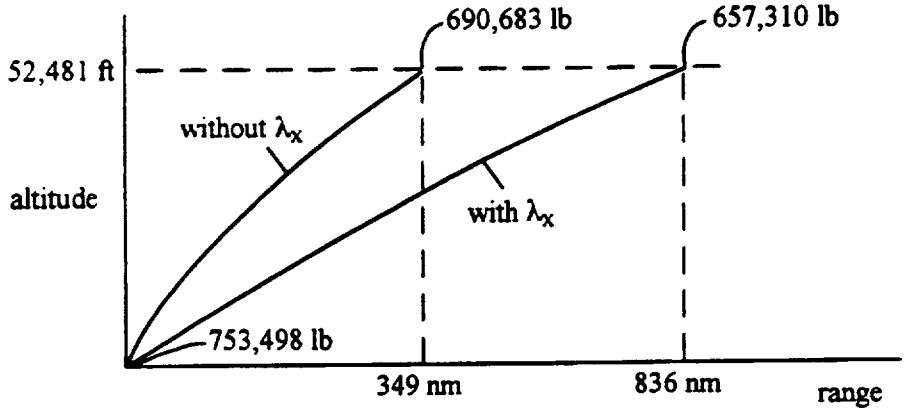

Figure 11. Sketch of trajectories with and without λ_x.

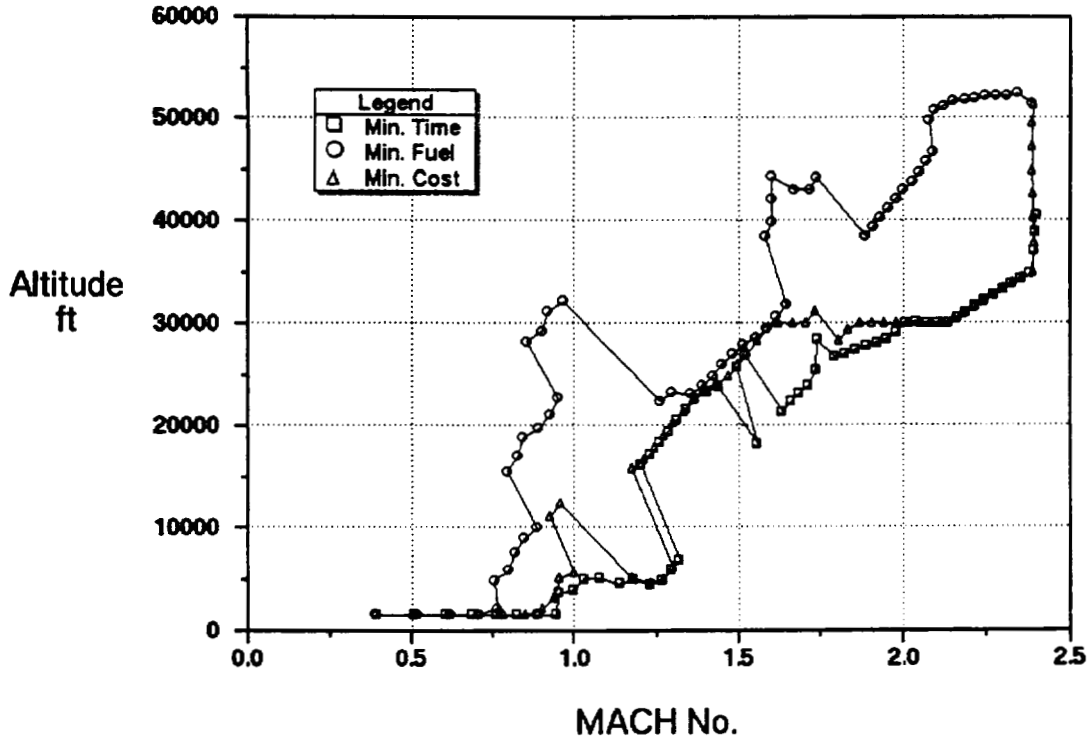

Figure 12. Energy climb path for minimum fuel, minimum time, and minimum cost.

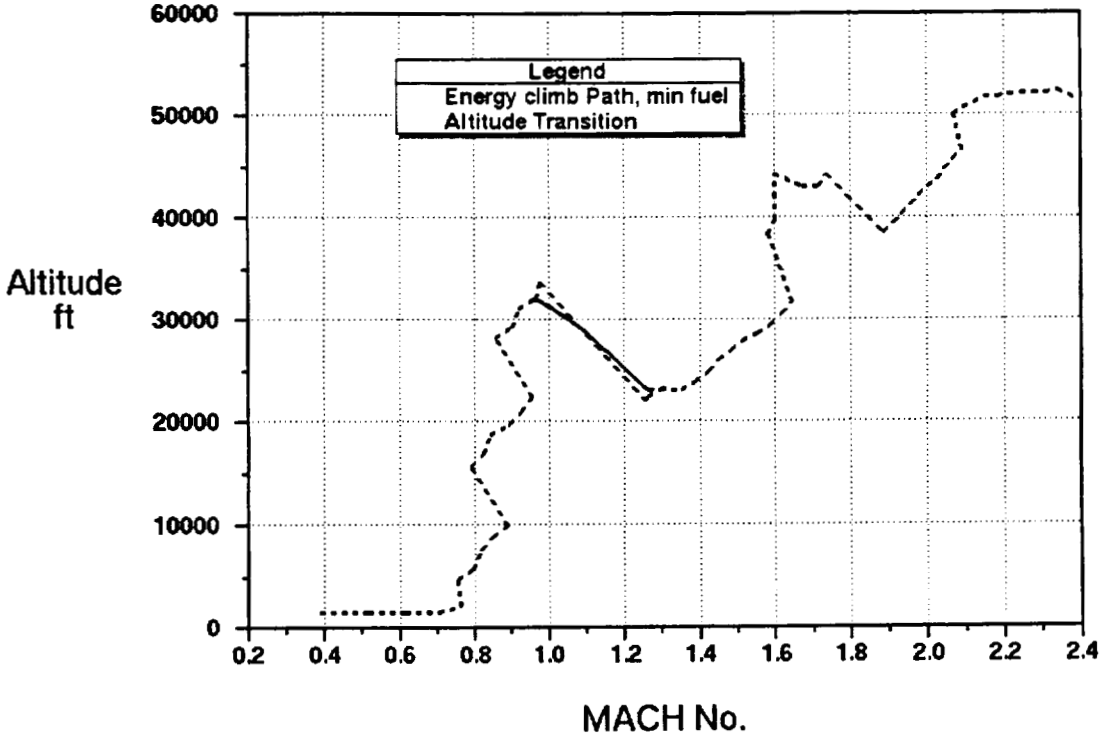

Figure 13. Transonic altitude transition for $N_1 = 0.97$, $N_2 = 1.05$, nonlinear determination of $\overline{v}$ and $\overline{\gamma}$.

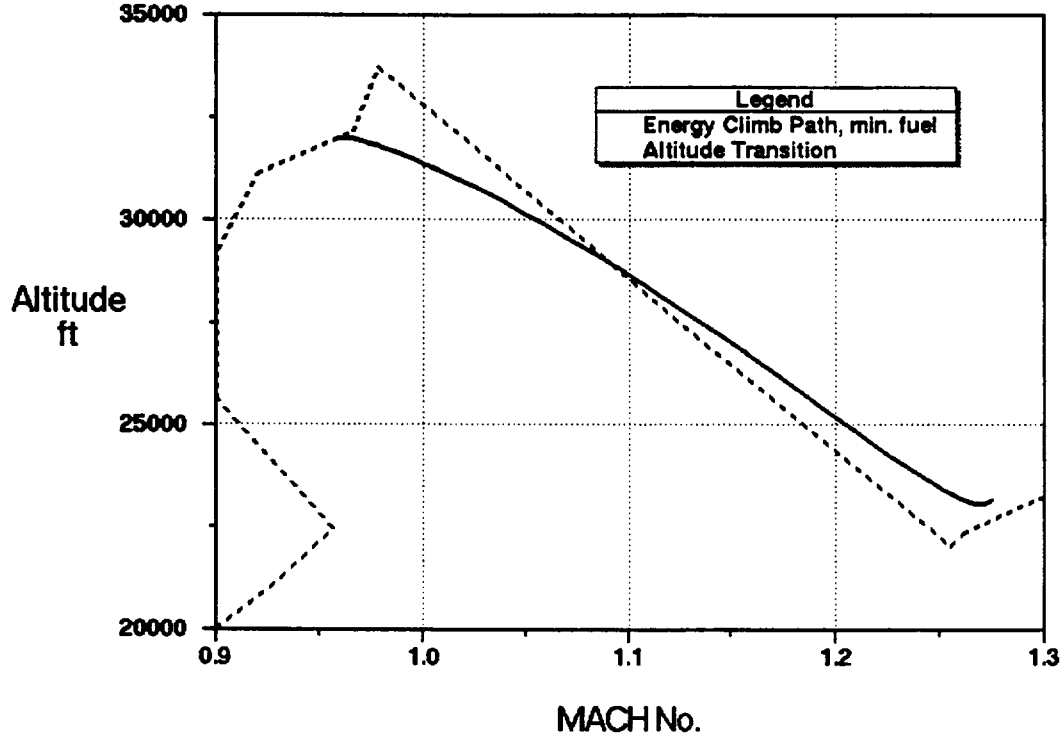

Figure 14. Altitude transition in the transonic region.

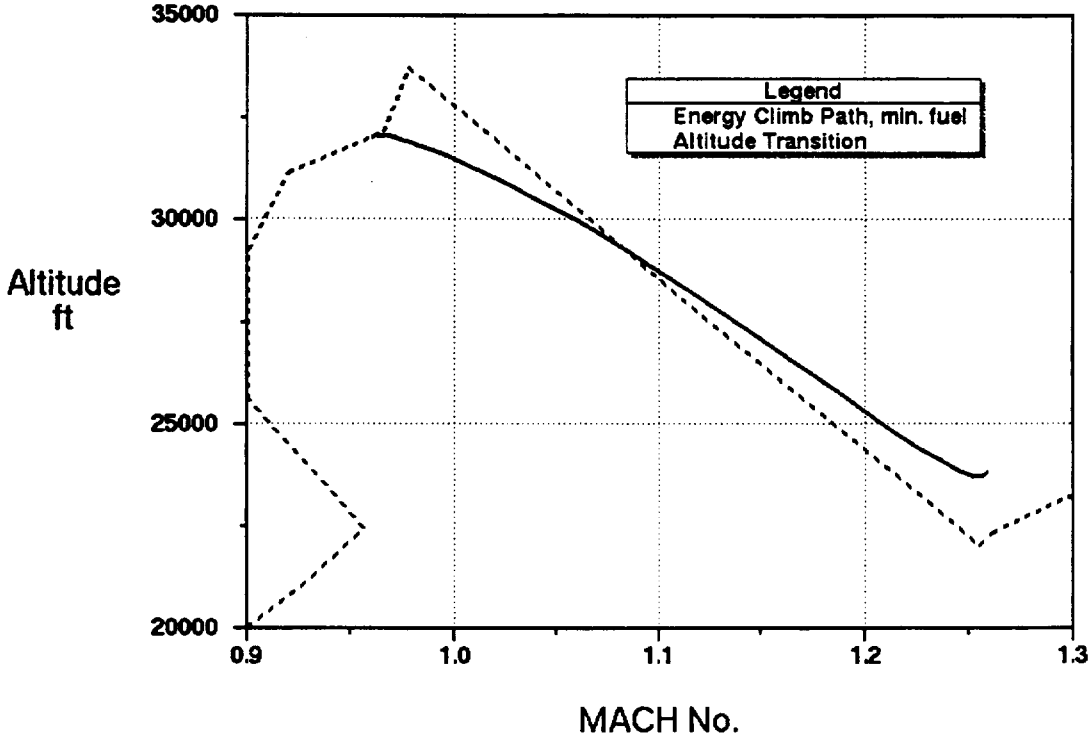

Figure 15. Altitude transition, linear determination of $\overline{v}$ and $\overline{\gamma}$.

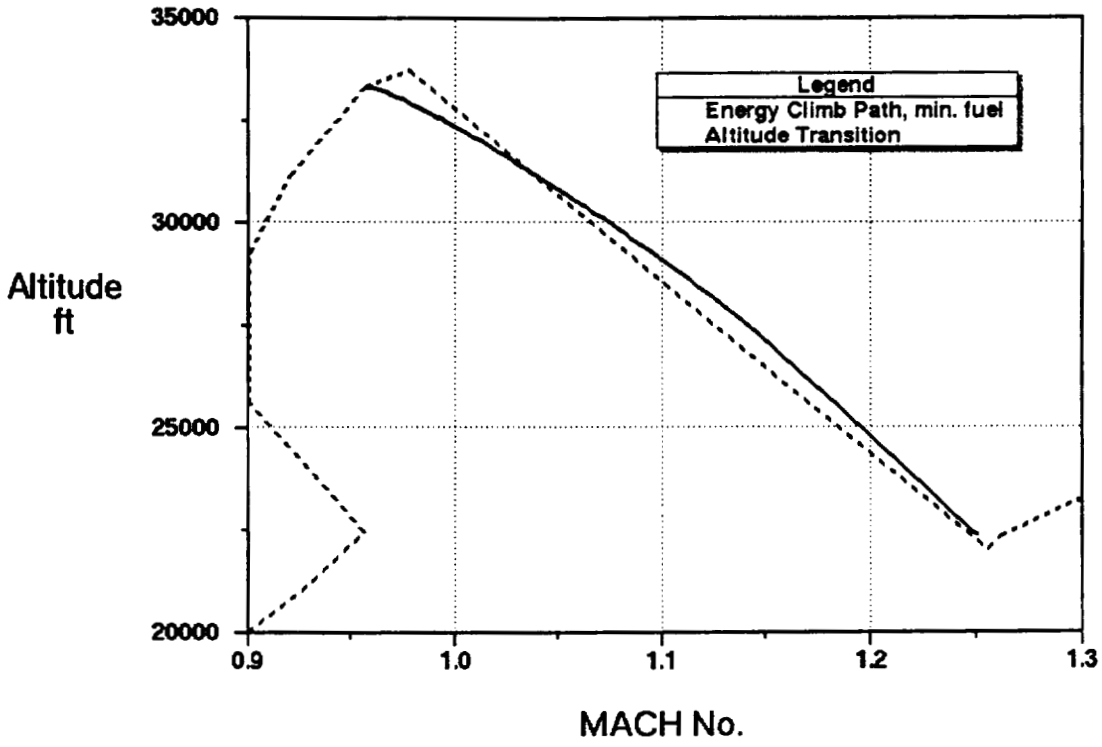

Figure 16. Altitude transition for $N_1 = 0.5$, $N_2 = 1.5$.

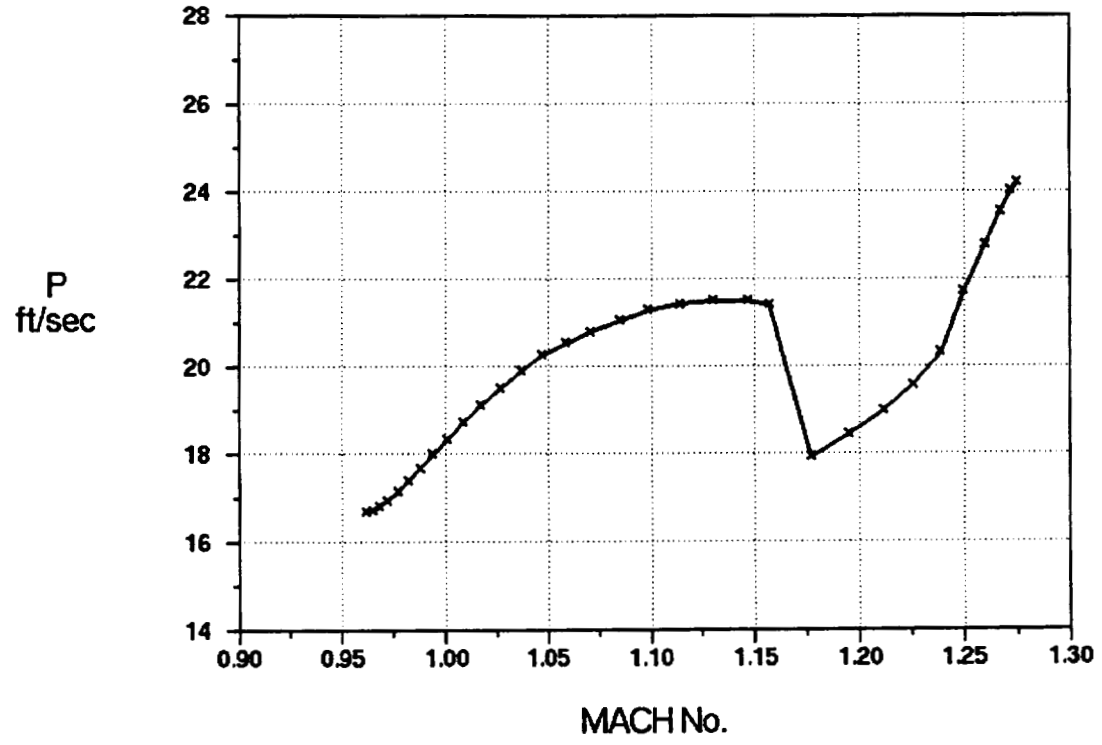

Figure 17. Energy rate during altitude transition, $N_1 = 0.97$, $N_2 = 1.05$.

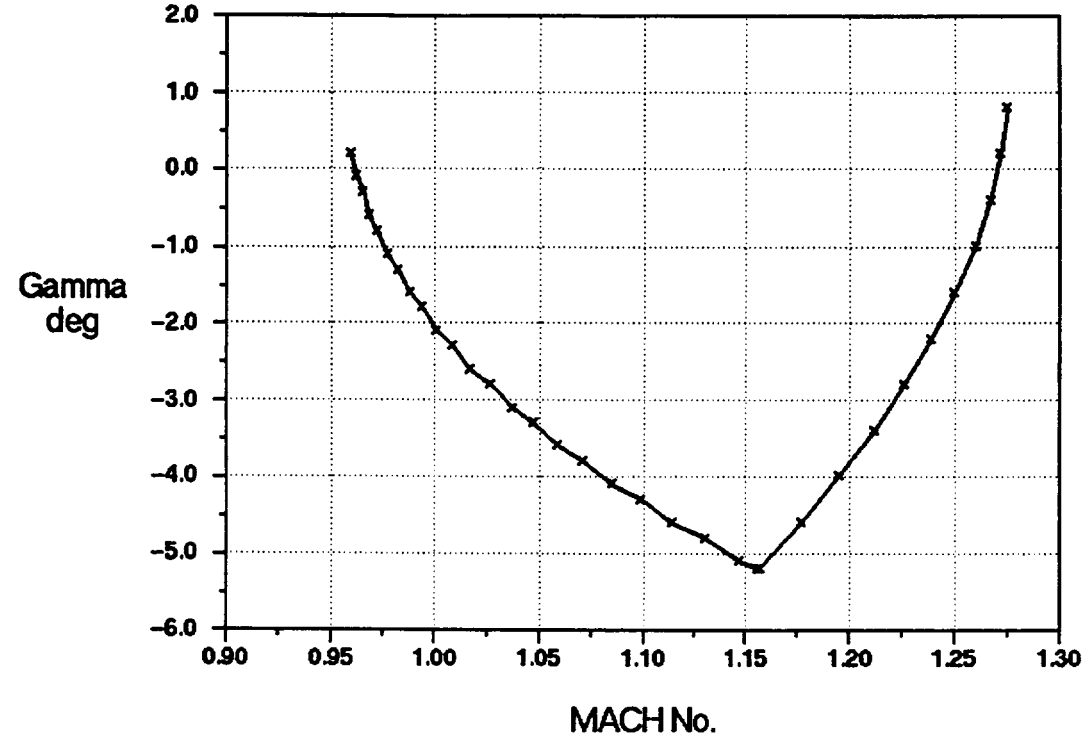

Figure 18. Flight path angle during altitude transition, $N_1 = 0.97$, $N_2 = 1.05$.

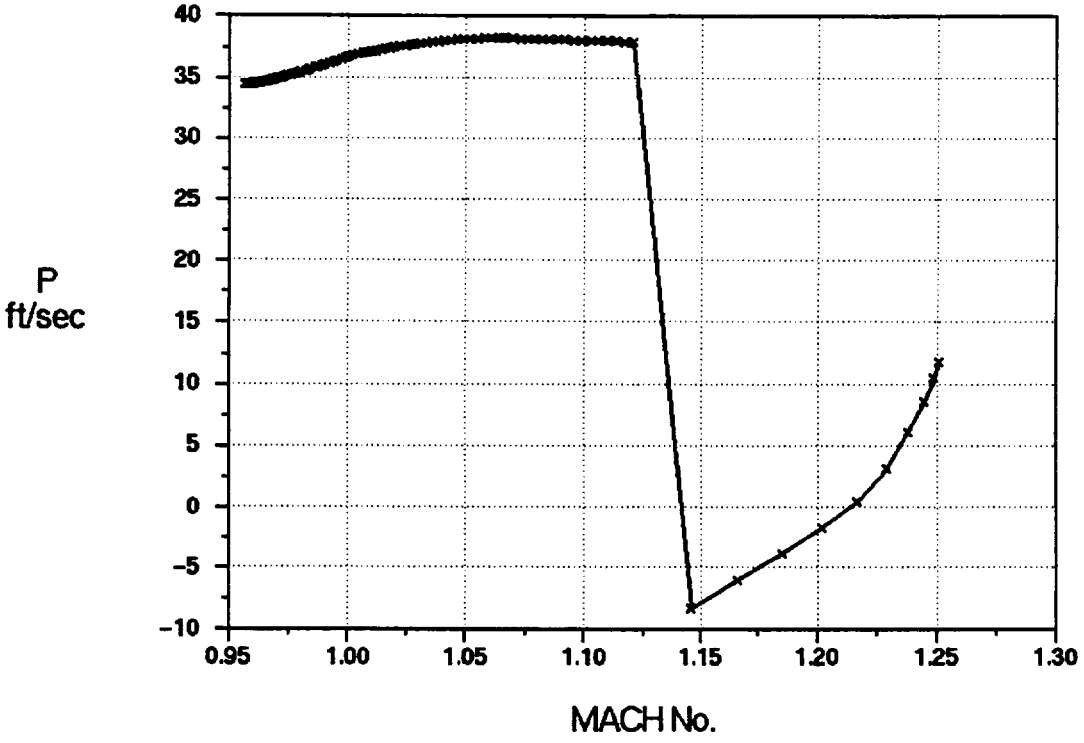

Figure 19. Energy rate during altitude transition, $N_1 = 0.5$, $N_2 = 1.5$.

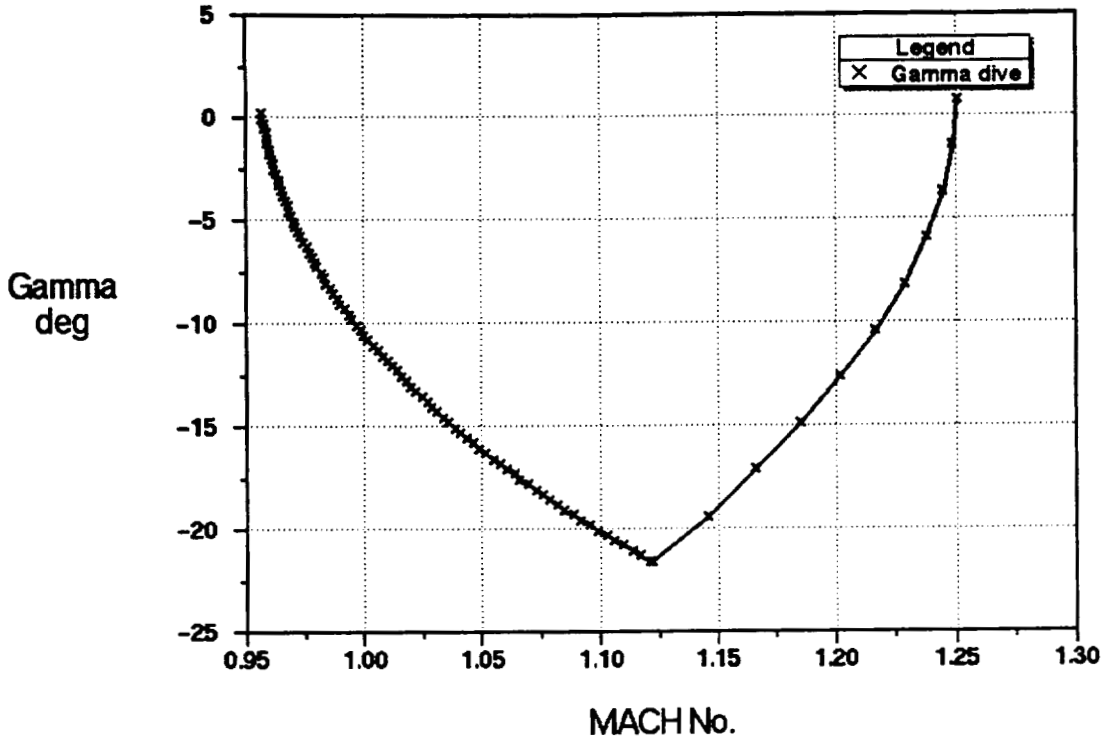

Figure 20. Flight path angle during altitude transition, $N_1 = 0.5$, $N_2 = 1.5$.

REPORT DOCUMENTATION PAGE

Form Approved
OMB No. 0704-0188

1. AGENCY USE ONLY *(Leave blank)*	2. REPORT DATE	3. REPORT TYPE AND DATES COVERED
	March 1998	Technical Memorandum

4. TITLE AND SUBTITLE

Optimization of Supersonic Transport Trajectories

5. FUNDING NUMBERS

522-41-42

6. AUTHOR(S)

Mark D. Ardema,* Robert Windhorst,* and James Phillips

7. PERFORMING ORGANIZATION NAME(S) AND ADDRESS(ES)

Ames Research Center
Moffett Field, CA 94035-1000

8. PERFORMING ORGANIZATION REPORT NUMBER

A-98-09997

9. SPONSORING/MONITORING AGENCY NAME(S) AND ADDRESS(ES)

National Aeronautics and Space Administration
Washington, DC 20546-0001

10. SPONSORING/MONITORING AGENCY REPORT NUMBER

NASA/TM—1998-112223

11. SUPPLEMENTARY NOTES

Point of Contact: James Phillips, Ames Research Center, MS 237-11, Moffett Field, CA 94035-1000
(650) 604-5789
*Santa Clara University, Santa Clara, California

12a. DISTRIBUTION/AVAILABILITY STATEMENT

Unclassified — Unlimited
Subject Category 08

12b. DISTRIBUTION CODE

13. ABSTRACT *(Maximum 200 words)*

This paper develops a near-optimal guidance law for generating minimum fuel, time, or cost fixed-range trajectories for supersonic transport aircraft. The approach uses a choice of new state variables along with singular perturbation techniques to time-scale decouple the dynamic equations into multiple equations of single order (second order for the fast dynamics). Application of the maximum principle to each of the decoupled equations, as opposed to application to the original coupled equations, avoids the two point boundary value problem and transforms the problem from one of a functional optimization to one of multiple function optimizations. It is shown that such an approach produces well known aircraft performance results such as minimizing the Brequet factor for minimum fuel consumption and the energy climb path. Furthermore, the new state variables produce a consistent calculation of flight path angle along the trajectory, eliminating one of the deficiencies in the traditional energy state approximation. In addition, jumps in the energy climb path are smoothed out by integration of the original dynamic equations at constant load factor. Numerical results performed for a supersonic transport design show that a pushover dive followed by a pullout at nominal load factors are sufficient maneuvers to smooth the jump.

14. SUBJECT TERMS

Supersonic aircraft trajectories, Singular perturbations,
Transonic altitude discontinuity

15. NUMBER OF PAGES

57

16. PRICE CODE

A04

17. SECURITY CLASSIFICATION OF REPORT	18. SECURITY CLASSIFICATION OF THIS PAGE	19. SECURITY CLASSIFICATION OF ABSTRACT	20. LIMITATION OF ABSTRACT
Unclassified	Unclassified		